DR 700

LBL-9093
GSRMP-5
UC-66a

State-of-the-Art Review of Geothermal Reservoir Modelling

George F. Pinder

Golder Associates

Geothermal Subsidence Research Management Program

March 1979

MASTER

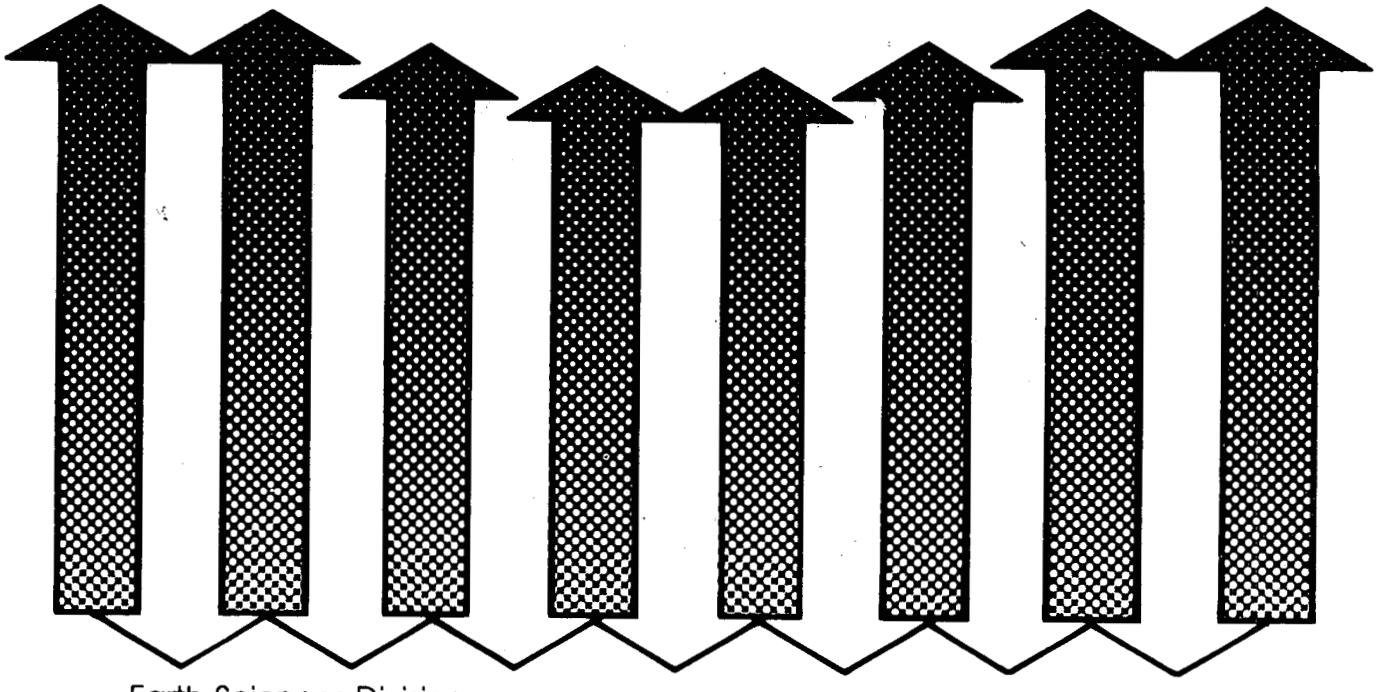

Earth Sciences Division
Lawrence Berkeley Laboratory
University of California

Prepared for the U.S. Department of Energy under Contract W-7405-ENG-48

DISCLAIMER

Printed in the United States of America
Available from
National Technical Information Service
U.S. Department of Commerce
5285 Port Royal Road
Springfield, VA 22161
Price Code: A08

STATE-OF-THE-ART REVIEW OF GEOTHERMAL RESERVOIR MODELLING

by

George F. Pinder

for

Golder Associates

March 1979

PREAMBLE

The following pages contain summaries of all published geothermal models known to the author which lie within the scope of this report. In preparing these summaries, it was often necessary to infer information not explicitly presented and to modify notation. I hope this was accomplished with a minimum of error. I wish to acknowledge the cooperation of Charles Faust and J. W. Pritchett for providing me with reports and papers not readily available elsewhere. I also wish to acknowledge the assistance of Edward Tang who reviewed the manuscript and to Dorothy Hannigan who typed it.

This research program was sponsored by the Division of Geothermal Energy of the U. S. Department of Energy under contract W-7405-ENG-48 through the Lawrence Berkeley Laboratory, Earth Sciences Division under Purchase Order number 3730302.

TABLE OF CONTENTS

1.0 INTRODUCTION

The simulation of subsidence in a geothermal reservoir involves the solution of equations governing fluid movement, energy transport, and reservoir skeleton deformation. The three phenomena are, of course, coupled and in the most rigorous formulation would be considered and approximated as a single system. In practice, however, deformation of the reservoir skeleton has only a minor impact on fluid flow and energy transport whereas these latter phenomena are very important in reservoir deformation. This type of one-way coupling is not unusual in mathematical physics and can be used effectively to enhance the efficiency of a geothermal reservoir subsidence code. The most important consequence of this is a decoupling of the fluid flow and energy transport from the deformation equations such that they can be solved sequentially rather than simultaneously without the introduction of significant error. Thus, the geothermal reservoir model, exclusive of skeletal deformation, can be viewed and analyzed meaningfully as a separate entity.

The objective of this report is to summarize and, to the degree possible, evaluate the state of the art in geotehrmal reservoir modelling. As used herein the term geothermal reservoir model refers to the representation of the dynamics and thermodynamics of a geothermal reservoir, without skeletal deformation, using the concepts of porous flow physics and the subsequent solution of the resulting assemblage of differential and partial differential equations. Only those models which have been developed exclusively for geothermal simulation will be considered within the scope of this report. Thus, we have exluded from this discussion models prepared for the simulation of steam injection processes in oil recovery (see for example, Coats et al. 1973; Coats, 1974; and Weinstein et al. 1974). We

will also focus attention primarily on the two and three dimensional distributed parameter models. It should be pointed out, however, that considerable success has been achieved in predicting the performance of the Wairakei geothermal field using zero dimensional or lumped parameter formulations (see, for example, Whiting and Ramey, 1969; Brigham and Morrow, 1974).

There are several distinct but interrelated elements of geothermal reservoir modelling. The most fundamental element is the conceptual model of the reservoir. While field data is relatively scarce and, at least in part, not freely available to the scientific community, there is nevertheless a general concensus of opinion on the fundamental aspects of the reservoir. It is believed, and in some reservoirs clearly demonstrated, that the primary conduits of energy transport are fractures. The porous medium blocks, delineated by these fractures, act as the long-term energy suppliers feeding the fracture system. One can visualize this system in two distinct ways and we will return to this later in the report.

Geothermal reservoirs can be classified on the basis of their fluid composition. The most common type of field is characterized by reservoir fluid which is predominantly water in the liquid phase. This type of field, often referred to as a hot water system, is found at Wairakei, New Zealand, Cerro Prieto, Mexico and many other locations around the world. Reservoirs which produce primarily steam are called vapour dominated. The major reservoirs of this class are found at the Geysers in California, at Larderello in Italy, and at the Matsukawa field in Japan. Hot water systems characteristically produce from 70 to 90 percent of their total mass as water at the surface while vapour dominated systems produce dry to superheated steam (Toronyi and Farouq Ali, 1977). The pressures of vapour dominated systems are below hydrostatic. Moreover, the initial temperatures

and pressures are very near those corresponding to the maximum enthalpy of saturated steam; 236°C and 31.8 kg./sq.cm (see figure 5). The regional distribution of fluids within a reservoir is essentially unknown.

The assumptions inherent in the conceptual model of the reservoir should dictate the framework of its mathematical description. In the case of geothermal reservoirs, however, the physical and mathematical foundations for multiphase mass and energy transport through fractured porous media do not exist. Consequently, all of the existing multiphase models assume the reservoir to be a porous medium. When fractures are included, they are highly idealized geometrically and, although the parameter values may differ, (Coats, 1977) employ the same governing equations as the porous medium. Fractured reservoir mass and energy transport has been considered in a formal way for hot water systems (O'Neill, 1977) but this has not yet been extended to a steam-water reservoir.

Given the theoretical constraint cited above, the governing flow and transport equations for geothermal reservoir simulation are obtained through one of three ways. The simplest approach is essentially a macroscopic mass balance. In other words, one assumes that the balance laws observed at the microscopic level are, with minor modification, valid for the porous medium as well. This approach does not provide insight into the micro-physics of energy transfer at the pore level but does provide a set of governing equations not unlike those obtained using more sophisticated techniques. A second approach involves the use of mixture theory as developed in continuum mechanics. This approach is more rigorous but, while recognizing the existence of pore level interaction, it does not provide

adequate insight into the nature of this interaction. The most promising approach to obtaining a rigorous formulation of the governing equations is through formal integration of the microscopic balance equations over the porous medium, possibly augmented through constitutive theory. In the development of the governing equations, we will employ this approach.

Having generated an appropriate set of governing equations, one is faced with the task of solving a set of highly non-linear partial-differential equations. In nearly all cases, this is approached numerically. There are several difficulties encountered in the numerical solution of the geothermal reservoir equations. The first task is to select a set of dependent variables since several possibilities exist. One must then decide upon a method of approximation. Currently, finite difference and finite element schemes are employed. One is now confronted with the problems associated with the simulation of convection dominated transport, namely numerical dispersion (oscillations) and diffusion (smearing of a sharp front). Possibly the most difficult task, however, remains; the efficient and accurate treatment of the highly non-linear coefficients. As we shall see virtually every geothermal model handles this problem differently.

From the reservoir engineering point of view, there are two additional factors to consider. The field application of a geothermal code requires a proper representation of the well-bore dynamics and thermodynamics. This is particularly important in the case of simulations in the immediate vicinity of the well. A second practical problem involves the reduction of the general three-dimensional system to an areal two-dimensional representation. This requires, of course, formal integration over the vertical. This integration should be carried out carefully so that essential elements of the reservoir physics are salvaged.

In this report, the general porous flow theory, which should be common to all models, will be formulated. Then each geothermal reservoir model known to the author will be examined. In particular, we will present the governing equations, method of approximation, treatment of the convection term, treatment of the nonlinear coefficients, solution of the resulting algebraic equations, and representation of the well-bore. We will briefly discuss example problems that have been treated. To facilitate a comparison of the various models, the attributes of each will be tabulated.

2.0 GOVERNING POINT EQUATIONS

The point of departure for the development of the equations governing mass and energy transport in either the porous medium or fractured porous medium model is the point balance equations. These are the expressions derived through averaging of the molecular level equations and generally encountered in continuum mechanics, fluid and solid mechanics, heat flow and other fields of science and engineering. The point balance equations for a continuum are

2.1 Mass Balance

$$\frac{\partial \rho}{\partial t} + \underset{\sim}{\nabla}\cdot(\rho \underset{\sim}{v}) = 0 \tag{2.1}$$

where ρ is the density $[ML^{-3}]$, and

$\underset{\sim}{v}$ is the mass average velocity $[Lt^{-1}]$

The first term describes the instantaneous rate of change in mass per unit volume and the second describes the net outward flow of mass from the point.

2.2 Momentum Balance

$$\frac{\partial}{\partial t}(\rho \underset{\sim}{v}) + \underset{\sim}{\nabla}\cdot(\rho \underset{\sim}{v}\underset{\sim}{v}) + \underset{\sim}{\nabla} p - \underset{\sim}{\nabla}\cdot \underset{\approx}{\tau} - \rho \underset{\sim}{g} = 0 \tag{2.2}$$

where p is the mechanical fluid pressure $[ML^{-1}t^{-2}]$, and

$\underset{\approx}{\tau}$ is the viscous stress tensor $(ML^{-1}t^{-2}]$, and

$\underset{\sim}{g}$ is the gravitational acceleration $[Lt^{-2}]$

The first term in (2.2) describes the instantaneous rate of change of momentum per unit volume, the second describes the outward flow of momentum per unit volume from the point, the third and fourth represent the loss of momentum per unit volume due to viscous stress dissipation and pressure forces and the fifth accounts for the gain in momentum per unit volume attributable to body forces, in our case gravity. Equation (2.2) may be rewritten as

$$(2.3) \qquad \underset{\sim}{v}\frac{\partial \rho}{\partial t} + \underset{\sim}{v}\cdot\nabla(\rho\underset{\sim}{v}) + \rho\frac{\partial \underset{\sim}{v}}{\partial t} + \rho\underset{\sim}{v}\cdot\nabla\underset{\sim}{v} + \nabla p - \nabla\cdot\underset{\approx}{\tau} - \rho\underset{\sim}{g} = 0$$

which, in light of (2.1) becomes

$$(2.4) \qquad \rho\frac{D\underset{\sim}{v}}{Dt_f} + \nabla p - \nabla\cdot\underset{\approx}{\tau} - \rho\underset{\sim}{g} = 0$$

where $$\frac{D(\cdot)}{Dt_f} \equiv \frac{\partial(\cdot)}{\partial t} + \underset{\sim}{v}_f\cdot\nabla(\cdot)$$

and is known as the substantial derivative. Because $\frac{D\underset{\sim}{v}}{Dt_f}$ is the acceleration, it is evident that (2.4) simply describes a balance of forces.

2.3 Energy Balance

$$(2.5) \qquad \frac{\partial}{\partial t}(\rho E) + \nabla\cdot\rho\underset{\sim}{v}E + \nabla\cdot\underset{\sim}{q} + \nabla\cdot p\underset{\sim}{v} - \nabla\cdot[\underset{\approx}{\tau}\cdot\underset{\sim}{v}] = 0$$

where $E = U + 1/2\ v^2 + \Phi$ and

E is the total energy per unit mass $[L^2t^{-2}]$,

U is the internal energy per unit mass $[L^2t^{-2}]$,

$1/2\ v^2$ is the kinetic energy per unit mass $[L^2t^{-2}]$,

Φ is the potential energy per unit mass $[L^2t^{-2}]$, and

$\underset{\sim}{q}$ is the heat flux vector $[L^3t^{-3}]$

The first term in (2.5) is the rate of gain of total energy per unit volume, the second is the rate of total energy loss per unit volume by convection, the third is the rate of loss of total energy per unit volume by conduction, the fourth is the rate of loss of total energy per unit volume by pressure forces and the last term is the rate of loss of total energy per unit volume by viscous forces.

Equation (2.5) can also be rewritten more compactly using the continuity equation (2.1)

$$(2.6) \qquad \rho \frac{DE}{Dt_f} + \nabla\cdot\underset{\sim}{q} + \nabla\cdot(\rho\underset{\sim}{v}) - \nabla\cdot[\underset{\approx}{\tau}\cdot\underset{\sim}{v}] = 0$$

In our investigations, it is sufficient to work with a simpler form of the total energy balance. Let us first use the momentum equation to obtain an expression for the kinetic energy. Thus premultiplying (2.4) by $\underset{\sim}{v}$, we obtain

$$(2.7) \qquad \rho \frac{D(1/2\ v^2)}{Dt_f} + \underset{\sim}{v}\cdot\nabla p - \underset{\sim}{v}\cdot\nabla\underset{\approx}{\tau} - \underset{\sim}{v}\cdot\rho\underset{\sim}{g} = 0$$

Substitution for E in (2.6) and subsequent subtraction of (7) yields

$$(2.8) \qquad \rho \frac{D}{Dt_f}(U+\Phi) + \nabla\cdot\underset{\sim}{q} + p\nabla\cdot\underset{\sim}{v} + \underset{\approx}{\tau}:\nabla\underset{\sim}{v} + \underset{\sim}{v}\cdot\rho\underset{\sim}{g} = 0$$

We can further simplify (2.8) by assuming that the body force can be expressed in terms of the gradient of a scalar function, i.e., $\underset{\sim}{g} = -\nabla\Phi$ (Bird et al, 1960)

$$(2.9) \qquad \rho \underset{\sim}{v}\cdot\underset{\sim}{g} = -\rho \underset{\sim}{v}\cdot\nabla\Phi = -\rho \frac{D}{Dt}\Phi + \rho \frac{\partial \Phi}{\partial t}$$

If, as in the case of gravity, we can assume Φ is time independent

$$\rho(\underset{\sim}{v}\cdot\underset{\sim}{g}) = -\rho \frac{D}{Dt}\Phi$$

and equation (2.8) becomes

$$(2.10) \qquad \rho \frac{DU}{Dt_f} + \nabla\cdot\underset{\sim}{q} + p\nabla\cdot\underset{\sim}{v} + \underset{\approx}{\tau}:\nabla\underset{\sim}{v} = 0$$

Equation (2.10) describes the internal energy balance. While some geothermal models elect to use internal energy as a dependent variable, others prefer to use enthalpy because it is a "field variable". From the definition of enthalpy h we have

$$(2.11) \qquad h = U + \frac{p}{\rho}$$

Thus, the energy balance (2.10) can be written in the equivalent form

$$(2.12) \qquad \rho \frac{Dh}{Dt_f} - \frac{Dp}{Dt_f} + \nabla\cdot\underset{\sim}{q} + \underset{\approx}{\tau}:\nabla\underset{\sim}{v} = 0$$

The three balance equations are now listed for convenience

$$(2.1) \qquad \frac{\partial \rho}{\partial t} + \nabla\cdot(\rho\underset{\sim}{v}) = 0 \qquad \text{(Mass)}$$

$$(2.4) \qquad \rho \frac{D\underset{\sim}{v}}{Dt_f} + \nabla \underset{\sim}{p} - \nabla \cdot \underset{\approx}{\tau} - \rho \underset{\sim}{g} = 0 \qquad \text{(Momentum)}$$

$$(2.10) \qquad \rho \frac{DU}{Dt_f} + \nabla \cdot \underset{\sim}{q} + p \nabla \cdot \underset{\sim}{v} + \underset{\approx}{\tau} : \nabla \underset{\sim}{v} = 0 \qquad \text{(Internal Energy)}$$

or

$$(2.12) \qquad \rho \frac{Dh}{Dt_f} - \frac{Dp}{Dt_f} + \nabla \cdot \underset{\sim}{q} + \underset{\approx}{\tau} : \nabla \underset{\sim}{v} = 0 \qquad \text{(Enthalpy)}$$

We now have three equations in six unknowns. It is tempting to introduce constitutive relationships at this point to reduce the indeterminancy of this system of equations. This is permitted provided one keeps in mind that once this is done, it precludes the possibility of introducing a macroscopic constitutive relationship at a later point in the development.

3.0 POROUS MEDIUM EQUATIONS

The purpose of this section is to illustrate a methodology for formulating the mass, energy, and momentum balance equations for a geothermal reservoir. The energy equation is selected as an example. This section can be skipped by the casual reader without loss of continuity in the discussion.

3.1 Averaging

We now face the task of formally integrating the balance equations over the porous medium to obtain a series of macroscopic rather than microscopic equations. Our objective requires that we define a smoothly varying functional relationship for each dependent variable such that the behavior of the system can be described using partial-differential equations. The procedure involves the definition of a volume of porous medium which is sufficiently large that microscopic effects can be averaged in a meaningful way, yet not so large that large scale heterogeneities become significant. In figure 1, we illustrate the nature of such a volume and denote it as a representative elementary volume (REV) (Bear, 1972). We assume that a property ψ_α (α = s,w,R) can be represented in a statistically meaningful way as the average defined as

$$(3.1) \qquad \langle\psi\rangle_\alpha \equiv \frac{1}{dV} \int_V \psi_\alpha \, dV$$

where ψ_α is non-zero only in the α phase. One can alternatively write

$$(3.2) \qquad \langle\psi\rangle_\alpha \equiv \frac{1}{dV} \int_V \psi\gamma_\alpha dV$$

where γ_α is defined for phase α as (Gray and Lee, 1977)

$$(3.3) \qquad \gamma_\alpha = \gamma_\alpha(\underset{\sim}{r},t) = \begin{cases} 1 & \underset{\sim}{r} \epsilon V_\alpha \\ 0 & \underset{\sim}{r} \epsilon V_\beta \end{cases} \qquad \text{for all } t$$

$$\alpha,\beta = s,w,R$$

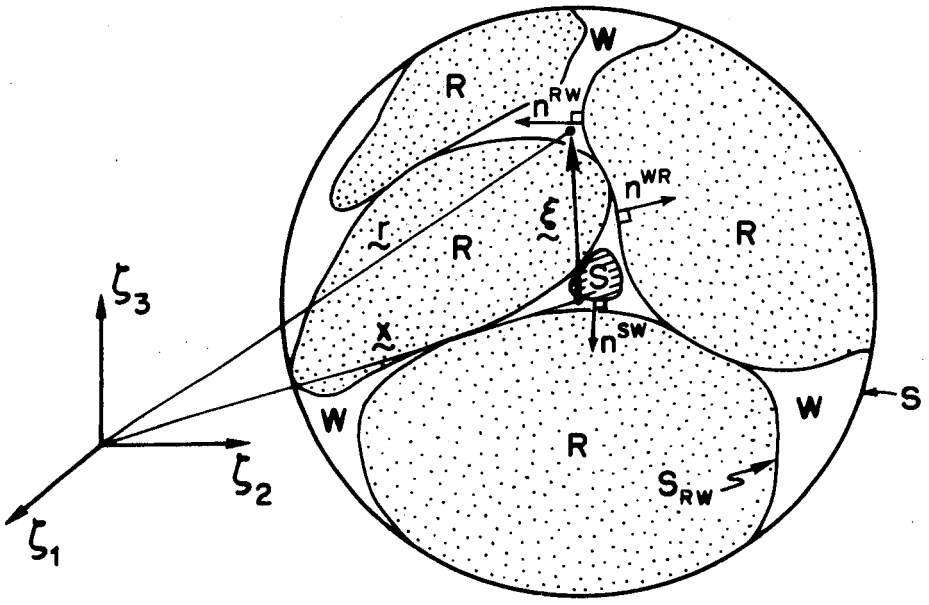

XBL 795-9559

Figure 1: Representative elementary volume (REV) containing steam (s), water (w) and rock (R) ($V_w + V_s + V_R = V$).

and ψ is defined simply as a property. Using γ_α one can formally define that part of $d\forall$ occupied by the α phase, $(d\forall_\alpha)$, as

$$(3.4) \qquad d\forall_\alpha = d\forall_\alpha(\underset{\sim}{x},t) = \int_{d\forall} \gamma_\alpha(\underset{\sim}{x} + \xi, t)dv_\xi$$

where dv_ξ is the microscopic element of volume. Thus, it becomes apparent that integration is being carried out over the microscopic local coordinate system $\underset{\sim}{\xi}$. This formulation leads naturally to the definition of the macroscopic element of area along dA

$$(3.5) \qquad dA_{\alpha\alpha} = dA_{\alpha\alpha}(\underset{\sim}{x},t) = \int_{dA} \gamma_\alpha(x+\xi,t)da_\xi$$

where da_ξ is the microscopic element of area. Note that dA_α is made up of two parts:

1) the part that makes up the boundary of dA, i.e. $dA_{\alpha\alpha}$

2) the part wholly within $d\forall$, i.e., it forms the interface of the α-phase with all other phases i.e.

$$\sum_{\beta\neq\alpha} dA_{\alpha\beta}$$

thus

$$(3.6) \qquad dA_\alpha = dA_{\alpha\alpha} + \sum_{\beta\neq\alpha} dA_{\alpha\beta}$$

It is critical to an understanding of the volume averaging approach to realize that the macroscopic variables will represent smooth functions. That is, in the absence of macroscopic shocks, there will be no discontinuities in these functions.

This conceptual model of a meaningful average is the one employed in all geothermal formulations published to date. There is, however, an important question that can be raised regarding the adequacy of this approach. The property ψ may be either intensive (e.g. density) or extensive (e.g. mass). In many instances the volume average of an intensive variable is of questionable validity, i.e.

$$\langle E \rangle_\alpha = \frac{1}{dV} \int_{dV} E \gamma_\alpha dv_\xi$$

This type of average appears, for example, in Assens (1977) and Faust and Mercer (1977). The averaging operator can be modified to circumvent this difficulty as suggested by Hassanizadeh and Gray (1979)

$$\overline{\psi}^\alpha = \frac{1}{\langle \rho \rangle_\alpha dV} \int_{dV} \rho E \gamma_\alpha dv_\xi \tag{3.7}$$

The use of this average provides a meaningful quantity because the integrand is now an extensive property. Moreover, it considerably reduces the complexity of surface integral terms which arise in the formal integration process. Similar mass-average surface-average operators may also be defined.

3.2 Averaging Theorems

While the various definitions of an average form the crux of the formal averaging procedures, there are several additional concepts that require consideration. We present these in the form of a series of theorems but omit the proofs. (for details see Gray and Lee, 1977)

Theorem 1: The integral of the time derivative of a function over dV_α is related to the derivative of the integral as

$$(3.8)\qquad \int_V \int_{dV} \frac{\partial \psi}{\partial t}\, \gamma_\alpha dv = \int_V \frac{\partial}{\partial t} \int_{dV} \psi \gamma_\alpha dv - \int_V \sum_{\beta \neq \alpha} \int_{dA_{\alpha\beta}} \psi \underset{\sim}{w} \cdot \underset{\sim}{n}^{\alpha\beta} da$$

where $\underset{\sim}{w}$ is the velocity of the $\alpha\beta$ interface, V is the volume of the entire domain, and we omit the subscript ξ on the local variables.

Theorem 2: The integral of the space derivative of a function over dV_α is related to the derivative of the integral as

$$(3.9)\qquad \int_V \int_{dV} (\underset{\sim}{\nabla}\psi)\gamma_\alpha dv = \int_V \underset{\sim}{\nabla} \int_{dV} (\psi \gamma_\alpha) dv + \int_V \sum_{\beta \neq \alpha} \int_{dA_{\alpha\beta}} \psi \underset{\sim}{n}^{\alpha\beta} da$$

Divergence Theorem for Discontinuous Media (Eringen and Suhubi, 1964).

$$\int_V \nabla \int_{dV} \Psi dv = \int_V \int_{dV} \underset{\sim}{\nabla} \Psi dv = \int_A \int_{dA} \Psi \underset{\sim}{n} da$$

Substitution of the divergence theorem into (3.9) yields (letting $\Psi \equiv \psi\gamma_\alpha$)

$$(3.10)\qquad \int_V \int_{dV} (\nabla\psi)\gamma_\alpha dv = \int_A \int_{dA} \psi\gamma_\alpha \underset{\sim}{n} da + \int_V \sum_{\beta\neq\alpha} \int_{dA_{\alpha\beta}} \psi \underset{\sim}{n}^{\alpha\beta} da$$

3.3 Perturbation Quantities

During the formal integration from microscopic to macroscopic one will encounter several non-linear terms (e.g., $\rho\underset{\sim}{v}\cdot\nabla\underset{\sim}{v}$ in the momentum equation (2.4)). There will be considerably fewer of these if mass averaging, i.e., (3.7), is used in lieu of (3.2), for selected variables. To accommodate non-linearities we expand ψ as follows (assuming mass averaging)

$$(3.11)\qquad \psi(\underset{\sim}{x}+\underset{\sim}{\xi},t) = \overline{\psi}^\alpha(\underset{\sim}{x},t) + \overline{\psi}^\alpha(\underset{\sim}{x}+\underset{\sim}{\xi},t)$$

The following identities are useful in simplifying complex integral relationships:

$$(3.12)\qquad 1)\ \overline{\overline{\psi}^\alpha}^\alpha = \frac{1}{\langle\rho\rangle_\alpha dV}\int_{dV} \rho(\psi - \overline{\psi}^\alpha)\gamma_\alpha dv = \overline{\psi}^\alpha - \overline{\psi}^\alpha = 0$$

$$(3.13)\qquad 2)\ \overline{\underset{\sim}{\psi}\overline{\phi}^\alpha}^\alpha = \overline{\gamma^\alpha}^\alpha \overline{\phi}^\alpha = 0 \qquad \text{(by equation 3.12)}$$

$$(3.14)\qquad 3)\ \overline{\psi\phi}^\alpha = \overline{(\overline{\psi}^\alpha + \gamma^\alpha)(\overline{\phi}^\alpha + \gamma^\alpha)}^\alpha = \overline{\psi}^\alpha\overline{\phi}^\alpha + \overline{\gamma^\alpha\gamma^\alpha}^\alpha$$

$$(3.15)\qquad 4)\ \overline{\rho\gamma^\alpha}^\alpha = \frac{1}{dA}\int_{dA} \rho\gamma^\alpha \underset{\sim}{n}\gamma_\alpha da = \frac{1}{dA}\int_{dV} \underset{\sim}{\nabla}(\rho\gamma^\alpha\gamma_\alpha)dv = \frac{\nabla}{dA}(\overline{\gamma}^\alpha\langle\rho\rangle_\alpha dv) = 0$$

(3.16) 5) $\overbrace{\rho\hat{\psi}^{\gamma\alpha}\,\overline{\phi}^{\alpha}}^{\alpha} = \overbrace{\rho\hat{\psi}^{\gamma\alpha}}\,\overline{\phi}^{\alpha} = 0$

3.4 Example Problem

Given the tools presented in the preceding sections (3.1 - 3.3) the next step is to apply these to equations (2.1), (2.4), (2.10) or (2.12). The simplest case is the mass transport equation (2.1). We will, therefore, consider this equation as an example. Rewriting (2.1) multiplying by γ_α and integrating over the porous medium we obtain

$$(3.17) \qquad \int_{V}\int_{dV}\left(\frac{\partial\rho}{\partial t} + \underset{\sim}{\nabla}\cdot(\rho\underset{\sim}{v})\right)\gamma_\alpha dv = 0$$

Let us consider the first term

$$(3.18) \qquad I_1 = \int_{V}\int_{dV}\frac{\partial\rho}{\partial t}\,\gamma_\alpha dv$$

Application of theorem 1 yields

$$(3.19) \qquad \int_{V}\int_{dV}\frac{\partial\rho}{\partial t}\,\gamma_\alpha dv = \int_{V}\frac{\partial}{\partial t}\int_{dV}\rho\gamma_\alpha dv - \int_{V}\sum_{\beta\neq\alpha}\int_{dA_{\alpha\beta}}\rho\underset{\sim}{w}\cdot\underset{\sim}{n}^{\alpha\beta}da$$

The second term in (3.17) can be rewritten using (3.9) as

$$(3.20)\qquad \int_{V}\int_{dV}\left(\underset{\sim}{\nabla}\cdot(\rho\underset{\sim}{v})\right)\gamma_\alpha dv = \int_{V}\underset{\sim}{\nabla}\cdot\int_{dV}(\rho\underset{\sim}{v})\gamma_\alpha dv + \int_{V}\sum_{\beta\neq\alpha}\int_{dA_{\alpha\beta}}(\rho\underset{\sim}{v})\cdot\underset{\sim}{n}^{\alpha\beta}da$$

Combination of (3.19) and (3.20) yields

$$(3.21)\qquad \int_{V}\left[\frac{\partial}{\partial t}\int_{dV}\rho\gamma_\alpha dv + \underset{\sim}{\nabla}\int_{dV}\cdot\,(\rho\underset{\sim}{v})\gamma_\alpha dv + \sum_{\beta\neq\alpha}\int_{dA_{\alpha\beta}}\rho(\underset{\sim}{v}-\underset{\sim}{w})\cdot\underset{\sim}{n}^{\alpha\beta}da\right] = 0$$

We can now use either volume or mass averaging i.e., (3.2) or (3.7). Mass averaging is the most straight-forward and yields directly

$$(3.22)\qquad \int_{V}\left[\frac{\partial}{\partial t}\langle\rho\rangle_\alpha + \underset{\sim}{\nabla}\cdot(\langle\rho\rangle_\alpha\underset{\sim}{\bar{v}}) + \sum_{\beta\neq\alpha}\frac{1}{dV}\int_{dA_{\alpha\beta}}\rho(\underset{\sim}{v}-\underset{\sim}{w})\cdot\underset{\sim}{n}^{\alpha\beta}da\right]dv = 0$$

Assuming certain smoothness conditions, this equation can be written as the point equation

$$(3.23)\qquad \frac{\partial}{\partial t}\langle\rho\rangle_\alpha + \underset{\sim}{\nabla}\cdot(\langle\rho\rangle_\alpha\underset{\sim}{\bar{v}}) + \sum_{\beta\neq\alpha}\frac{1}{dV}\int_{dA_{\alpha\beta}}\rho(\underset{\sim}{v}-\underset{\sim}{w})\cdot\underset{\sim}{n}^{\alpha\beta}da$$

Let us now develop the macroscopic equation using the volume average. The first task is to expand the product $\rho\underset{\sim}{v}$

$$(3.24)\qquad \rho\underset{\sim}{v} = (\langle\rho\rangle^\alpha + \tilde{\rho}^\alpha)(\langle\underset{\sim}{v}\rangle^\alpha + \tilde{\underset{\sim}{v}}^\alpha)$$

where $\langle\rho\rangle^{\alpha} = \dfrac{\langle\rho\rangle_{\alpha}}{\varepsilon_{\alpha}}$ and is called the intrinsic phase average density and $\varepsilon_{\alpha} = \dfrac{\mathcal{V}_{\alpha}}{\mathcal{V}}$.

Expansion of (3.24) yields

$$\rho\underset{\sim}{v} = \langle\rho\rangle^{\alpha}\langle\underset{\sim}{v}\rangle^{\alpha} + \tilde{\rho}^{\alpha}\langle\underset{\sim}{v}\rangle^{\alpha} + \tilde{\underset{\sim}{v}}^{\alpha}\langle\rho\rangle^{\alpha} + \tilde{\rho}^{\alpha}\tilde{\underset{\sim}{v}}^{\alpha} \tag{3.25}$$

Because we require $\langle\rho\underset{\sim}{v}\rangle$ in (3.21) we average (3.25) to yield

$$\langle\rho\underset{\sim}{v}\rangle_{\alpha} = \langle\langle\rho\rangle^{\alpha}\langle\underset{\sim}{v}\rangle^{\alpha}\rangle_{\alpha} + \langle\rho\,\tilde{\underset{\sim}{v}}^{\alpha}\tilde{}\rangle_{\alpha} = \varepsilon_{\alpha}\langle\rho\rangle^{\alpha}\langle\underset{\sim}{v}\rangle^{\alpha} + \langle\tilde{\rho}^{\alpha}\tilde{\underset{\sim}{v}}^{\alpha}\rangle_{\alpha} \tag{3.26}$$

The second term in (3.17) now becomes

$$\int_{\mathcal{V}}\int_{d\mathcal{V}} \left(\nabla\cdot(\rho\underset{\sim}{v})\right)\gamma_{\alpha}\,dv = \int_{\mathcal{V}}\int_{d\mathcal{V}} \left(\nabla\cdot\varepsilon_{\alpha}\langle\rho\rangle^{\alpha}\langle\underset{\sim}{v}\rangle^{\alpha}\right)\gamma_{\alpha}\,dv + \int_{\mathcal{V}}\int_{d\mathcal{V}} \left(\nabla\cdot(\langle\tilde{\rho}^{\alpha}\tilde{\underset{\sim}{v}}^{\alpha}\rangle_{\alpha})\right)\gamma_{\alpha}\,dv \tag{3.27}$$

Application of the averaging relationships yields

$$\int_{\mathcal{V}}\int_{d\mathcal{V}} \left(\nabla\cdot(\rho\underset{\sim}{v})\right)\gamma_{\alpha}\,dv = \int_{\mathcal{V}} \nabla\cdot \int_{d\mathcal{V}} (\varepsilon_{\alpha}\langle\rho\rangle^{\alpha}\langle\underset{\sim}{v}\rangle^{\alpha})\gamma_{\alpha}\,dv \tag{3.28}$$

$$+ \int_{\mathcal{V}} \nabla\cdot \int_{d\mathcal{V}} (\langle\tilde{\rho}^{\alpha}\tilde{\underset{\sim}{v}}^{\alpha}\rangle_{\alpha})\gamma_{\alpha}\,dv + \int_{\mathcal{V}} \sum_{\beta\neq\alpha} \int_{dA_{\alpha\beta}} (\rho\underset{\sim}{v})\cdot\underset{\sim}{n}^{\alpha\beta}\,da$$

Substituting (3.28), (3.19) and (2.2) in (3.17), we obtain

$$(3.29)\qquad \int_V \frac{\partial}{\partial t}\langle\rho\rangle_\alpha + \nabla\cdot(\langle\rho\rangle^\alpha\langle\underset{\sim}{v}\rangle) + \sum_{\beta\neq\alpha}\frac{1}{dV}\int_{dA_{\alpha\beta}}\rho(\underset{\sim}{v}-\underset{\sim}{w})\cdot\underset{\sim}{n}^{\alpha\beta}\,da$$

$$+\int_V \nabla\cdot\langle\rho^\alpha\underset{\sim}{\tilde{v}}^\alpha\underset{\sim}{\tilde{v}}^\alpha\rangle_\alpha\,dV = 0$$

The appropriate point equation becomes

$$(3.30)\qquad \frac{\partial}{\partial t}\langle\rho\rangle_\alpha + \nabla\cdot(\langle\rho\rangle^\alpha\langle\underset{\sim}{v}\rangle) + \sum_{\beta\neq\alpha}\frac{1}{dV}\int_{dA_{\alpha\beta}}\rho(\underset{\sim}{v}-\underset{\sim}{w})\cdot\underset{\sim}{n}^{\alpha\beta}\,da$$

$$+\nabla\cdot\langle\rho^\alpha\underset{\sim}{\tilde{v}}^\alpha\underset{\sim}{\tilde{v}}^\alpha\rangle_\alpha = 0$$

The surface integral describes mass movement across the interface as encountered, for example, in the change of phase from water to steam. Examination of (3.23), obtained using the mass average, and (3.30) obtained using the volume average, reveals an additional perturbation term $\nabla\cdot\langle\rho^\alpha\underset{\sim}{\tilde{v}}^\alpha\underset{\sim}{\tilde{v}}^\alpha\rangle$ arises in the volume average approach. Assens (1976) indicates that this accounts for dispersion. In a homogeneous fluid we would not expect such a term to be significant.

The macroscopic balance equations for momentum and energy are, of course, considerably more complicated. We can write a general macroscopic conservation equation (Gray and Hassanizadeh, 1978).

$$(3.31)\qquad \frac{\partial}{\partial t}\left(\langle\rho\rangle_\alpha \bar{\psi}^\alpha\right) + \nabla\cdot\left(\langle\rho\rangle_\alpha \bar{\underset{\sim}{v}}^\alpha \bar{\psi}^\alpha\right) - \nabla\cdot\bar{\underset{\sim}{i}}^\alpha - \langle\rho\rangle_\alpha \bar{f}^\alpha - \langle\rho\rangle_\alpha e^\alpha - \langle\rho\rangle_\alpha \hat{I}^\alpha$$

$$- \langle\rho\rangle_\alpha \bar{G}^\alpha = 0$$

where $$\hat{I}^\alpha = \frac{1}{\langle\rho\rangle_\alpha dV} \sum_{\beta\neq\alpha} \int_{dA_{\alpha\beta}} \underset{\sim}{n}^{\alpha\beta}\cdot\underset{\sim}{i}\, da\ ,$$

$\underset{\sim}{i}$ is a surface flux vector,

$$\bar{i}^\alpha = \frac{1}{dA}\int_{dA} [\underset{\sim}{i} - \rho\tilde{\psi}^\alpha \tilde{\underset{\sim}{v}}^\alpha]\cdot\underset{\sim}{n}_\alpha da\ ,$$

$$\bar{\underset{\sim}{i}}\cdot\underset{\sim}{N} = \bar{i}_N$$

f is an external supply

$$e^\alpha = \frac{1}{\langle\rho\rangle_\alpha dV} \sum_{\beta\neq\alpha} \int_{dA} \rho\psi(\underset{\sim}{w}-\underset{\sim}{v})\cdot\underset{\sim}{n}^{\alpha\beta} da,\ \text{and}$$

G is a net production.

The appropriate macroscopic balance equation is readily obtained using (3.31) and table 1. One can readily verify the form of the mass balance equation through substitution of row 1 in table 1 into (3.31).

Quantity	ψ	$\underset{\sim}{i}$	f	G
Mass	1	$\underset{\sim}{0}$	0	0
Linear Momentum	$\underset{\sim}{v}$	$\underset{\approx}{\tau}$	$\underset{\sim}{g}$	0
Angular Momentum	$\underset{\sim}{r}\times\underset{\sim}{v}$	$\underset{\sim}{r}\times\underset{\approx}{\tau}$	$\underset{\sim}{r}\times\underset{\sim}{g}$	0
Energy	$U + \frac{1}{2}v^2$	$\underset{\approx}{\tau}\cdot\underset{\sim}{v} + \underset{\sim}{q}$	$\underset{\sim}{g}\cdot\underset{\sim}{v} + h$	0
Entropy	\$	$\underset{\sim}{\phi}$	b	Γ

Table 1: Properties for substitution into the general balance equation (3.31) where $\underset{\sim}{r}$ is the position vector, U is the internal energy density function, \$ is the internal entropy density function, $\underset{\approx}{\tau}$ is the stress tensor, $\underset{\sim}{q}$ is the heat flux vector, $\underset{\sim}{\phi}$ is the entropy flux vector, $\underset{\sim}{g}$ is the external supply of momentum (body force), h is the external supply of energy, b is the external supply of entropy, Γ is the total entropy production. (after Hassanazadeh and Gray, 1979)

While (3.31) provides an accurate representation of the physics of the system, it cannot be solved directly because of the presence of microscopic variables within the macroscopic equations, e.g. $\tilde{\psi}$, $\underset{\sim}{i}$ etc. Thus, it is necessary to introduce a series of constitutive relationships to make the system of equations tractable. The rigor dedicated to this step largely dictates the accuracy of the final set of governing equations. Formulations currently available in the literature (Assens, 1976; Faust and Mercer, 1977; Voss, 1978) have not attempted a rigorous formulation based, for example, on constitutive theory. Moreover, all attempts to date have employed volume rather than mass averaging. In the discussion of each model we will provide the governing equations used in each and the interested reader can deduce the approximations inherent in the reduction of (3.31).

3.5 Equation Reduction

As an illustration of the constitutive assumptions employed in formulating the final set of partial-differential equations, we will present the energy equation as developed by Voss (1978). To simplify notation, we will omit the averaging brackets: variables defined as microscopic will be denoted as $\tilde{(\cdot)}$. We will begin with the volume averaged equations which have been summed over each phase.

$$(3.32)\qquad \frac{\partial}{\partial t}\left[(1-\varepsilon)\rho_R r_R + \varepsilon(S_s\rho_s r_s + S_w\rho_w r_w)\right]$$

$$+ \underset{\sim}{\nabla}\cdot\left[(1-\varepsilon)\rho_R r_R \underset{\sim}{v}_R + \varepsilon(S_s\rho_s r_s \underset{\sim}{v}_s + S_w\rho_w r_w \underset{\sim}{v}_w)\right]$$

$$+ \underset{\sim}{\nabla}\cdot[(1-\varepsilon)q_R + \varepsilon(S_s\underset{\sim}{q}_s + S_w\underset{\sim}{q}_w)]$$

$$+ \underset{\sim}{\nabla}\cdot[(1-\varepsilon)(\underset{\approx}{\tau}_R\cdot\underset{\sim}{v}_R) + \varepsilon(S_s\underset{\approx}{\tau}_s\cdot\underset{\sim}{v}_s + S_w\underset{\approx}{\tau}_w\cdot\underset{\sim}{v}_w)]$$

$$- \frac{\partial}{\partial t}[(1-\varepsilon)p_R + \varepsilon(S_s p_s + S_w p_w)] - [(1-\varepsilon)\rho_R\underset{\sim}{v}_R + \varepsilon(S_s\rho_s\underset{\sim}{v}_s + S_w\rho_w\underset{\sim}{v}_w)]\cdot\underset{\sim}{g}$$

$$+ \frac{1}{d\forall}\int_{A_R(t)}\tilde{\underset{\sim}{q}}_R\cdot\underset{\sim}{n}^R da + \frac{1}{d\forall}\int_{A_s(t)}\tilde{\underset{\sim}{q}}_s\cdot\underset{\sim}{n}^s da + \frac{1}{d\forall}\int_{A_w(t)}\tilde{\underset{\sim}{q}}_w\cdot\underset{\sim}{n}^w da$$

$$+ \frac{1}{d\forall}\int_{A_R(t)}(\tilde{\underset{\approx}{\tau}}_R\cdot\tilde{\underset{\sim}{v}}_R)\cdot\underset{\sim}{n}^R da + \frac{1}{d\forall}\int_{A_s(t)}(\tilde{\underset{\approx}{\tau}}_s\cdot\tilde{\underset{\sim}{v}}_s)\cdot\underset{\sim}{n}^s da + \frac{1}{d\forall}\int_{A_w(t)}(\tilde{\underset{\approx}{\tau}}_w\cdot\tilde{\underset{\sim}{v}}_w)\,\underset{\sim}{n}^w da$$

$$+ \frac{1}{d\forall}\int_{A_R(t)}\tilde{p}_R(\tilde{\underset{\sim}{w}}_R\cdot\underset{\sim}{n}^R)da + \frac{1}{d\forall}\int_{A_s(t)}\tilde{p}_s(\tilde{\underset{\sim}{w}}_s\cdot\underset{\sim}{n}^s)da + \frac{1}{d\forall}\int_{A_w(t)}\tilde{p}_w(\tilde{\underset{\sim}{w}}_w\cdot\underset{\sim}{n}^w)da$$

$$+ \frac{1}{d\forall}\int_{A_R(t)}\tilde{\rho}_R\tilde{r}_R(\tilde{\underset{\sim}{v}}_R-\tilde{\underset{\sim}{w}}_R)\cdot\underset{\sim}{n}^R da + \frac{1}{d\forall}\int_{A_s(t)}\tilde{\rho}_s\tilde{r}_s(\tilde{\underset{\sim}{v}}_s-\tilde{\underset{\sim}{w}}_s)\cdot\underset{\sim}{n}^s da$$

$$+ \frac{1}{d\forall}\int_{A_w(t)}\tilde{\rho}_w\tilde{r}_w(\tilde{\underset{\sim}{v}}_w-\tilde{\underset{\sim}{w}}_w)\cdot\underset{\sim}{n}^w da = 0$$

In (3.32) $(1-\varepsilon)$ is the volumetric fraction of solid matrix and ε is the local porosity; (εS_s) and (εS_w) are the volumetric fractions of steam and water respectively where S_s and S_w are the local saturations of steam and water, $S_s + S_w = 1$; the quantity r_α is the sum of kinetic energy and enthalpy, $r_\alpha = h_\alpha + 1/2\ v_\alpha^2$.

Voss (1978) now assumes that the solid matrix is mechanically non-reactive and rigid such that $\varepsilon \neq \varepsilon(t)$, $r_R = h_R$, $\underset{\sim}{v}_R = \tilde{\underset{\sim}{v}}_R = \tilde{\underset{\sim}{w}}_R = 0$, $\rho_R \neq \rho_R(t)$ and the pressure in the matrix p_R is independent of time and space. These are reasonable assumptions in describing the reservoir hydrodynamics. These assumptions reduce (3.32) to the form

$$
\begin{aligned}
(3.33)\quad & (1-\varepsilon)\rho_R \frac{\partial h_R}{\partial t} + \varepsilon \frac{\partial}{\partial t}(S_s\rho_s r_s + S_w\rho_w r_w) + \underset{\sim}{\nabla}\cdot[\varepsilon(S_s\rho_s r_s \underset{\sim}{v}_s \\
& \quad (1) \qquad\qquad (2) \qquad\qquad (3) \\
& + S_w\rho_w r_w \underset{\sim}{v}_w)] + \underset{\sim}{\nabla}\cdot[(1-\varepsilon)\underset{\sim}{q}_R + \varepsilon(S_s\underset{\sim}{q}_s + S_w\underset{\sim}{q}_w)] \\
& \qquad\qquad\qquad\qquad (4) \\
& + \underset{\sim}{\nabla}\cdot[\varepsilon(S_s\underset{\approx}{\tau}_s\cdot\underset{\sim}{v}_s + S_w\underset{\approx}{\tau}_w\cdot\underset{\sim}{v}_w)] - \varepsilon\frac{\partial}{\partial t}(S_s p_s + S_w p_w) \\
& \qquad\qquad (5) \qquad\qquad\qquad\qquad (6) \\
& - \varepsilon(S_s\rho_s\underset{\sim}{v}_s + S_w\rho_w\underset{\sim}{v}_w)\cdot\underset{\sim}{g} + \frac{1}{d\forall}\int_{A_R(t)} (\tilde{\underset{\sim}{q}}_R\cdot\underset{\sim}{n}^R)da \\
& \qquad (7) \qquad\qquad\qquad\qquad (8) \\
& + \frac{1}{d\forall}\int_{A_s(t)} (\tilde{\underset{\sim}{q}}_s\cdot\underset{\sim}{n}^s)da + \frac{1}{d\forall}\int_{A_w(t)} (\tilde{\underset{\sim}{q}}_w\cdot\underset{\sim}{n}^w)da \\
& \qquad (9) \qquad\qquad\qquad\qquad (10) \\
& + \frac{1}{d\forall}\int_{A_s(t)} (\tilde{\underset{\approx}{\tau}}_s\cdot\tilde{\underset{\sim}{v}}_s)\cdot\underset{\sim}{n}^s da + \frac{1}{d\forall}\int_{A_w(t)} (\tilde{\underset{\approx}{\tau}}_w\cdot\tilde{\underset{\sim}{v}}_w)\cdot\underset{\sim}{n}^w da \\
& \qquad\qquad (11) \qquad\qquad\qquad\qquad (12) \\
& + \frac{1}{d\forall}\int_{A_s(t)} \tilde{p}_s(\tilde{\underset{\sim}{w}}_s\cdot\underset{\sim}{n}^s)da + \frac{1}{d\forall}\int_{A_w(t)} \tilde{p}_w(\tilde{\underset{\sim}{w}}_w\cdot\underset{\sim}{n}^w)da \\
& \qquad\qquad (13) \qquad\qquad\qquad\qquad (14) \\
& + \frac{1}{d\forall}\int_{A_s(t)} \tilde{\rho}_s\tilde{r}_s(\tilde{\underset{\sim}{v}}_s - \tilde{\underset{\sim}{w}}_s)\cdot\underset{\sim}{n}^s da + \frac{1}{d\forall}\int_{A_w(t)} \tilde{\rho}_w\tilde{r}_w(\tilde{\underset{\sim}{v}}_w - \tilde{\underset{\sim}{w}}_w)\cdot\underset{\sim}{n}^w da = 0 \\
& \qquad\qquad (15) \qquad\qquad\qquad\qquad (16)
\end{aligned}
$$

To further simplify (3.33) several assumptions are introduced which are common to many geothermal models:

(3.34) $\rho = S_s\rho_s + S_w\rho_w$ where ρ is the local average density of the fluid,

(3.35) $\rho\psi = S_s\rho_s\psi_s + S_w\rho_w\psi_w$ where ψ is an intensive property, e.g. r, $1/2\ v^2$, h and

(3.36) $\underset{\sim}{v} = \frac{1}{\rho}(S_s\rho_s\underset{\sim}{v}_s + S_w\rho_w\underset{\sim}{v}_w)$ where $\underset{\sim}{v}$ is the mass-average velocity.

Employing (3.34) and (3.35) the second and third terms in (3.33) become

(3.37) $$\varepsilon \frac{\partial}{\partial t}(S_s\rho_s r_s + S_w\rho_w r_w) = \varepsilon \frac{\partial}{\partial t}(\rho r),$$

(3.38) $$\underset{\sim}{\nabla}\cdot[\varepsilon(S_s\rho_s r_s\underset{\sim}{v}_s + S_w\rho_w r_w\underset{\sim}{v}_w)]$$

$$= \underset{\sim}{\nabla}\cdot(\varepsilon\rho r\underset{\sim}{v}) + \underset{\sim}{\nabla}\cdot[(\frac{\varepsilon}{\rho})\rho_s\rho_w S_s S_w(r_s-r_w)(\underset{\sim}{v}_s-\underset{\sim}{v}_w)]$$

where we have used the identity (Voss, 1978)

(3.39) $$S_s\rho_s r_s\underset{\sim}{v}_s + S_w\rho_w r_w\underset{\sim}{v}_w = \rho r\underset{\sim}{v} + (\frac{1}{\rho})\rho_s\rho_w S_s S_w(r_w-r_s)(\underset{\sim}{v}_w-\underset{\sim}{v}_s)$$

While the surface integration expressed in (3.33) is over all interfaces, i.e., s, w, R, all the fluid and interface velocities are zero on fluid-rock interfaces. The surface integrals now become

(3.40) $$I_2 = \int_{A_{ws}(t)} [\tilde{\rho}_w \tilde{r}_w (\tilde{\underset{\sim}{v}}_w - \underset{\sim}{w}) - \tilde{\rho}_s \tilde{r}_s (\tilde{\underset{\sim}{v}}_s - \underset{\sim}{w}) + (\tilde{p}_w - \tilde{p}_s)\underset{\sim}{w}$$

$$+ (\tilde{\underset{\sim}{\tau}}_w \cdot \tilde{\underset{\sim}{v}}_w - \tilde{\underset{\sim}{\tau}}_s \cdot \tilde{\underset{\sim}{v}}_s)] \cdot \underset{\sim}{n}^{ws} da$$

$$+ \int_{A_{ws}} (\tilde{\underset{\sim}{q}}_w - \tilde{\underset{\sim}{q}}_s) \cdot \underset{\sim}{n}^{ws} da + \int_{A_{Rw}} (\tilde{\underset{\sim}{q}}_R - \tilde{\underset{\sim}{q}}_w) \cdot \underset{\sim}{n}^{Rw} da + \int_{A_{sR}} (\tilde{\underset{\sim}{q}}_s - \tilde{\underset{\sim}{q}}_R) \cdot \underset{\sim}{n}^{sR} da$$

According to the jump energy balance the sum of these integrals must be zero, i.e., $I_2 = 0$. The macroscopic energy flux $\underset{\sim}{q}_\alpha$ can be defined

(3.41) $$\underset{\sim}{q}_\alpha = -\kappa_\alpha \underset{\sim}{\nabla} T_\alpha$$

where T_α is the temperature of the α phase and κ_α is the thermal conductivity of that phase (κ may be tensorial). Term 4 in equation (3.33) can now be written

(3.42) $$\underset{\sim}{\nabla} \cdot [(1-\varepsilon)\underset{\sim}{q}_R + \varepsilon(S_s \underset{\sim}{q}_s + S_w \underset{\sim}{q}_w)]$$

$$= - \underset{\sim}{\nabla} \cdot [(1-\varepsilon)\kappa_R \underset{\sim}{\nabla} T + \varepsilon(S_s \kappa_s + S_w \kappa_w)\underset{\sim}{\nabla} T]$$

$$= - \underset{\sim}{\nabla} \cdot (\kappa \underset{\sim}{\nabla} T)$$

where $T = T(\underset{\sim}{x},t)$ is the equilibrium temperature of the three constituents at any point in the system and κ is an average thermal conductivity defined as

$$\kappa \equiv (1-\varepsilon)\kappa_R + \varepsilon(S_s\kappa_s + S_w\kappa_w) \tag{3.43}$$

Consider now the viscous stress work contribution to the energy balance. Voss (1978) argues that, because the internal and kinetic energies have been considered together in this equation, the transfer of energy due to friction on the solid grains is implicitly accounted for. Thus, term 4 must represent only internal fluid interactions and may be neglected.

Term 6 in (3.33) can be written

$$-\varepsilon \frac{\partial}{\partial t}(S_s p_s + S_w p_w) = -\varepsilon \frac{\partial}{\partial t}(S_s p_c) - \varepsilon \frac{\partial}{\partial t} p_w \tag{3.44}$$

where p_c is the capillary pressure

$$p_c \equiv p_s - p_w \tag{3.45}$$

In general, the capillary pressure is neglected since, for steam-water systems relatively little is known concerning its existence or behaviour. This is, of course, an assumption subject to experimental verification.

Substitution of (3.37 - 3.45) into (3.33) yields the simplified energy equation

$$(1-\varepsilon)\rho_R \frac{\partial h_R}{\partial t} + \varepsilon \frac{\partial}{\partial t}(\rho r) + \underset{\sim}{\nabla}\cdot(\varepsilon \rho r \underset{\sim}{v}) \tag{3.46}$$

$$+ \nabla\cdot\left[\left(\frac{\varepsilon}{\rho}\right)S_s S_w \rho_s \rho_w (r_s - r_w)(\underset{\sim}{v}_s - \underset{\sim}{v}_w)\right] - \nabla\cdot(\kappa\nabla T)$$

$$- \varepsilon \frac{\partial p_w}{\partial t} - \varepsilon\rho(\underset{\sim}{v}\cdot\underset{\sim}{g}) = 0$$

where we have used (3.36) in modifying the gravity work term. An equivalent form of the energy equation can be determined from (3.46) by substitution of the mass conservation equation for the fluid

$$(3.47) \qquad (1-\varepsilon)\rho_R \frac{\partial h_R}{\partial t} + \varepsilon\rho \frac{\partial r}{\partial t} + \varepsilon\rho \underset{\sim}{v}\cdot\nabla r$$

$$+ \nabla\cdot\left[\left(\frac{\varepsilon}{\rho}\right)S_s S_w \rho_s \rho_w (r_s - r_w)(\underset{\sim}{v}_s - \underset{\sim}{v}_w)\right] - \nabla\cdot(\kappa\nabla T)$$

$$- \varepsilon \frac{\partial p_w}{\partial t} - \varepsilon\rho(\underset{\sim}{v}\cdot\underset{\sim}{g}) = 0$$

Finally, one can argue that the internal energy is much greater than the kinetic and consequently a reasonable approximation is

$$(3.48) \qquad r \simeq h$$

We also implicitly assume, however, that the derivatives of r and h are also approximately equal; this is not intuitively obvious. Substitution of (3.48) into (3.47) yields

$$(3.49) \qquad (1-\varepsilon)\rho_R \frac{\partial h_R}{\partial t} + \varepsilon\rho \frac{\partial h}{\partial t} + \varepsilon\rho \underset{\sim}{v}\cdot\nabla h$$

$$+ \underset{\sim}{\nabla}\cdot\left[\left(\frac{\varepsilon}{\rho}\right)S_s S_w \rho_s \rho_w (h_s - h_w)(\underset{\sim}{v}_s - \underset{\sim}{v}_w)\right] - \underset{\sim}{\nabla}\cdot(\kappa \underset{\sim}{\nabla} T)$$

$$- \varepsilon \frac{\partial p_w}{\partial t} - \varepsilon\rho(\underset{\sim}{v}\cdot\underset{\sim}{g}) = 0$$

The approximation (3.48) was tested by Voss (1978) and found to be satisfactory.

Equation (3.49) is now in a form amenable to solution. To solve (3.49) in conjunction with the mass and momentum conse equations, it is necessary to employ the thermodynamic relationships of the steam tables. This will be discussed in more detail in section 5 on the specific models.

3.6 Deformation Equations

While we focused attention in the previous section on the development of an energy relationship for the fluid, a similar development with different constitutive assumptions can be formulated for a solid. Employing the same averaging relationships presented above, Bear and Pinder (1978) have developed the system of equations describing porous media deformation in multiphase flow. They did not, however, treat the non-isothermal case which arises in geothermal simulation. The multiphase isothermal case was solved by Safai (1977) for a series of hypothetical subsidence problems. In the work by Bear and Pinder (1978), they demonstrated that under mild constraints the volume averaged equations reduce to those developed by Biot (1956) and Verruijt (1969). These equations, modified to accommodate non-elastic deformation and non-isothermal flow, appear to be suitable for simulating the geothermal system.

Brownell, et al (1975) have presented equations for a deformable geothermal reservoir. The macroscopic equations are presented directly (without the use of averaging). The rock grains are assumed to be a linear thermoelastic material. The authors argue that this is a reasonable assumption for the range of temperatures and pressures encountered in geothermal reservoirs. In addition to the grain deformation, a constitutive expression for porosity was required. While the functional form of this expression was not given, it was suggested that the porosity would, in general, depend upon mixture pressure p_m (i.e., $p_m = \varepsilon p + (1-\varepsilon)p_R$, fluid pressure p_f and deviatoric stress $\underset{\sim}{\tau}$.

In summary, the equations describing porous media deformation and fluid flow arise from the same balance equations, (2.1, 2.4, 2.10, 2.12). When these point equations are properly integrated over the porous medium, a coupled set of partial differential equations describing fluid flow and matrix deformation will arise. This system of equations becomes tractable upon introduction of appropriate constitutive assumptions. There is no apparent justification for decomposing the problem into separate flow and deformation components. In other words, the reservoir model must, in some way, account for deformation and the deformation model must account for the fluid flow and energy transport. Because the main purpose of this report is not subsidence, we will not present in detail the formulation of the governing equations.

4.0 FRACTURED MEDIUM EQUATIONS

4.1 Discrete Fracture Model

There are two schools of thought regarding the mathematical description of fractured geothermal reservoirs. One approach is to consider each fracture as a discrete entity defined by its size and orientation. Generally, a different set of governing equations will be assumed for the fracture than the adjacent porous medium. This approach was employed by Coats (1977) in his analysis of multiphase geothermal reservoirs. He employed a variable grid finite-difference network to simulate this system (see figure 2). In simulating the fracture flow he used sufficiently large permeabilities ($10\text{-}20 \times 10^{-8}$ cm^2) to render viscous forces negligible relative to gravitational forces. The corresponding matrix permeability was 10^{-11} cm^2 with a porosity of 0.2. A zero capillary pressure was used for the fractures and a linear relationship between $p_c = 0$ at $S_w = 1$ and $p_c = 10$ at $S_w = 0$ was used for the porous medium. The rock relative permeability was described by

$$k_{rw} = [(S_w - S_{wc})/(1 - S_{wc})]^{n_w} \tag{4.1}$$

$$k_{rs} = k_{rscw} [(S_s - S_{sc})/(1 - S_{wc} - S_{sc})]^{n_s} \tag{4.2}$$

where

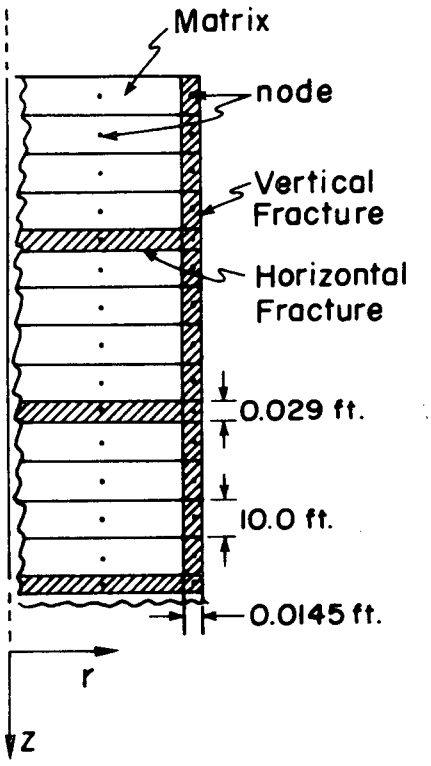

XBL 795-9558

Figure 2: Discrete fracture system modelled used finite differences (after Coats, 1977). The number of vertical blocks employed in the original experiment by Coats was 31.

S_{wc} is the irreducible water saturation = 0.2,

S_{sc} is the critical steam saturation = 0.0,

k_{rscw} is the relative permeability to steam at irreducible water saturation = 0.5,

$n_w = n_s = 2.0$.

The fracture relative permeability was given by

$$k_r = S_s$$

He observed that the numerical solution exhibited the following interesting features:

1) Due to the discontinuity in the capillary pressure between blocks and horizontal fractures, there was poor recovery of water from the matrix blocks.

2) The horizontal fractures rapidly approach 100% steam. The water draining vertically downward from the blocks into these fractures flows preferentially down into the top of the next lower matrix block rather than laterally into the vertical fracture.

3) In comparison with a standard porous-medium simulation of the system, the fractured porous medium transition zone is considerably lower than observed in the standard porous medium model when viewed either from the fractures or the intervening porous blocks.

Coats concludes:

> "Considering the basic difference in mechanisms for the conventional and more correct matrix-fissure calculations, we hold little hope for forcing accuracy from a conventional simulation".

The veracity of this conclusion rests, in large part, on the degree to which the proposed model represents the physical system. The experiment suggests,

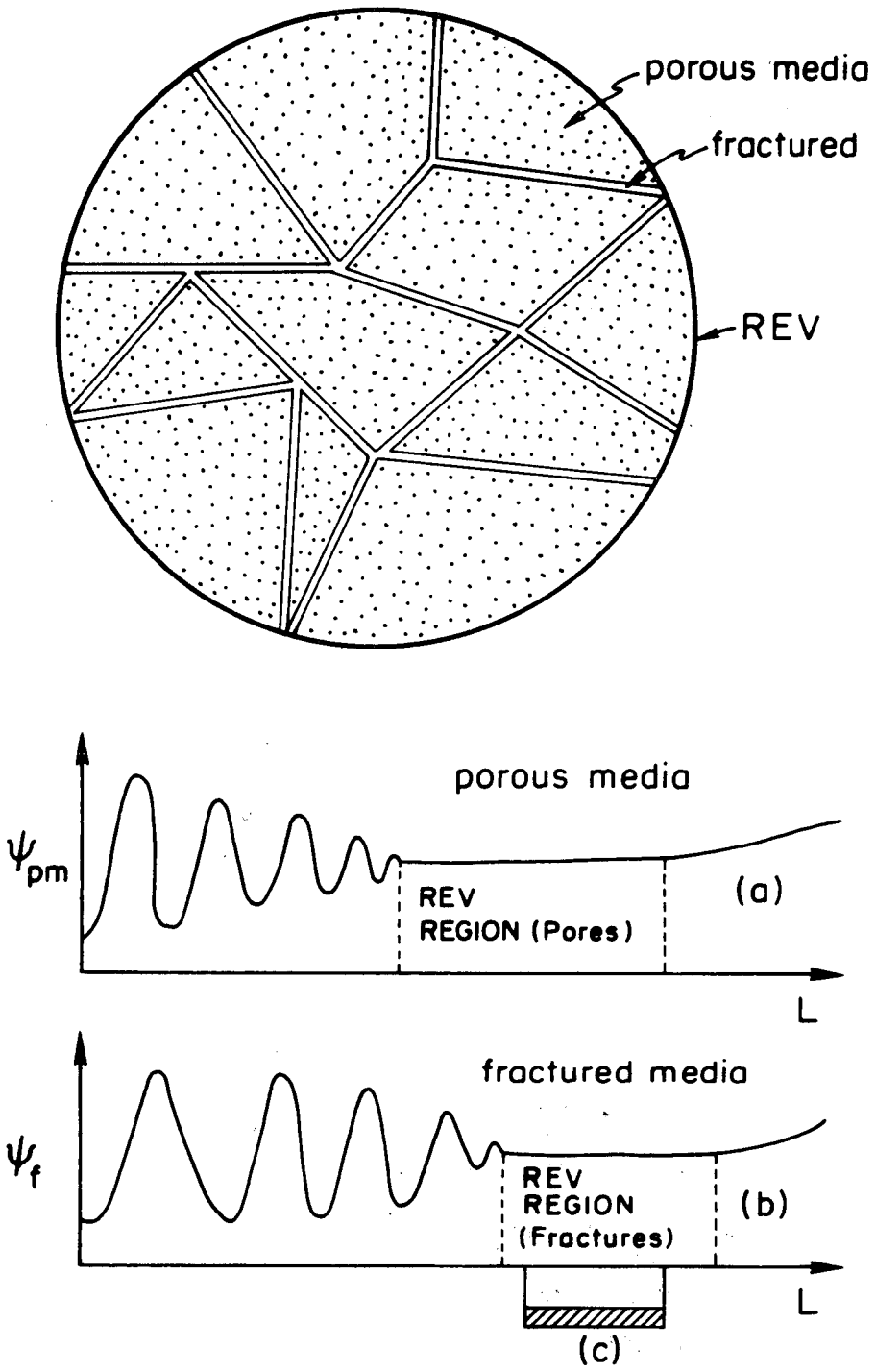

Figure 3: Conceptual model for overlapping continua, curve (a) is the plot of a property ψ measured for different volume (REV) L^3 of porous media; curve (b) is the plot of a property ψ measured for different volumes (REV) L^3 of fractured porous media. The region (c) is the common region where both the porous medium and fracture medium physics can be represented as though each were a continuum.

however, that a fractured porous medium may behave fundamentally different than its non-fractured counterpart.

4.2 Random Fracture Model

The principal difficulty associated with the discrete fracture model, whether formulated using finite difference or more flexible finite element schemes, is the inability to establish fracture geometry in the field. This is, of course, essential input into the discrete fracture model. There is, however, a second approach to the problem which is designed to circumvent this difficulty. The conceptual model is illustrated in figure 3. As in the porous medium case, we select a REV which manifests certain statistical properties. We assume the REV is sufficiently large that a porous media property ψ_{pm} is well behaved but not so large that the sample is affected by non-homogeneities (see figure 3). These are the same constraints introduced earlier for the porous medium equations. In the fracture flow model, however, we impose an additional constraint. We require that the REV be sufficiently large that a fracture property ψ_f is also well behaved in a statistical sense. The REV must also be sufficiently small that large scale non-homogeneities in the material do not significantly influence the mean parameter value. Thus, we must restrict our consideration to REVs which reside within the area of (c) of figure 3c. In other words, we are required to work at a level where overlapping porous and fracture continua are meaningful. Whether such a physical system is realizable in the field remains to be determined experimentally. Certainly such a system will exist if we relegate large scale discontinuities, faults for example, to a separate but coupled system analogous to that defined for the discrete-fracture system.

If we accept the existence of a system such as illustrated in figure 3b, the ground rules are established for the formal integration

of the point equations (2.1, 2.4, 2.10 and 2.12) over the fractured porous media. To date, the only energy transport formulation based on this type of approach is that of O'Neill (1977). He restricts his work, however, to single phase energy transport and does not address the more general multiphase system encountered in geothermal systems. If one assumes that two phases, α, are fracture water and pore water, the equation development is similar to that employed in formulating the porous media equations using volume averaging. Because of the lengthy development required to properly present this approach, we omit it in this report and refer the interested reader to the original work (O'Neill, 1977). Note that the field parameters arising out of this type of approach are volume averages and similar in concept to permeability in a porous medium formulation. The discrete fracture geometry no longer appears explicitly in the governing equations. Work is currently going on to extend O'Neill's work to the case of a steam-water system.

5.0 SUMMARY OF EXISTING MODELS

In this section we will present the salient features of existing geothermal models. Each model will be identified by the authors of the referenced publication(s). The summary will include the governing equations, a description of the numerical procedure used to solve these equations, an outline of problems considered and a brief discussion of advantages and disadvantages, strengths and weaknesses of each model. We will consider only distributed parameter multiphase models thereby excluding the zero dimensional models of Whiting and Ramey (1969) and Brigham and Morrow (1974) and

the single-phase models of Mercer and Pinder (1975), Lippmann et al. (1977), Riney et al. (1977), and Sorey (1975). The many analytical convective models are also beyond the scope of this report (e.g. Kassoy, 1976).

5.1 Model of Lasseter, Witherspoon and Lippmann

The model by Lasseter, Witherspoon and Lippmann was one of the first two phase geothermal models. It is described in the papers by Lasseter, Witherspoon and Lippmann (1975), Lasseter, T. J. (1975), and Assens (1976).

5.1.1 Governing Equations:

The governing equations were formulated by Lasseter et al (1975) using a macroscopic mass and internal energy balance. He obtains, for internal energy

$$(5.1) \qquad V_f \rho_f \frac{DU_f}{Dt_R} + m_R \frac{DU_R}{Dt_R} - \int_A (U_f - U_f^a)\rho_f^a \underset{\sim}{v}^a \cdot \underset{\sim}{n} da - \int_A \kappa^a \underset{\sim}{\nabla} T^a \cdot \underset{\sim}{n} da$$

$$- Q + U_f R V = 0$$

where $V_f = V_f(t)$ volume of fluid occupying the control volume V,

m_R is the mass of rock within V,

$U_f^a, \rho_f^a, \kappa^a$ and T^a are the fluid internal energy, fluid density, effective thermal conductivity of the fluid solid matrix, and matrix temperature evaluated along the surface A,

Q is the internal energy injection rate from sources within V, and

R is the mass injection rate per unit volume from sources within V.

It is, perhaps, worth noting that an internal energy balance is not a viable concept in an irreversible thermodynamic system. Only a total energy balance is meaningful. We also observe that during the development of (5.1) it is assumed that the variable U_f can be moved through the area integration. Because this variable is spatially dependent, it is not apparent how this procedure can be justified. At a later stage, it is possible to remove kinetic and potential energy employing the momentum equation and certain assumptions on the form of the potential energy function. Lasseter et al (1975) recognized the limitations of the formulation and suggested that a compressible work and viscous dissipation term should be added to the equations. They surmised, however, that these terms would be small. (this was, in part, demonstrated to be true by Garg and Pritchett, 1977)

Essentially, the same model was proposed by Assens (1976) although a volume averaging approach was employed to formulate the governing equations. His energy equations was reduced to a point equation for the solid and fluid combined

$$(5.2) \qquad \frac{\partial}{\partial t}(\varepsilon_R \rho_R U_R + \varepsilon_f \rho_f U_f) + \underset{\sim}{\nabla}\cdot(\varepsilon_f \rho_f \underset{\sim}{v}_f U_f) - \underset{\sim}{\nabla}\cdot\underset{\approx}{\kappa}\cdot\underset{\sim}{\nabla}T$$

$$+ p(\underset{\sim}{\nabla}\cdot[\varepsilon_w \underset{\sim}{v}_w + \varepsilon_s \underset{\sim}{v}_s]) - Q_R - Q_f = 0$$

Negligible viscous dissipation was also an assumption in this formulation.

The momentum conservation equation is given by Darcy's law summed for each fluid phase, i.e.,

$$(5.3) \qquad \rho_f \underset{\sim}{v}_f + (M_s\rho_s + M_w\rho_w)\underset{\sim}{\nabla} p_f - (M_s\rho_s^2 + M_w\rho_w^2)\underset{\sim}{g} = 0$$

where M_α is the mobility of the α phase and defined as

$$(5.4) \qquad M_\alpha = \frac{kk_{r\alpha}}{\mu_\alpha},$$

$k_{r\alpha}$ is the relative permeability of the α phase,

k is the permeability $[L^2]$, and

μ_α is the dynamic viscosity $[ML^{-1}t^{-1}]$

Mass conservation is straight-forward and given by

$$(5.15) \qquad \frac{\partial}{\partial t}(\epsilon_f\rho_f) + \underset{\sim}{\nabla}\cdot(\rho_f \underset{\sim}{v}_f) - R = 0$$

5.1.2 Assumptions:

Because many of the assumptions inherent in this model also hold for the remaining models, we will list them only once. When in the discussion of other models additional assumptions are introduced or some on the list relaxed, they will be noted.

1) the porous medium can be assumed to be a continuum,
2) the reservoir is a porous medium, fractures do not materially influence either the dynamics or thermodynamics of the system,
3) the system is locally in thermodynamic equilibrium,
4) the thermodynamic pressure is essentially the same as the mechanical fluid pressure,
5) Darcy's law for a multiphase fluid is valid,
6) the various hypotheses inherent in the averaging formalism are valid,
7) incompressible, non reacting solid,
8) non deformable solid matrix,
9) fluid inertia is negligible (related to 5),
10) negligible viscous dissipation,
11) negligible capillary pressure,
12) temperature equilibrium between the fluid phases,
13) temperature equilibrium between the solid and fluid,
14) negligible pressure work,
15) the equation of state for water, determined using flat interfaces, is valid in the reservoir.

5.1.3 Numerical Approximations:

The numerical scheme used to solve (5.2), (5.3), and (5.5) has been called the integrated finite-difference method. While the general approach has been known for some time, it has recently been cleverly implemented in a computer code by Edwards (1972) which he called TRUMP. This code forms the foundation of the Lasseter, Witherspoon and Lippmann model. The basic idea is to solve (5.1) directly without reducing it to a point equation. The volume V is selected to be a multi-faceted sphere (a polygon in two space dimensions) where the flux across each face is approximated using a finite difference approximation of these first order terms. To apply this approach, it is necessary to rewrite (5.3) and (5.5) as integral equations. Substitution of (5.3) into (5.5) and integration over V yields

$$(5.6)\qquad \int_{V}\left[\frac{\partial}{\partial t}(\epsilon_f\rho_f)dv\right] - \int_{A}\left[(M\rho)^*\cdot\nabla p_f - (M\rho^2)^*\underset{\sim}{g}\right]\cdot\underset{\sim}{n}da - \int_{V} Rdv = 0$$

where $(M\rho)^* \equiv M_s\rho_s + M_w\rho_w$

$$(M\rho^2)^* \equiv M_s\rho_s^2 + M_w\rho_w^2$$

The finite difference approximation to (5.1) and (5.6) are (see figure 4 for nomenclature)

$$(5.7)\qquad \left(V_f\rho_f + m_R\frac{dU_R}{dU_f}\right)_n \frac{\delta U_{fn}}{\Delta t} - \sum_m \left\{[U^n_{wnm}S^n_{wnm} + U^n_{vnm}S^n_{vnm} - U^n_{fn}]F^n_{nm} + \frac{A_{nm}}{D_{nm}}\kappa_{nm}(T^n_m - T^n_n)\right\} - Q_{fn} + U_{fn}R_nV_n - \theta\sum_m\left[\delta U_{up}F^n_{nm} + \frac{A_{nm}}{D_{nm}}\kappa_{nm}\left\{\frac{\partial T_m}{\partial U_{fm}}\delta U_{fm} - \frac{\partial T_n}{\partial U_{fn}}\delta U_{fn}\right\}\right] = 0$$

where F_{nm} is the fluid flow rate between the nodes n and m (positive if into n),

n is the time level when used as a superscript,

U_{up} is the energy of the upstream node,

T_n is the temperature at the node n, and

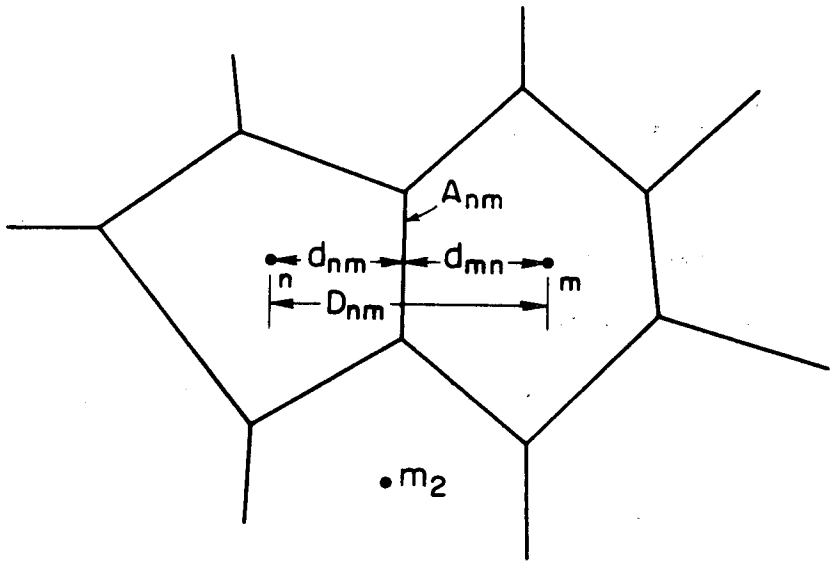

XBL 795-9556

Figure 4: Discretization by the integrated finite difference method (after Lasseter, Witherspoon and Lippmann, 1975).

ρ_f is held constant in the partial differentiation

The incremental form δU is obtained from the relationship

$$U = \theta U^{n+1} + (1-\theta)U^n = U^n + \theta(U^{n+1} - U^n) \equiv U^n + \theta\delta U$$

Thus, θ is the weighting parameter which locates the spatial operator in the time domain. Numerical round-off error is reduced when one solves for δU rather than U. Note that (5.7) is now written in one dependent variable δU_f (assuming a suitable choice for δU_{up} is made).

To achieve this reduction in unknowns, thermodynamic relationships derived from the steam tables were introduced, i.e., $\frac{dT_n}{dU_{fn}}$. These relationships are highly non-linear coefficients which make the solution of the two parameter (here U_f and ρ_f) reservoir simulation problem very difficult (see figure 5). In this model, the change in the vapour saturation of the flux is assumed to be the change in the vapour saturation at the upstream node. This type of upstream weighting of the convective term is necessary because of the hyperbolic behavior of this equation. Upstream weighting was also applied to U, i.e. $\delta U_{nm} = \delta U_{up}$.

To present the finite-difference form of the flow equation, we proceed in two steps because of the complexity of the thermodynamic coefficients. Let us first finite difference (5.6)

$$(5.8) \qquad \left(\varepsilon + \rho_f \frac{\partial \varepsilon}{\partial \rho}\right)_n V_n \frac{\delta \rho_{fn}}{\Delta t}$$

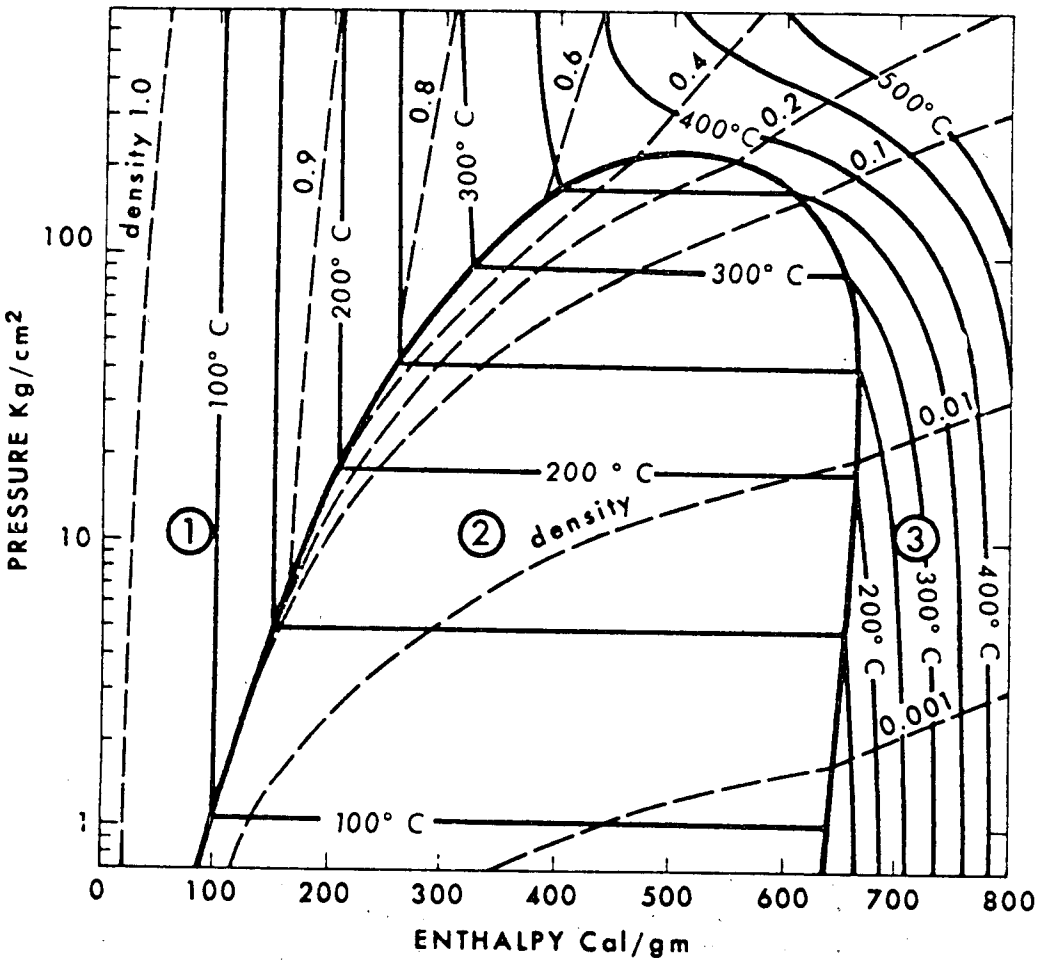

XBL 795-9555

Figure 5: Pressure-enthalpy diagram for water and steam with thermodynamic regions: 1) compressed water, 2) two-phase steam and water, and 3) superheated steam (after Faust and Mercer, 1977a).

$$= \sum_m A_{nm} \left[(M\rho)^*_{nm} \left(\frac{p_m - p_n}{D_{nm}} \right) - (M\rho^2)^*_{nm} \gamma_{nm} g \right] + R_n V_n$$

where γ_{nm} is the direction cosine between the normal from node n to m and the gravitational acceleration vector. Equation (5.8) contains the dependent variable p which we now eliminate through the use of the steam tables.

(5.9)
$$\left(\epsilon + \rho_f \frac{\partial \epsilon}{\partial \rho_f} \right)_n V_n \frac{\delta \rho_{fn}}{\Delta t}$$

$$= \sum_m A_{nm} \left[(M\rho)^*_{nm} \left(\frac{p^n_m - p^n_n}{D_{nm}} \right) - (M\rho^2)^*_{nm} \gamma_{nm} g \right]$$

$$+ \theta \sum_m A_{nm} \left\{ \left[X_{nm} \frac{d_{mn}}{D_{nm}} - \frac{(M\rho)^*_{nm}}{D_{nm}} \frac{\partial p_n}{\partial \rho_{fn}} \right] \delta \rho_{fn} \right.$$

$$\left. + \left[X_{nm} \frac{d_{nm}}{D_{nm}} + \frac{(M\rho)^*_{nm}}{D_{nm}} \frac{\partial p_m}{\partial \rho_{fm}} \right] \delta \rho_{fm} \right\} + R_n V_n$$

where

$$X_{nm} = \left(\frac{\partial (M\rho)^*}{\partial \rho} \right)_{nm} \left(\frac{p^n_m - p^n_n}{D_{nm}} \right) - \left(\frac{\partial (M\rho^2)^*}{\partial \rho_f} \right)_{nm} \gamma_{nm} g \ ,$$

$$(M\rho)^*_{nm} = \frac{D_{nm}(M\rho)^*_n(M\rho)^*_m}{d_{nm}(M\rho)^*_m + d_{mn}(M\rho)^*_n}$$

$$(M\rho^2)^*_{nm} = \frac{(M\rho^2)^*_n(M\rho)^*_m d_{nm} + (M\rho^2)^*_m(M\rho)^*_n d_{mn}}{d_{nm}(M\rho)^*_m + d_{mn}(M\rho)^*_n}, \quad \text{and}$$

internal energy is held constant in the differentiation.

5.1.4 Solution of Approximating Equations:

Equations (5.7) and (5.9) form a coupled set of highly non-linear finite difference equations in terms of the internal energy of the fluid U_f and fluid density ρ_f. The salient features of the method used to solve these equations, as determined from the publication by Lasseter, Witherspoon and Lippmann, can be summarized as follows:

a) The density equation (5.9) is solved at $t+\Delta t$ using initial estimates of the internal energy ($t = 0$).

b) The mass flux is calculated explicitly from the density and internal energy.

c) The internal energy equation is solved for $t+2\Delta t$ using the density solution obtained at $t+\Delta t$.

d) The time weighting parameter θ is computed for each time step; it is the same for all nodes during that step.

e) The linearized algebraic equations are solved iteratively using a scheme similar to, but different from, successive over-relaxation. The procedure was first derived by Evans et al, 1954.

5.1.5 Example Problem

Two problems were considered in the paper of Lasseter, Witherspoon and Lippmann (1975). The first is an axisymmetric cross section discretized into a uniform net with 10 rows and 25 columns. A hot water circulation system is established through a localized heat and mass source at the base. When a dynamic steady state is achieved forced convection is introduced by fluid withdrawal from a node located along the well-bore edge of the model. The problem was not used to illustrate the accuracy of the model.

The second problem is an idealized representation of the Geysers field. It is also axisymmetric with 15 evenly spaced rows of nodes and 10 nodes in the horizontal with increasing spacing with radius. The system is almost completely filled with steam initially. Steam is withdrawn from three nodes along the well-bore side of the model. The solution is illustrative of the physical processes encountered, but not designed to demonstrate model accuracy.

5.1.6 Model Evaluation:

This model played an important role in the development of geothermal reservoir simulators. It demonstrated that the combined-fluid-flow concept suggested by Garg (1974) was workable. Many of the later models assumed this general methodology. The use of the thermodynamic relationships to reduce the number of dependent variables was an important contribution. The integrated finite difference scheme could be used effectively in some problems because of its flexibility through the use of irregular elements.

The major deficiencies in the model lie in the fundamental equations and the solution of the approximating equations. The energy equation should be developed completely followed by appropriate term by term reduction. In the representation of T and P in terms of U_f and ρ_f, it is assumed $T = T(U_f)$ and $p = p(\rho_f)$. While this assumption is consistent with the numerical scheme, it requires additional investigation. A well bore model is also required before realistic simulations are undertaken. The numerical scheme does not appear to solve the non-linear equations. In this highly non-linear problem this is a serious deficiency. The model does not appear to have been "verified" against experimental data or single phase flow analytical solutions. No mass and energy balance calculations have been presented but the two phase example problem suggests some difficulties may have been encountered. In summary, this model was an important step in the development of geothermal reservoir models but could not be considered an engineering tool. More recent variations on this code which have not been published may have rectified these deficiencies.

5.2 Model of Brownell, Garg and Prichett

Brownell, Garg, and Pritchett were among the first to consider the solution of the multiphase problem using two dependent variables. Information relevant to their model can be found in Brownell et al (1975), Pritchett (1975), and Garg et al (1975). There are also several papers devoted to the development of the governing equations for geothermal reservoir simulation (Brownell, Garg and Pritchett, 1977; Garg and Pritchett, 1977) and a number of comprehensive reports (Garg et al, 1977; Pritchett et al., 1975; Pritchett et al.,1976; Garg et al., 1978; Pritchett, 1978).

5.2.1 Governing Equations

The governing equations are obtained using a mixture theory approach. For the rigid rock matrix case (analogous to the model of Lasseter, Witherspoon and Lippmann) we obtain for mass

$$\frac{\partial}{\partial t}(\varepsilon S_w \rho_w) + \underset{\sim}{\nabla}\cdot(\varepsilon S_w \rho_w \underset{\sim}{v}_w) + m = 0 \qquad \text{(water)} \tag{5.10a}$$

$$\frac{\partial}{\partial t}(\varepsilon S_s \rho_s) + \underset{\sim}{\nabla}\cdot(\varepsilon S_s \rho_s \underset{\sim}{v}_s) - m = 0 \qquad \text{(steam)} \tag{5.10b}$$

where m is the mass transfer rate from liquid to vapour due to phase change. In application the mixture (rock-liquid-vapour) is of primary importance, thus (5.10a) and (5.10b) are summed to give:

$$\varepsilon \frac{\partial}{\partial t}(S_w \rho_w + S_s \rho_s) + \underset{\sim}{\nabla}\cdot(\varepsilon S_w \rho_w \underset{\sim}{v}_w + \varepsilon S_s \rho_s \underset{\sim}{v}_s) = 0 \quad \text{(combined mass)} \tag{5.11}$$

This equation no longer contains the condensation term.

In place of the momentum equation, one uses the multiphase Darcy's law:

$$\varepsilon S_w \underset{\sim}{v}_w + \frac{k k_{rw}}{\mu_w}(\underset{\sim}{\nabla} p_w - \rho_w \underset{\sim}{g}) = 0 \tag{5.12a}$$

$$\varepsilon S_s \underset{\sim}{v}_s + \frac{k k_{rs}}{\mu_s}(\underset{\sim}{\nabla} p_s - \rho_s \underset{\sim}{g}) = 0 \qquad \text{(momentum)} \tag{5.12b}$$

Assuming capillary pressure to be negligible (5.12) can be substituted into (5.11) to yield

$$(5.13)\qquad \varepsilon \frac{\partial}{\partial t}(S_w\rho_w + S_s\rho_s) - \underset{\sim}{\nabla}\cdot\left(\frac{\rho_w kk_{rw}}{\mu_w}[\underset{\sim}{\nabla}p_f - \rho_w\underset{\sim}{g}] + \frac{\rho_s kk_{rs}}{\mu_s}[\underset{\sim}{\nabla}p_f - \rho_s\underset{\sim}{g}]\right) - R$$

$$= 0$$

where R is added as the source term.

The energy equation, written in terms of internal energy, is

$$(5.14)\qquad \frac{\partial}{\partial t}[(1-\varepsilon)\rho_R U_R] + \frac{D}{Dt_w}(\varepsilon S_w\rho_w U_w) + \frac{D}{Dt_s}(\varepsilon S_s\rho_s U_s) - \underset{\sim}{\nabla}\cdot\underset{\approx}{\kappa}\cdot\underset{\sim}{\nabla}T - Q_f = 0 \qquad \text{(energy)}$$

where $\underset{\approx}{\kappa}$ is the mixture thermal conductivity. In the simulator (5.14) and (5.13) are simplified, using standard assumptions, (see below), to give

$$(5.15)\qquad \frac{\partial}{\partial t}[(1-\varepsilon)\rho_R U_R + \varepsilon\rho_f U_f] - \underset{\sim}{\nabla}\cdot\rho_f U_f\left[\beta_w\frac{kk_{rw}}{\mu_w}(\underset{\sim}{\nabla}p_f - \rho_w\underset{\sim}{g}) + \beta_s\frac{kk_{rs}}{\mu_s}(\underset{\sim}{\nabla}p_f - \rho_s\underset{\sim}{g})\right] - \underset{\sim}{\nabla}\cdot\underset{\approx}{\kappa}\cdot\underset{\sim}{\nabla}T - Q_f = 0 \qquad \text{(energy)}$$

where $\beta_w = \frac{(1-\bar{Q})}{S_w}\left[1 - \bar{Q}\frac{U_{vap}}{U_f\rho_f}\right]$; $\beta_s = \frac{\bar{Q}}{S_s}\left[1 + (1-\bar{Q})\frac{U_{vap}}{U_f\rho_f}\right]$

$$(5.16) \qquad \varepsilon \frac{\partial}{\partial t} \rho_f - \nabla \cdot \left[\frac{\rho_f k(1-\bar{Q})\, k_{rw}}{S_w \mu_w} (\nabla p_f - \rho_w g) + \frac{\rho_f k Q k_{rs}}{S_s \mu_s} (\nabla p_f - \rho_s g) \right] - R$$

$$= 0$$

where $\bar{Q}$ is the steam quality i.e. $\bar{Q} \equiv \rho_s/(\rho_\ell + \rho_s)$ and U_{vap} is the latent heat of vaporization per unit fluid volume. The set of equations (5.15) and (5.16) are solved in terms of internal energy and fluid density. Pritchett (1975) points out that this choice of variables results in an exact conservation of mass and energy since these are the dependent variables rather than an auxiliary property. The solution of (5.15) and (5.16) requires auxiliary information on the relationship between the dependent variables U_f and ρ_f and the other unknown quantities such as pressure, temperature, steam quality, vapour saturation, latent heat of vapourization, viscosity, and thermal conductivity. In this model, large data tables combined with interpolation schemes are used for this purpose. The relative permeabilities are given by the equations of Corey et al (1956).

$$(5.17a) \qquad k_{rw} = (S_w^*)^4$$

$$(5.17b) \qquad k_{rs} = (1-S_w^{*2})(1-S_w^*)^2$$

$$(5.17c) \qquad S_w^* = (S_w - S_{wc})/(1 - S_{wc} - S_{sc})$$

Other identities employed in the development of (5.16) and not presented earlier include:

$$(5.18) \qquad \rho_w = \rho_f \left(\frac{1-\bar{Q}}{1-S_s} \right)$$

$$(5.19) \qquad \rho_v = \rho_f \left(\frac{\bar{Q}}{S_s} \right)$$

In addition the following constitutive relationship attributed to Budiansky (1970) is used

$$(5.20) \qquad (1-\varepsilon)\left[\frac{2}{3} + \frac{1}{3}\left(\frac{\kappa_R}{\kappa} \right)\right]^{-1} + \varepsilon \left\{ S_w \left[\frac{2}{3} + \frac{1}{3}\left(\frac{\kappa_w}{\kappa} \right)\right]^{-1} + S_s \left[\frac{2}{3} + \frac{1}{3}\left(\frac{\kappa_s}{\kappa} \right)\right]^{-1} \right\} = 1$$

and the assumption

$$U_R = C_{VR} T_R$$

where C_{VR} is the constant volume heat capacity of the solid.

In addition to the geothermal reservoir model, Garg has a subsidence model which works either interactively or in tandem with the reservoir model. The governing equations are derived from the fundamental balance laws augmented by constitutive relationships from solid mechanics. The momentum balance yields

$$(5.21) \quad -\underset{\sim}{\nabla}[(1-\varepsilon)p_R + \varepsilon p_f] + \underset{\sim}{\nabla}\cdot\underset{\approx}{\tau}_R + [(1-\varepsilon)\rho_R + \varepsilon S_w\rho_w + \varepsilon S_s\rho_s]\underset{\sim}{g} = 0$$

where p_R is the solid pressure, and

$\underset{\approx}{\tau}_R$ is the deviatoric stress tensor for porous rock

It is necessary to compliment (5.21) with the following constitutive relationships:

$$(5.22)\ 1) \quad \dot{\underset{\approx}{\varepsilon}} = \frac{1}{2}[\nabla\underset{\sim}{v}_R + (\nabla\underset{\sim}{v}_R)^t] = \frac{\dot{\varepsilon}}{3}\underset{\approx}{I} + \dot{\underset{\approx}{e}}$$

where

$\dot{\underset{\approx}{\varepsilon}}$ is the bulk strain rate tensor for rock,

$\dot{\underset{\approx}{e}}$ is the deviatoric part of the strain rate tensor,

$(\nabla\underset{\sim}{v}_R)^t$ denotes the transpose of $(\nabla\underset{\sim}{v}_R)$.

$$(5.23)\ 2) \quad \varepsilon^e = \frac{\rho_{oR}}{\rho_R} - 1 = \left(\frac{1-\varepsilon}{1-\varepsilon_o}\right)(1+\bar{\varepsilon}) - 1$$

where $\bar{\varepsilon}$ is the bulk volumetric strain

ε^e is the rock grain volumetric strain

3) the rock grain is a linear thermoelastic material

$$(5.24) \quad p_R = -K_R(\varepsilon^e - 3\eta_R T_R)$$

where $K_R(\eta_R)$ denotes the coefficient of linear thermal expansion for the rock grain

4) shear stresses are linearly related to shear strains $\underset{\sim}{e}$ through Hooke's law

(5.25) $$\underset{\sim}{\tau}_R = 2\mu_p \underset{\sim}{e}$$

where μ_p is the shear modulus of the porous rock.

(5.26) 5) $$\epsilon = \epsilon_o[1 + \alpha(p_T - p_f)]$$

where $p_T = (1-\epsilon)p_R + \epsilon p_f$

(5.27) $$\alpha \equiv \alpha(p_T - p_f) = \frac{1}{\epsilon_o}\left[\frac{1}{K_R} - \frac{(1-\epsilon_o)}{K}\right] ,$$

K is the bulk modulus of the porous rock, (may have a hysteretic effect), and

$p_T - p_f$ is the effective pressure.

This model is generally run in sequence with the reservoir model (Pritchett, 1978).

5.2.2 Assumptions:

The assumptions differ from those presented in 5.1.2 as follows:

1) The solid is not assumed incompressible in the presence of the deformation model,
2) The solid matrix is not assumed non-deformable in the presence of the deformation model,

3) The assumption of negligible pressure work and viscous dissipation are demonstrated theoretically and through numerical experiment rather than assumed (Garg and Pritchett, 1977)

5.2.3 Numerical Approximations:

The geothermal reservoir model is approximated using standard finite difference methods with the following features:

1) First order space terms are represented using a one-sided difference in the upstream direction (upstream weighting).

2) Equations are formulated in 1-D areal, 1-D cylindrical, 1-D spherical, 2-D areal or cross section, 2-D axisymmetric, and 3-D cartesian geometries.

The subsidence model is approximated using a standard finite element formulation, modified to account for material non-linearities. The code is also designed to accommodate plastic deformation. The code is 2-D (axisymmetric[+])

5.2.4 Well-bore Model:

Recently a "near well-bore" model was added to this simulator which permits calculations with wells that penetrate more than one zone (Pritchett, 1978). The relationship between well-block pressure, sandface pressure and flow rate for a single well in a single zone is computed by the model. The well blocks are then coupled together by insisting that the pressure distribution in the open interval in the well be hydrostatic. One version of the well bore model accounts for the discharge of methane in solution in a geothermal fluid (single water phase).

[+]assumed by author.

5.2.5 Solution of the Approximating Equations

The iterative alternating direction implicit procedure ADIP is used to solve the reservoir simulation equations. In this scheme, the multi-dimensional problem is decomposed into a series of one-dimensional problems. This corresponds to a particular form of matrix decomposition. In linear cases, it is often possible to solve the series of one-dimensional problems without iteration. For large time steps, however, it is generally advisable to iterate between the rows and column solutions. There is question that ADIP, when applicable, is an exceedingly powerful numerical approach.

Each one-dimensional problem is generally solved using direct methods. The Thomas algorithm, an efficient Gaussian elimination method, is particularly effective. In geothermal simulation, these one-dimensional problems are highly non-linear and must be solved iteratively. That is to say one must iterate within, as well as between, each row and column calculation. While the details of the algorithms are not available, Pritchett (1978) reports that the iteration scheme designed to accommodate the non-linearity employs a Newton Raphson procedure within each one-dimensional calculation. Additional information on the methodology can be found in Pritchett et al. (1975).

When the solution oscillates across the steam-water boundary of the thermodynamic diagram (figure 5), the oscillations are damped by requiring that the amplitude of each oscillation decrease by a specified amount (Pritchett, 1978). This is the only model developed to date that employs an ADIP approach.

The consolidation model is probably solved using a direct solution algorithm (Gaussian elimination) although this has not been stated explicitly.

5.2.6 Example Problems:

This model has been applied to a number of test problems:

1) One dimensional simulations of the laboratory experiments by Kruger and Ramey (1974) and Arihara (1974).

2) Injection into and production from a hypothetical right circular cylinder. Production takes place from a central vertical crack and fluid reinjection is into two similar cracks located at the reservoir periphery. The reservoir initially contains pressurized water. This model consisted of 384 nodes.

3) A homogeneous, isotropic, initially isothermal circular reservoir with a well located at the center. The initial pressure in the reservoir is specified such that in the three cases considered the first is in a liquid state, the second is a pure vapor reservoir and the third is initially liquid but yields two-phase flow near the well as the simulation proceeds. The purpose of these experiments was to demonstrate the significance, or lack thereof, of the pressure-work and viscous dissipation terms in the energy equation.

4) Preliminary calculations on the Wairakei geothermal field.

The one-dimensional simulation (1) was an attempt to verify the accuracy of the code. Several groups have used those experiments as a means of demonstrating the validity of their models. Unfortunately, several material parameters are unknown in this experiment and only one thermodynamically independent variable was measured at the exit point. Thus, an ability to reproduce the experiment numerically is a necessary but not sufficient condition to demonstrate its veracity. The second experiment is important in that the system must move from pressurized water to a steam-water mixture; a good test for any geothermal model.

In addition to the test problems, a two-dimensional vertical cross section of Wairakei was simulated. The section was selected to pass through the principal features of the reservoir. A successful history

match of pressure decline in the system was achieved.

An analysis was also performed of the Salton Sea geothermal reservoir. A two-dimensional, areal simulation was performed to establish the importance of lithologic variations on the response of the reservoir to production.

To demonstrate the application of their simulator to problems involving subsidence and methane production, a model of the Brazoria County, Texas project was undertaken. Vertical and horizontal displacements were computed for a problem case in cylindrical coordinates.

A similar model was developed to demonstrate the ability of their simulator to describe the precipitation of salt during flashing of geothermal brines. Simulations using 70 and 100 percent salt-saturated brine were successfully conducted. For the 70 percent case precipitation of salt in the pores did not occur: it did occur, however, in the 100 percent case.

5.2.7 Model Evaluation:

The Brownell, Garg and Pritchett model(s) appears to be theoretically sound and should be computationally efficient. The code employs governing equations which have been carefully derived and appear to encompass the salient physics of the geothermal system. It is the only model which incorporates a non-isothermal subsidence formulation and salt precipitation. The numerical scheme is one of the most efficient currently available for reservoir engineering problems.

While the model(s) are generally of high caliber, they have some negative aspects. The finite-difference formulation on a rectangular net is somewhat limiting in terms of flexibility in discretization when

compared with integrated finite differences or finite elements. This is largely offset by the efficiency of the ADIP algorithm. The use of an artificial constraint in the solution of the non-linear equations is undesirable and casts suspicion on the convergence properties of the non-linear algorithm. Information on mass and energy balances would assist in evaluating this possibility.

5.3 Model of Faust and Mercer

The model of Faust and Mercer was developed in parallel with but independent from the work of Brownell, Garg and Pritchett. While many of the features of the two models are similar, others are distinctly different. The essential elements of the Faust and Mercer model are described in a number of publications (Faust and Mercer, 1975 ; Mercer and Faust, 1975; Faust 1976; Faust and Mercer, 1977a; Faust and Mercer, 1977b; Faust and Mercer, 1978a; Faust and Mercer, 1978b).

5.3.1 Governing Equations:

The governing equations for this model were formulated using a volume averaging approach (Faust, 1976; Faust and Mercer, 1977b). The resulting equations for mass and momentum are the same as presented for the model of Brownell, Garg, and Pritchett. Because Faust and Mercer wish to solve the energy equation in terms of enthalpy rather than internal energy, they use (2.12) as the point of departure for formulating their energy equations. Writing (2.12) in combination with the continuity equation, one obtains

$$(5.28) \qquad \frac{\partial}{\partial t}(\rho h) + \underset{\sim}{\nabla}\cdot(\rho \underset{\sim}{v} h) - \frac{Dp}{Dt_f} + \underset{\sim}{\nabla}\cdot\underset{\sim}{q} + \underset{\approx}{\tau}:\underset{\sim\sim}{\nabla v} = 0$$

Assuming viscous dissipation can be neglected, Faust and Mercer present the following macroscopic energy balance equations

$$(5.29a) \qquad \frac{\partial}{\partial t}(\varepsilon S_s \rho_s h_s) + \underset{\sim}{\nabla}\cdot(\varepsilon S_s \rho_s h_s \underset{\sim}{v}_s) - \frac{D}{Dt_s}(\varepsilon S_s p_s) + \underset{\sim}{\nabla}\cdot(\underset{\sim}{q}_{1s} + \underset{\sim}{q}_{2s})$$

$$- Q_s' - R_s h_s' = 0 \qquad \text{(steam)}$$

$$(5.29b) \qquad \frac{\partial}{\partial t}(\varepsilon S_w \rho_w h_w) + \underset{\sim}{\nabla}\cdot(\varepsilon S_w \rho_w h_w \underset{\sim}{v}_w) - \frac{D}{Dt_w}(\varepsilon S_w p_w) + \underset{\sim}{\nabla}\cdot(\underset{\sim}{q}_{1w} + \underset{\sim}{q}_{2w})$$

$$- Q_w' - R_w h_w' = 0 \qquad \text{(water)}$$

$$(5.29c) \qquad \frac{\partial}{\partial t}[(1-\varepsilon)\rho_R h_R] + \underset{\sim}{\nabla}\cdot\underset{\sim}{q}_{1R} - Q_R' = 0$$

(rock)

where h_s' is the enthalpy of the source fluid, Q_α' are interphase energy exchange terms and $q_{1\alpha}$ and $q_{2\alpha}$ are heat flux by virtue of conduction and dispersion respectively. Imposing the generally accepted assumptions on (5.29) the three separate energy relationships can be combined to yield

$$(5.30)\quad \frac{\partial}{\partial t}\left[(1-\varepsilon)\rho_R h_R + \varepsilon\rho_f h_f\right] + \underset{\sim}{\nabla}\cdot(\varepsilon S_s \rho_s h_s \underset{\sim}{v}_s) + \underset{\sim}{\nabla}\cdot(\varepsilon S_w \rho_w h_w \underset{\sim}{v}_w) - \frac{\partial \varepsilon p_f}{\partial t}$$

$$- (\varepsilon S_s \underset{\sim}{v}_s + \varepsilon S_w \underset{\sim}{v}_w)\cdot\underset{\sim}{\nabla} p_f - \underset{\sim}{\nabla}\cdot(\kappa \underset{\sim}{\nabla} T) - R_s h'_s - R_w h'_w = 0$$

where

$$(5.40)\quad \sum_{\alpha}\sum_{i} \underset{\sim}{q}_{\alpha i} = -\kappa \underset{\sim}{\nabla} T$$

The final form of the balance equations is obtained by combining the mass conservation equation for the three phases and by introducing the momentum balance into the mass and energy balances. Thus, we obtain, assuming $\frac{Dp}{Dt_\alpha} = 0$,

$$(5.41)\quad \frac{\partial}{\partial t}(\varepsilon\rho_f) - \underset{\sim}{\nabla}\cdot\left[\frac{\underset{\approx}{k} k_r \rho_s}{\mu_s}(\underset{\sim}{\nabla} p_f - \rho_s \underset{\sim}{g})\right] - \underset{\sim}{\nabla}\cdot\left[\frac{\underset{\approx}{k} k_{rw}\rho_w}{\mu_w}(\underset{\sim}{\nabla} p_f - \rho_w \underset{\sim}{g})\right] - R_f$$

$$= 0$$

$$(5.42)\quad \frac{\partial}{\partial t}\left[\varepsilon\rho_f h_f + (1-\varepsilon)\rho_R h_R\right] - \underset{\sim}{\nabla}\cdot\left[\frac{\underset{\approx}{k} k_{rs}\rho_s h_s}{\mu_s}(\underset{\sim}{\nabla} p_f - \rho_s \underset{\sim}{g})\right]$$

$$- \underset{\sim}{\nabla}\cdot\left[\frac{\underset{\approx}{k} k_{rw}\rho_w h_w}{\mu_w}(\underset{\sim}{\nabla} p_f - \rho_w \underset{\sim}{g})\right] - \underset{\sim}{\nabla}\cdot\left[\kappa_m \left(\frac{\partial T}{\partial p}\right)_h \underset{\sim}{\nabla} p_f + \kappa_m \left(\frac{\partial T}{\partial h}\right)_p \underset{\sim}{\nabla} h_f\right]$$

$$- R_s h'_s - R_w h'_w = 0$$

It is interesting to compare (5.41) and (5.42) with the final form of the equations used by Brownell, Garg and Pritchett (5.15) and (5.16). The difference in these two equations is due to the fact that for (5.15) and (5.16) the solution variables are U_f and ρ_f while for (5.41) and (5.42) the solution variables are h_f and p_f.

Faust and Mercer (1978a) have also provided balance equations which are vertically integrated over the reservoir. The procedure for vertical integration is well known and was used for some time in surface water hydrodynamics before being introduced into hydrology. It is, nevertheless, a useful tool to assure that a consistent areal formulation is obtained from the three dimensional equations. In some ways, the procedure is analogous to the volume averaging introduced earlier and suffers from the same limitations. The basic rules follow. Let us assume that the operator in question is $L(\psi) = 0$. Integration over ψ yields:

$$\int_{z_1}^{z_2} L(\psi)\,dz = 0 \tag{5.43}$$

One now applies Leibnitz' rule to the various terms in L. Consider for example an extensive quantity ψ such that

$$\int_{z_1}^{z_2} \frac{\partial \psi}{\partial x}\,dz = \frac{\partial}{\partial x}\int_{z_1}^{z_2} \psi dz + \psi(x,y,z_1,t)\frac{\partial z_1}{\partial x} - \psi(x,y,z_2,t)\frac{\partial z_2}{\partial x} \tag{5.44}$$

We now define the averaging operator

$$\langle\psi\rangle = \frac{1}{b}\int_{z_1}^{z_2} \psi dz \; ; \qquad b \equiv z_2 - z_1 \tag{5.45}$$

Equation (5.45) can now be used in an obvious way to modify (5.44)

$$(5.46) \qquad \int_{z_1}^{z_2} \frac{\partial \psi}{\partial x}\, dz = b\langle\psi\rangle + \psi(x,y,z_1,t)\frac{\partial z_1}{\partial x} - \psi(x,y,z_2,t)\frac{\partial z_2}{\partial x}$$

When non-linear terms are encountered, we draw on theory which is again analogous to the volume averaging theory developed earlier. Let a property $\hat{\psi}$ be defined such that (see figure 6)

$$(5.47) \qquad \psi = \langle\psi\rangle + \hat{\psi}$$

One can then treat the product $\langle\psi\gamma\rangle$ as the equivalent expression

$$(5.48) \qquad \langle\psi\gamma\rangle = \langle\psi\rangle\langle\gamma\rangle + \langle\hat{\psi}\hat{\gamma}\rangle$$

which can be readily handled.

While this formalism leads naturally to an averaged equation in the areal plane, one must be careful that at each stage of the integration meaningful variables are generated. Making certain assumptions regarding the orientation of coordinate axes and the time invariance of the thickness of the reservoir, one obtains for the vertically averaged form of (5.41) and (5.42) (Faust and Mercer, 1978a)

$$(5.49) \qquad b\frac{\partial}{\partial t}\langle\varepsilon\rho_f\rangle - \frac{\partial}{\partial x}\left[b\langle\omega_x\rangle\left\langle\frac{\partial p_f}{\partial x}\right\rangle + \left\langle\hat{\omega}_x\frac{\partial \hat{p}_f}{\partial x}\right\rangle\right]$$

$$- \frac{\partial}{\partial y}\left[b\left(\langle\omega_y\rangle\left\langle\frac{\partial p_f}{\partial y}\right\rangle + \left\langle\hat{\omega}_y\frac{\partial \hat{p}_f}{\partial y}\right\rangle\right)\right]$$

$$- b\langle R_f\rangle + \underset{\sim}{v}_f\Big|_{z_1} \cdot\underset{\sim}{\nabla}(z-z_1) - \underset{\sim}{v}_f\Big|_{z_2} \cdot\underset{\sim}{\nabla}(z-z_2) = 0$$

where $\underset{\sim}{v}_f \equiv \varepsilon S_s \rho_s \underset{\sim}{v}_s + \varepsilon S_w \rho_w \underset{\sim}{v}_w$, and

$$R_f \equiv R_w + R_s$$

(5.50) $$b\frac{\partial}{\partial t}\left[\left(\langle\varepsilon\rho_f h_f\rangle + \langle\rho_R h_R\rangle - \langle\varepsilon\rho_R h_R\rangle\right] - \frac{\partial}{\partial x}\left[b\left(\langle\omega_{hx}\rangle\left\langle\frac{\partial p_f}{\partial x}\right\rangle + \left\langle\hat{\omega}_{hx}\frac{\partial \hat{p}_f}{\partial x}\right\rangle\right)\right]$$

$$- \frac{\partial}{\partial y}\left[b\left(\langle\omega_{hy}\rangle\left\langle\frac{\partial p_f}{\partial y}\right\rangle + \left\langle\hat{\omega}_{hy}\frac{\partial \hat{p}_f}{\partial y}\right\rangle\right)\right] - \frac{\partial}{\partial x}\left[b\langle\omega_{cp}\rangle\left\langle\frac{\partial p_f}{\partial x}\right\rangle\right.$$

$$\left. + \langle\omega_{ch}\rangle\left\langle\frac{\partial h_f}{\partial x}\right\rangle + \left\langle\hat{\omega}_{cp}\frac{\partial \hat{p}_f}{\partial x}\right\rangle + \left\langle\hat{\omega}_{ch}\frac{\partial \hat{h}_f}{\partial x}\right\rangle\right)\Big] - \frac{\partial}{\partial y}\left[b\left(\langle\omega_{cp}\rangle\left\langle\frac{\partial p_f}{\partial y}\right\rangle\right.\right.$$

$$\left.\left. + \langle\omega_{ch}\rangle\left\langle\frac{\partial h_f}{\partial y}\right\rangle + \left\langle\hat{\omega}_{cp}\frac{\partial \hat{p}_f}{\partial y}\right\rangle + \left\langle\hat{\omega}_{ch}\frac{\partial \hat{h}_f}{\partial y}\right\rangle\right)\right] - b\left(\langle R_s h_s'\rangle + \langle R_w h_w'\rangle\right)$$

$$+ h_f \underset{\sim}{v}_f\Big|_{z_1} \cdot\underset{\sim}{\nabla}(z-z_1) - h_f \underset{\sim}{v}_f\Big|_{z_2} \cdot\underset{\sim}{\nabla}(z-z_2) + \underset{\sim}{\lambda}_m\Big|_{z_1} \cdot\underset{\sim}{\nabla}(z-z_1) - \underset{\sim}{\lambda}_m\Big|_{z_2} \cdot\underset{\sim}{\nabla}(z-z_2)$$

$$= 0$$

where

$$\omega_x = \frac{k_{xx}k_{rw}\rho_w}{\mu_w} + \frac{k_{xx}k_{rs}\rho_s}{\mu_s} \quad , \tag{5.51}$$

$$\omega_{hx} = \frac{k_{xx}k_{rw}\rho_w h_w}{\mu_w} + \frac{k_{xx}k_{rs}\rho_s h_s}{\mu_s} \tag{5.52}$$

$$\omega_{cp} = \kappa_m \left(\frac{\partial T}{\partial p_f}\right)_{h_f} \tag{5.53}$$

$$\omega_{ch} = \kappa_m \left(\frac{\partial T}{\partial h_f}\right)_{p_f} \tag{5.54}$$

$$\omega_{gz} = \frac{k_{zz}k_{rw}\rho_w^2 g}{\mu_w} + \frac{k_{zz}k_{rs}\rho_s^2 g}{\mu_s} \quad , \tag{5.55}$$

$$\omega_{hgz} = \frac{k_{zz}k_{rw}\rho_w^2 g h_w}{\mu_w} + \frac{k_{zz}k_{rs}\rho_s^2 g h_s}{\mu_s} \quad , \tag{5.56}$$

$$\underset{\sim}{v}_f\Big|_{z_1} \cdot \underset{\sim}{\nabla}(z-z_1) = -\left(\omega_x \frac{\partial p_f}{\partial x}\right)\Big|_{z_1} \frac{\partial z_1}{\partial x} - \left(\omega_y \frac{\partial p_f}{\partial y}\right)\Big|_{z_1} \frac{\partial z_1}{\partial y} + \left(\omega_z \frac{\partial p_f}{\partial z} + \omega_{gz}\right)\Big|_{z_1} , \tag{5.57}$$

$$h_f \underset{\sim}{v}_f\Big|_{z_1} \cdot \underset{\sim}{\nabla}(z-z_1) = -\left(\omega_{hx} \frac{\partial p_f}{\partial x}\right)\Big|_{z_1} \frac{\partial z_1}{\partial x} - \left(\omega_{hy} \frac{\partial p_f}{\partial y}\right)\Big|_{z_1} \frac{\partial z_1}{\partial y} + \left(\omega_{hz} \frac{\partial p_f}{\partial z} + \omega_{hgz}\right)\Big|_{z_1} , \tag{5.58}$$

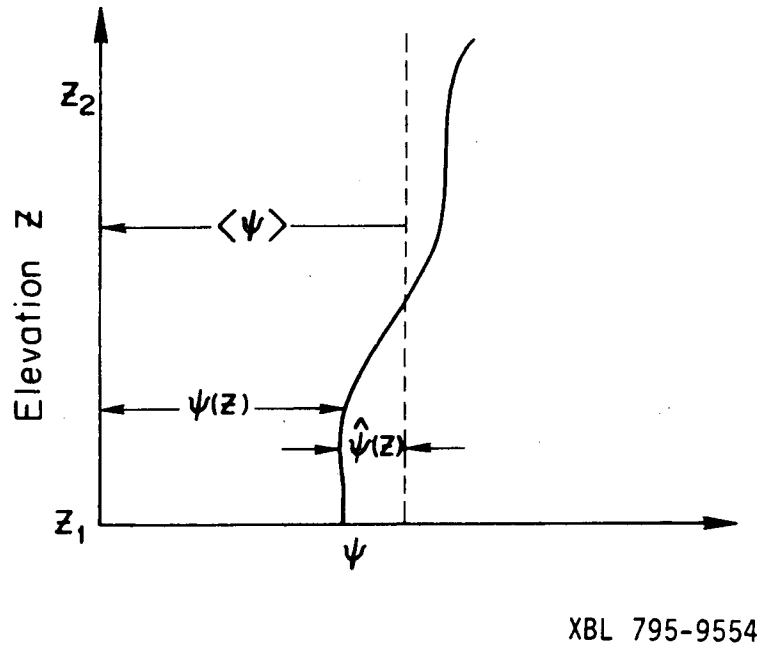

XBL 795-9554

Figure 6: Definition sketch for the vertical integration of the parameter ψ (z) = $\langle\hat{\psi}\rangle$(z) (after Faust and Mercer, 1978a).

$$(5.59)\qquad \underset{\sim}{\lambda}_m\Big|_{z_1} \cdot \underset{\sim}{\nabla}(z-z_1) = -\left(\omega_{cp}\frac{\partial p_f}{\partial x} + \omega_{ch}\frac{\partial h_f}{\partial x}\right)\Big|_{z_1}\frac{\partial z_1}{\partial x}$$

$$-\left(\omega_{cp}\frac{\partial p_f}{\partial y} + \omega_{ch}\frac{\partial h_f}{\partial y}\right)\Big|_{z_1}\frac{\partial z_1}{\partial y} + \left(\omega_{cp}\frac{\partial p_f}{\partial z} + \omega_{ch}\frac{\partial h}{\partial z}\right)\Big|_{z_1}$$

and similar expressions can be written for z_2.

Let us now examine (5.50). Terms of the form $\langle \varepsilon \rho_f h_f \rangle$ are meaningful in the sense that the integrand $(\varepsilon \rho_f h_f)$ is an extensive variable. This is not true, however, for all terms in (5.50). Consider, for example, the term $\left\langle \frac{\partial h_f}{\partial y} \right\rangle$. The integrand in this case is not an extensive variable and its volume integral appears to have no physical meaning. In other words, we are employing variables which are mathematical abstractions without physical interpretation. The impact of this questionable step in the formulation is difficult to judge but certainly warrants additional study.

Faust and Mercer (1978a) now investigate the evaluation of the averaged terms appearing in (5.49 - 5.59). Employing a definition of hydrostatic pressure and Leibnitz' rule, one obtains for pressure

$$(5.60)\qquad \left\langle \frac{\partial p_f}{\partial x} \right\rangle = \frac{\partial}{\partial x}\langle p_f \rangle - \langle \rho_f g \rangle \frac{\partial \langle D \rangle}{\partial x} - \frac{1}{b}\langle \hat{z}\hat{\rho}_f g \rangle \frac{\partial \langle D \rangle}{\partial x}$$

where $\frac{\partial}{\partial x}\langle D \rangle = -\frac{1}{2}\left(\frac{\partial z_1}{\partial x} + \frac{\partial z_2}{\partial x}\right)$

and for enthalpy

$$(5.61) \qquad \left\langle \frac{\partial h_f}{\partial x} \right\rangle = \frac{\partial}{\partial x} \langle h_f \rangle - \frac{1}{b} \left(\langle h_f \rangle - h_f \Big|_{z_1} \right) \frac{\partial z_1}{\partial x} + \frac{1}{b} \left(\langle h_f \rangle - h_f \Big|_{z_2} \right) \frac{\partial z_2}{\partial x}$$

To evaluate the averaged coefficients Faust and Mercer (1978a) assume local vertical equilibrium. They have used field data and simulation runs to establish the equilibrium form of pressure and enthalpy. They assume that, in the absence of significant capillary pressure, steam and water segregate due to gravity and a steam cap is produced with a water saturation equal to residual water saturation. Below the cap, the saturation is unity. This provides a series of relationships which are subsequently used in obtaining the averaged values of the coefficients appearing in (5.49) and (5.50). Certain relatively mild assumptions must be made to achieve the final form. The principal assumption here is vertical equilibrium - an assumption which can in a sense be checked using a three-dimensional simulator.

5.3.2 Assumptions:

The only new assumption associated with this model involves the two dimensional formulation wherein one assumes the reservoir has a high degree of vertical communication such that vertical gradients can be disregarded.

5.3.3 Numerical Approximations:

A standard finite difference scheme is used for the primary simulator. The grid is block centered (nodes are placed in the center of each block). The grid blocks may change size but must remain rectangles. In formulating the coefficients of the difference equations, the following rules were observed:

1) Density, viscosity, $\left(\frac{\partial T}{\partial p_f}\right)_{h_f}$, and $\left(\frac{\partial T}{\partial h_f}\right)_{p_f}$ are evaluated as arithmetic averages of values in adjacent blocks.

2) Relative permeabilities and enthalpies are usually assigned the upstream value.

3) Other space dependent terms are determined as harmonic means of the values in the two adjacent blocks.

The same basic scheme is used for both the two and three-dimensional models.

5.3.4 Solution of the Approximating Equations:

The resulting set of finite-difference approximating equations are highly non-linear, as with all preceeding models. Faust and Mercer (1978a) use a slightly different scheme for approximating the three and two-dimensional equations. The three-dimensional model uses a fully implicit scheme to approximate the transmissivity, accumulation, and source terms. (i.e., these parameters are evaluated at the new time level (n+1)) To achieve this implicit formulation, Newton-Raphson iteration was applied to these non-linear terms. For the areal model, only the accumulation and source terms were treated implicitly and Picard iteration was used for the transmissivity.

The three-dimensional model is solved using a block iterative scheme called slice successive over-relaxation (SSOR) (see Wattenbarger and Thurnaw, 1976). The blocks in this case are vertical cross-sections of the grid. Each block (a two-dimensional problem) is solved implicitly using a standard band solver based on Gaussian elimination. Each node carries an unknown value of pressure and enthalpy. The SSOR is imbedded within the Newton-Raphson iteration. This is in contrast to the Brownell, Garg and Pritchett model (section 5.2) where the Newton-Raphson iteration is

imbedded within each one-dimensional implicit solution generated using ADIP. The advantage to solving only linear equations in SSOR is that the matrix must be decomposed only once per Newton-Raphson iteration.

In the areal model, the two equations (5.49 and 5.50) are solved sequentially. This is the approach taken by Lasseter, Witherspoon and Lippmann (section 5.1). The scheme used by Faust and Mercer is described in Coats et al. 1974. In this scheme, Gaussian elimination is applied to the linearized Newton-Raphson equations in such a way as to upper triangularize the 2x2 blocks associated with each node. Consider, for example, the typical pair of equations written for an arbitrary node

$$\begin{bmatrix} c_{11} & c_{12} \\ c_{21} & c_{22} \end{bmatrix} \begin{Bmatrix} \delta p_f^{n+1} \\ \delta h_f^{n+1} \end{Bmatrix} = \begin{bmatrix} 1 & 0 \\ 0 & 1 \end{bmatrix} \begin{Bmatrix} y_1 \\ y_2 \end{Bmatrix} + \begin{Bmatrix} r_1 \\ r_2 \end{Bmatrix} \tag{5.62}$$

where, for the flow equation (5.49 and 5.50)

$$\delta p_f = p_f^{k+1} - p_f^k \quad , \quad \delta h_f = h_f^{k+1} - h_f^k$$

$$c_{11} = \frac{\partial M}{\partial p_f} \frac{V_b}{\Delta t}$$

$$c_{12} = \frac{\partial M}{\partial h_f} \frac{V_b}{\Delta t}$$

$$c_{21} = \frac{\partial x}{\partial p_f} \frac{V_b}{\Delta t} - \frac{\partial (R_s h_s' + R_w h_w')}{\partial p_f}$$

$$c_{22} = \frac{\partial x_f}{\partial h_f} \frac{V_b}{\Delta t} - \frac{\partial (R_s h_s' + R_w h_w')}{\partial h_f}$$

$$x \equiv [\varepsilon\rho_f h_f + (1-\varepsilon)\rho_R h_R]$$

$$M \equiv \varepsilon\rho_f$$

V_b is the grid-block volume

$$y_1 = \Delta[(T_w^* + T_s^*)\,\Delta\,(\delta p_f^{n+1})]$$

$$y_2 = \Delta[T_h^*\Delta(\delta p_f^{n+1})] + \Delta[T_c^*\Delta(\delta h_f^{n+1})]$$

$$r_1 = \Delta[(T_w^* + T_s^*)\Delta p_f^{n+1}] + bR_f - (M^{n+1} - M^n)\,\frac{V_b}{\Delta t}$$

$$r_2 = \Delta(T_h^*\Delta p_f^{n+1}) + \Delta(T_c^*\Delta h_f^{n+1}) + bR_s h_s' - bR_w h_w' - (E^{n+1} - E^n)\,\frac{V_b}{\Delta t}$$

$$T_\alpha^* = \frac{kA\rho_\alpha k_{r\alpha}}{\ell\mu_\alpha}$$

$$T_c^* = \frac{K_m A}{\ell}\left(\frac{\partial T}{\partial h_f}\right)_{p_f}$$

$$T_h^* = T_w^* h_w + T_s^* h_s + \frac{K_m A}{\ell}\left(\frac{\partial T}{\partial p_f}\right)_{h_f}$$

where K_m is a combined isotropic conduction - thermal dispersion coefficient and A and ℓ are the grid cross sectional areas perpendicular to the flow direction and the length increment in the flow direction respectively. The finite difference operator Δ is defined, in the x direction for example,

$$\Delta_x(a\Delta_x b^{n+1}) = a_{i+1/2jk}(b^{n+1}_{i+1jk} - b^{n+1}_{ijk}) - a_{i-1/2jk}(b^{n+1}_{ijk} - b^{n+1}_{i-1jk})$$

where $P(x,y,z) = P(i\Delta x, j\Delta y, k\Delta z)$.

Application of Gaussian elimination to (5.62) yields (Faust and Mercer, 1978b)

$$(5.63)\quad \begin{bmatrix} c_{11} & c_{12} \\ 0 & c_{22} - \frac{c_{21}}{c_{11}} c_{12} \end{bmatrix} \begin{Bmatrix} \delta p_f^{n+1} \\ \delta h_f^{n+1} \end{Bmatrix} = \begin{bmatrix} 1 & 0 \\ -\frac{c_{21}}{c_{11}} & 1 \end{bmatrix} \begin{Bmatrix} y_1 \\ y_2 \end{Bmatrix} + \begin{Bmatrix} r_1 \\ r_2 - r_1 \frac{c_{21}}{c_{11}} \end{Bmatrix}$$

Note that [c] contains only time matrix information. This is because only the accumulation and source terms were treated implicitly. One can now solve a set of N equations in δh_f^{n+1} and subsequently a set of N equations in δp_f^{n+1}. The coefficient matrices involved are symmetric and can be solved efficiently using D4 ordering (Price and Coats, 1974). One must iterate between sequential solutions within each Newton-Raphson iteration. Only one decomposition per Newton-Raphson iteration is required. Faust and Mercer (1978b) claim this procedure (sequential solution and D4 ordering) reduces the computational effort required to solve the set of algebraic equations to $\frac{1}{4}$ to $\frac{1}{16}$ of that required for simultaneous solution and normal ordering.

It is not apparent from the available literature how the transition from a water to a steam-water system is accomplished. It

reportedly involves a modified Newton-Raphson scheme similar to that presented later in Huyakorn and Pinder (section 5.6) (Faust, 1978).

5.3.5 Example Problems:

The model of Faust and Mercer has been tested extensively and applied to a number of physical situations. In addition they have compared their model against other methodologies. Some of the problems they consider are:

1) one-dimensional single phase flow: a problem which has an analytical solution

2) one-dimensional experiment of Kruger and Ramey (1974): reproduction of this experiment should be considered a necessary but not sufficient condition for model verification. This problem was solved using finite difference and finite element techniques.

3) hypothetical cross section with two phase flow: designated to evaluate the validity of assumptions used in the vertically integrated areal model. The model consists of either 48 or 80 equally spaced grid blocks.

4) hypothetical three-dimensional reservoir: used to evaluate the ability of the areal model to reproduce three-dimensional systems.

5) hypothetical three-dimensional reservoir solved using areal, vertically integrated model

6) vertical cross sectional model of Wairakei, New Zealand.

7) vertically integrated three-dimensional model of Wairakei, New Zealand, Faust (1978c)

The primary objective of many of the simulations was the justification of vertical integration in simulating three-dimensional problems. Their general conclusions are as follows: (Faust and Mercer, 1978b).

a) assumption of vertically uniform properties is suitable for hot water systems and two phase systems in thin reservoirs.

b) assumption of no gravity segregation or vertical variation in thermodynamic properties, for most two-phase problems gives erroneous pressures and saturations leading to an incorrect prediction of early reservoir depletion.

c) the cross-section and three-dimensional models converge to the pressure solution of the vertical equilibrium model as $\Delta z \rightarrow 0$.

d) the vertical equilibrium model is most useful for reservoirs less than 500 meters thick with relatively high permeability and a thin steam cap.

5.3.6 Model Evaluation:

The model of Faust and Mercer is the most thoroughly tested and documented multiphase geothermal model available in the public domain. It has been carefully developed and employs the most current methodologies in both the theoretical formulation and numerical solution of the resulting approximate equations. The reduction of the three-dimensional formulation to two dimensions through vertical integration is important. Considerable savings in both man hours and computer time can be realized using the vertically integrated model.

The only major deficiency in this model is the lack of an accurate well-bore simulator. Thus, the model is essentially restricted from application in near well bore regions.

There are several minor theoretical questions which require further study.

1) the vertical integration of intensive variables leading to non-physical parameters.

2) the method of representing the non-linear coefficients in the neighborhood of the phase transition boundary

3) the accuracy of the numerical solutions, i.e., some information on global and local mass and energy balances. (this apparently has been included in a recent paper).

5.4 Model of Toronyi and Farouq Ali

The Toronyi and Farouq Ali model was possibly the first of the multi-phase models. It was first described in the thesis of Toronyi (1974) and later in a journal article (Toronyi and Farouq Ali, 1975). The model is more restrictive than those discussed thus far inasmuch as the fluid must be two phases.

5.4.1 Governing Equations:

The governing equations are obtained through a macroscopic mass and energy balance. As in earlier cases, the mass and energy balance relationships are derived for a mixture, i.e., the water and steam are combined to form a single fluid. Combination of Darcy's law written for the two phases and the continuity equation written for each phase and summed yields

$$(5.64)\qquad \frac{\partial}{\partial t}\left(\epsilon\rho_w S_w + \epsilon\rho_s S_s\right)$$

$$- \underset{\sim}{\nabla}\cdot\left[\frac{\underset{\approx}{k}k_{rw}\rho_w}{\mu_w}\cdot\left(\underset{\sim}{\nabla}p_f - \rho_w\underset{\sim}{g}\right) + \frac{\underset{\approx}{k}k_{rs}\rho_s}{\mu_s}\cdot\left(\underset{\sim}{\nabla}p_f - \rho_s\underset{\sim}{g}\right)\right] - R_f = 0$$

This expression is similar to the continuity of mass expressions presented earlier, eg. equation (5.13).

The conservation of energy equation is expressed in terms of enthalpies. The simplest form of this formulation yields

$$(5.65)\qquad \frac{\partial}{\partial t}\left[\epsilon(\rho_w h_w S_w + \rho_s h_s S_s) + (1-\epsilon)\rho_R h_R\right]$$

$$+ \underset{\sim}{\nabla}\cdot(\rho_w h_w \epsilon S_w \underset{\sim}{v}_w + \rho_s h_s \epsilon S_s \underset{\sim}{v}_s) - \underset{\sim}{\nabla}\cdot(\kappa\underset{\sim}{\nabla}T) - Q_f = 0$$

This equation is an approximation to the true energy balance inasmuch as the pressure work term does not appear. Coats (1977) claims this to be an erroneous formulation wherein an enthalpy balance relationship was used. It is not clear from the paper by Toronyi and Farouq Ali whether such a balance was implied, but no mention is made of the assumption of negligible pressure work. Substitution of Darcy's law into (5.65) yields

$$(5.66)\qquad \frac{\partial}{\partial t}\left[\varepsilon(\rho_w h_w S_w + \rho_s h_s S_s) + (1-\varepsilon)\rho_R h_R\right]$$

$$- \underset{\sim}{\nabla}\cdot\left[\frac{\underset{\simeq}{k}k_{rw}\rho_w h_w}{\mu_w}\cdot(\underset{\sim}{\nabla}p_f - \rho_w\underset{\sim}{g}) + \frac{\underset{\simeq}{k}k_{rs}\rho_s h_s}{\mu_s}\cdot(\underset{\sim}{\nabla}p_f - \rho_s\underset{\sim}{g})\right]$$

$$- \underset{\sim}{\nabla}\cdot(\kappa\underset{\sim}{\nabla}T) - Q_f = 0$$

We note that in the original paper by Toronyi and Farouq Ali (1975), there appears to be a typographical error and the sign of the convective term is incorrect.

To this point, the form of the equations is totally general. Only when the constitutive equations are introduced and the dependent variables selected does the restriction to the two phase region appear. The density, viscosity and enthalpy for both water and steam are assumed functionally dependent on pressure and temperature at saturated conditions. The temperature and pressure within the reservoir are related by

$$(5.67)\quad \text{(Farouq Ali, 1970)}\qquad T = 115.1\, p_f^{0.225}$$

where p_f has the units of lb_f/sq.in. and T is in °F. The dependent variables are chosen as saturation and pressure: this choice is obviously meaningful only in the two phase region (see figure 5).

5.4.2 Assumptions:

The principal new assumption is that the fluid is two phase only. A second relationship of interest is the functional dependence of $\varepsilon = \varepsilon(p)$, i.e., the function is assumed separable into spacial and pressure dependent parts.

$$\varepsilon = \varepsilon_1(x,y)\varepsilon_2(p_f) \tag{5.68}$$

$$\varepsilon_2 = [1 + c_r(p-p_o)] \tag{5.69}$$

where c_r is the rock compressibility.

5.4.3 Numerical Approximations:

The equations (5.64) and (5.66) are approximated using standard finite-difference procedures with the following idiosyncrasies:

1) saturation dependent terms are assumed non-linear and evaluated at the new (n+1) time level

2) backward difference approximation is used for the time derivative

3) for pressure dependent terms, a linear average of adjacent grid point values is used

4) for saturation dependent terms, upstream saturations are used based on fluid potentials

5) permeability is taken as the harmonic mean of adjacent grid point values

The well bore model is formulated as follows: let the heat sink term in the energy equation be written:

$$Q = h_w R + (h_s - h_w) R_s \tag{5.70}$$

The steam production rate is determined by fractional flow as

$$R_s = \sigma_s R \tag{5.71a}$$

where

$$\sigma_s = \frac{k_{rs}}{k_{rs} + \Lambda k_{rw}} \text{ , and} \tag{5.71b}$$

$$\Lambda = \frac{\mu_s}{\mu_w} \frac{\rho_w}{\rho_s} \tag{5.71c}$$

Substitution of (5.71a) into (5.70) yields, in finite difference form,

$$Q_{ij}^{n+1} = \left[h_w^n + \frac{(h_s^n - h_w^n) k_{rs}^{n+1}}{k_{rs}^{n+1} + \Lambda^n k_{rw}^{n+1}} \right]_{ij} R_{ij}^{n+1}$$

where Q_{ij}^{n+1} appears in the energy equation (5.66) and R_{ij}^{n+1} appears in the flow equation (5.64).

5.4.4 Solution of the Approximating Equations:

When N nodes are considered a system of 2N equations is generated by the finite difference equations. These non-linear equations are solved using a Newton-Raphson technique. At each iteration, a direct solution scheme is used to solve the linearized equations.

5.4.5 Example Problems:

Several example problems were run using a two-dimensional areal and cross-sectional model. The cross-section does not appear to have been formulated in cylindrical coordinates although a "well" was involved in the simulation. The models involved 36 nodes each.

A 5 x 2 x 2 x 2 factorial experiment was run where the factors were as follows: initial saturation 1.0, 0.8, 0.6, 0.4, 0.2; porosity 0.05 and 0.35; initial pressure 650 psia and 450 psia; permeability 1.0 and 0.10 darcy. For the cross section, the initial saturations were 0.50, 0.40, 0.30, 0.20, and 0.10. The convergence tolerance used was 10^{-9} and the typical mass and energy residuals were 10^{-12} - 10^{-15} and 10^{-9} - 10^{-11} respectively. The percent error in both incremental and cumulative mass balances was 10^{-9} to 10^{-10}. A stability parameter was defined as the dimensionless throughput.

$$N_{TP} = \frac{R\Delta t}{m_p} \tag{5.73}$$

where m_p is the total mass per cell containing the well

Δt is the time step size , and

R is the total mass production rate

The maximum stable value of N_{TP} was from about 1.0 to 33. It is interesting that for higher levels of initial saturation N_{TP} was not a good measure of stability. Toronyi and Farouq Ali (1975) suggest this is due to the importance of thermal effects, such as flashing, on the stability of the system.

5.4.6 Model Evaluation:

The Toronyi-Farouq Ali model was an important contribution in the development of geothermal simulators. It was designed to examine various geothermal reservoir phenomena under the constraint of two phase flow. Several interesting aspects of geothermal reservoir behavior were elucidated.

The formulation of the governing equations was not presented in any detail. The final expressions, however, are the same as those generated by others for the case of negligible pressure work. The choice of saturation and pressure as dependent variables has the advantage of eliminating problems associated with the transition from water to steam. The obvious disadvantage is that the model is not readily applicable to the majority of geothermal reservoirs.

The numerical scheme appears sound. The general approach is mathematically sound. Moreover, mass and energy balances are presented such that the accuracy of the non-linear algorithm can be evaluated. The choice of a stability criteria is worthwhile although the one that was selected probably has little relevance to a model designed to simulate the transition from pure liquid water to steam.

5.5 Model of Coats

While the particular model we identify with Coats was published in 1977, he and his colleagues presented earlier a number of related simulators. (Coats, 1974, Coats et al., 1974) We focus on the paper Coats (1977) because it describes a scheme designed specifically for geothermal reservoir simulation. It will become apparent in the course of this discussion that the Coats model is probably the most advanced formulation for the general simulation of multi-dimensional reservoirs.

5.5.1 Governing Equations:

The governing equations are formulated using a macroscopic balance approach. The mass and energy balance is formulated for the combined steam-water mixture, as in earlier examples. The mass balance is,+

$$(5.74)\qquad \frac{\partial}{\partial t}(\varepsilon\rho_w S_w + \varepsilon\rho_s S_s) - \underset{\sim}{\nabla}\cdot\left[\frac{\underset{\approx}{k}k_{rs}\rho_s}{\mu_s}\cdot(\underset{\sim}{\nabla}p_s - \rho_s\underset{\sim}{g}) + \frac{\underset{\approx}{k}k_{rw}\rho_w}{\mu_w}\cdot(\underset{\sim}{\nabla}p_w - \rho_w\underset{\sim}{g})\right] - R_f = 0$$

This is similar to (5.64), the mass balance of Toronyi and Farouq Ali, but we do not assume a single fluid pressure, i.e., capillary pressure may exist.

The energy equation, with potential and kinetic terms ignored, becomes

$$(5.75)\qquad \frac{\partial}{\partial t}[\varepsilon(\rho_w S_w U_w + \rho_s S_s U_s) + (1-\varepsilon)\rho_R c_{pR} T] - \underset{\sim}{\nabla}\cdot\left[\frac{\underset{\approx}{k}k_{rw}\rho_w h_w}{\mu_w}\cdot(\underset{\sim}{\nabla}p_w - \rho_w\underset{\sim}{g}) + \frac{\underset{\approx}{k}k_{rs}\rho_s h_s}{\mu_s}\cdot(\underset{\sim}{\nabla}p_s - \rho_s\underset{\sim}{g})\right]$$

$$- \underset{\sim}{\nabla}\cdot\underset{\approx}{\kappa}\cdot\underset{\sim}{\nabla}T - Q_{HL} - Q_H = 0$$

+The continuous form is not presented and here the partial differential equations are formulated from the difference equations.

where Q_{HL} is a heat gain rate and

Q_H is an enthalpy injection rate.

We have not specified the form of Q_{HL} or Q_H as in the case of the Faust and Mercer model (5.42). All of the functions in (5.74) and (5.75) can be expressed as single valued functions of T, S_s, p_s. Note that the water saturation and pressure are also known through the relationships

$$S_w + S_s = 1 \tag{5.76}$$

$$p_c = p_s - p_w \tag{3.45}$$

where, once again, p_c is the capillary pressure.

Examination of figure 5 reveals that the three variables T, S_s, p_s are not independent everywhere on the thermodynamic diagram. In the water region 1) the two independent variables are pressure p_w and temperature T. The independent variables in region 2) are pressure p_s and saturation S_s: this we have seen was the choice of Toronyi and Farouq Ali in their two-phase model: in the superheated steam region 3) temperature and pressure are once again the dependent variables of choice. In the water region U_w is assumed to be a single-valued function of temperature and the density is obtained from

$$\rho_w \simeq \rho_{ws}(T)[1 + c_w(T)(p_s - p_{ss}(T))] \tag{5.77}$$

where the subscript ss denotes saturated conditions. Constitutive relationships are also obtained for the other variables functionally related to the dependent variables of choice. Thus, the algorithm employs three different formulations of the governing equations; one for each of the

regions indicated in figure 5. The question which arises is how does one operate in the vicinity of the water-multiphase fluid boundary of the thermodynamic diagram? In other words, the troublesome non-linearity has been artifically removed from the governing equations but must, nevertheless, exist in the model formulation. Coats (1977) does not detail the iterative procedure involved.

5.5.2 Assumptions:

The assumption of zero capillary pressure is relaxed in this model. There is also an attempt to employ a discrete fracture reservoir formulation (see section 4.1). A sophisticated well bore model is employed.

5.5.3 Numerical Approximations:

The appropriate governing equations are approximated using standard block-centered finite-difference approximations. Idiosyncrasies of this particular formulation follow:

1) relative permeabilities and enthalpies are evaluated at the upstream grid block conditions

2) interblock ρ_α/μ_α and γ_α are evaluated as arithmetic averages of their values in the two grid blocks.

5.5.4 Well-bore Model:

Coats (1977) has gone to considerable trouble to formulate a meaningful well-bore model. The development is long and rather tedious but essentially addresses the following possible cases:

1) the production rates of water phase, steam phase and total water and enthalpy from a given layer

2) the information obtained in 1) but extended to consider the case of a multilayer well completion

3) the formulation presented in 2) but assuming a semi-implicit well treatment (the model otherwise is totally implicit)

4) in single well problems defined in cylindrical geometry, the well is treated implicitly by simply incorporating the well bore in the reservoir grid system. Because of the unique flow characteristics of the well bore, one must either employ a code suitable to fully developed turbulent multiphase flow or modify the normal Darcy formulation through the use of psuedo relative permeabilities which accomplish the same effect. A problem encountered in this type of formulation involves the throughput ratio in the very small well-bore blocks.

5.5.5 Solution of Approximating Equations

The totally implicit solution of the approximating algebraic equations is achieved using Newton-Raphson iteration. While this accounts for the relatively weak non-linearity within a phase region (see figure 5), it does not indicate the technique employed in resolving the extreme non-linearity encountered in moving between phases.

The convergence criteria associated with the Newton-Raphson change $\delta(\cdot)^+$ is reported as

$$\text{Max}|\delta p_{s\ ijk}| \leq 0.1$$

$$\text{Max}|\delta T_{ijk}| \leq 1°F$$

$$\text{Max}|\delta S_{s\ ijk}| \leq 1\%$$

The time truncation error was examined using sequentially smaller time steps. For the problem considered time steps of 1000 days produced an "acceptable" error. The rate of convergence of the method was such that the first time step required 20-23 iterations while each additional step required only two to three. In the one-dimensional problem considered, convergence was achieved using a throughput rate, here defined as,

---

+Note that $\delta(\cdot)$ here denotes changes between iterations rather than time levels.

(5.78) $$\tilde{N}_{TP} \equiv \frac{q^m \Delta t}{V_p}$$

of 52.45×10^6. In (5.78), V_p is the finite-difference grid block pore volume and q_v is the total volumetric flow rate through the grid block. In a two-dimensional problem twice as large a throughput ratio was achieved and this was under a range of saturations, i.e., $0 \leq S_s \leq 0.8993$. Note that this corresponds to a value of approximately 30 in the Toronyi and Farouq Ali model. It would be very interesting to know the mass and energy balance achieved in the Coats model.

The 2N algebraic equations generated at each iteration level are solved using a "reduced band width direct solution" algorithm attributed to Price and Coats (1974). This is the same scheme employed by Faust and Mercer (1978b) in their vertically integrated, areal, two-dimensional model (section 5.3.4).

5.5.6 Example Problems:

A number of problems have been run using the Coats simulator. They are summarized as follows:

1) a radial test problem designed to compare the simulators calculated deliverability against an analytical determined value. In addition, this problem was used to examine stability and time-truncation error. In these experiments, zero capillary pressure was used. A maximum deviation between the numerical and analytical of approximately 10% was observed. This is probably within the tolerance associated with the discrepancy between the assumptions required in the analytical solution and those realized in the numerical simulator. Time steps of 1000 days resulted in a small truncation error and stable throughput ratios of 10^7 were observed. Nine nodes were used in this model.

2) a problem cast in cylindrical coordinates with 50 nodes. A straight-line pseudo capillary pressure curve was used such that $p_c = 18.45$ psi when $S_w = S_{wc} = 0.2$ and $p_c = -18.45$ when $S_w = 1.0$. To demonstrate spacial convergence, the problem was also run using twice as many nodes in the vertical i.e. a total of 100 nodes in the problem. The time truncation error was also examined and $\Delta t = 500$ days produced little

truncation error. A stable throughput ratio of 10^8 was achieved with a saturation change from 0 to 0.8993. This problem was run using several initial pressures, permeabilities of 100 and 500 md and porosity values of 0.05 and 0.35. Average computer time for the 50 node problem was 0.016 seconds per grid block-time step. This figure compares with 0.01 seconds for semi-implicit models used by Coats.

3) a two-dimensional (cylindrical) discrete fracture model was formulated and tested. The details of this problem were presented earlier (section 4.1).

4) a three-dimensional (5x5x5) model of a vertical fracture in a hot, dry rock. Tests were conducted to achieve a suitable spacial truncation error. Several matrix permeabilities were considered. The model considered only one half of the symmetric problem. An automatic time step selector was used which employs steps ranging from 0.1 days to 500 days.

5.5.7 Model Evaluation:

The Coats (1977) model represents the state of the art in geothermal reservoir engineering. It incorporates, in addition to the features of other models considered, the possibility of discrete fracture representation (albeit somewhat idealized) in addition to an effective well bore model. The stability and time truncation aspects of the algorithm employed are quite impressive.

While stable solutions for difficult problems were achieved it is not apparent how the iterative algorithm which employs three different equations was applied at the phase transition boundary. Because no mass or energy balances were employed, the convergence characteristics of the algorithm are not evident. Moreover, none of the experimental problems simulated by others were attempted by Coats. It would be particularly interesting to investigate the impact of non-zero capillary pressure since it is one of the few models currently available to handle this situation.

5.6 Model of Huyakorn and Pinder

The model of Huyakorn and Pinder is principally of interest because it demonstrates that a finite element formulation can be used to solve the multiphase geothermal reservoir equations. It should be considered as an alternative formulation to that presented by Faust (1976) wherein he experienced difficulties when applying a standard Galerkin formulation. The Huyakorn and Pinder model is presented in Huyakorn and Pinder (1977).

5.6.1 Governing Equations:

The governing equations were not formulated from first principles but rather adopted directly from Mercer and Faust (1975). The mass and energy balance for the combined water-steam system in a horizontal column can be written

$$(5.79)\qquad \frac{\partial}{\partial t}\left(\varepsilon S_w \rho_w + \varepsilon S_s \rho_s\right) - \frac{\partial}{\partial x}\left[\left(\frac{kk_{rw}\rho_w}{\mu_w} + \frac{kk_{rs}\rho_s}{\mu_s}\right)\frac{\partial p_f}{\partial x}\right] = 0 \qquad \text{(mass)}$$

$$(5.80)\qquad \frac{\partial}{\partial t}\left(\varepsilon S_w \rho_w h_f + \varepsilon S_s \rho_s h_f + (1-\varepsilon)\rho_R h_R\right) - \frac{\partial}{\partial x}\left[\left(\frac{kk_{rs}\rho_s h_s}{\mu_s} + \frac{kk_{rw}\rho_w h_w}{\mu_w}\right)\frac{\partial p_f}{\partial x}\right] - \frac{\partial}{\partial x}\left(\kappa \frac{\partial T}{\partial p_f}\right)_{h_f}\frac{\partial p_f}{\partial x} - \frac{\partial}{\partial x}\left(\kappa \frac{\partial T}{\partial h_f}\right)_{p_f}\frac{\partial h_f}{\partial x}$$

$$= 0 \qquad \text{(energy)}$$

The nonlinear coefficients appearing in (5.79) and (5.80) eg. $\left(\frac{\partial T}{\partial p_f}\right)_{h_f}$ are obtained from formulae written in terms of p_f and h_f.

5.6.2 Assumptions:

The standard assumptions outlined earlier are applicable to this model.

5.6.3 Numerical Approximation:

The numerical scheme used to approximate (5.79) and (5.80) is a modification of the Galerkin finite element method. Because this formulation is not as well known as standard finite difference approximations we will outline it here. Let us rewrite (5.79) and (5.80) in an equivalent but more compact form

$$(5.81) \qquad L_f(p) \equiv \frac{\partial F}{\partial t} - \frac{\partial}{\partial x}\left(\tau \frac{\partial p}{\partial x}\right) = 0$$

$$(5.82) \qquad L_e(p,h) \equiv \frac{\partial H}{\partial t} - \frac{\partial}{\partial x}\left(\lambda \frac{\partial p}{\partial x}\right) - \frac{\partial}{\partial x}\cdot\left(\beta \frac{\partial h}{\partial x}\right) = 0$$

where $\tau = \tau_w + \tau_s$

$$\tau_\alpha = \frac{k k_{r\alpha} \rho_\alpha}{\mu_\alpha} \quad , \quad \alpha = w,s$$

$$F \equiv \varepsilon\rho$$

$$\rho \equiv S_w\rho_w + S_s\rho_s$$

$$\lambda \equiv \kappa \left(\frac{\partial T}{\partial p_f}\right)_{h_f} + h_s \tau_s + h_w \tau_w \qquad (h_w \leq h \leq h_s)$$

$$\lambda \equiv \kappa \left(\frac{\partial T}{\partial p_f}\right)_{h_f} + \tau_\alpha h_\alpha \qquad (h < h_w \text{ or } h > h_s)$$

$$\beta \equiv \kappa \left(\frac{\partial T}{\partial h_f}\right)_{p_f}$$

$$H \equiv \varepsilon \rho_f h_f + (1-\varepsilon)\rho_R h_R$$

The first step in the numerical development is the representation of the unknown functions and the coefficients using finite series involving undetermined coefficients and basis functions (we drop the subscript on p_f and h_f for clarity)

(5.83a) $$p(x,t) \simeq \hat{p}(x,t) = N_J(x) p_J(t)$$

(5.83b) $$h(x,t) \simeq \hat{h}(x,t) = N_J(x) h_J(t)$$

(5.83c) $$\rho(x,t) \simeq \hat{\rho}(x,t) = N_J(x) \rho_J(t)$$

(5.83d) $$F(x,t) \simeq \hat{F}(x,t) = N_J(x) F_J(t)$$

(5.83e) $$\lambda(x,t) \simeq \hat{\lambda}(x,t) = N_J(x) \lambda_J(t)$$

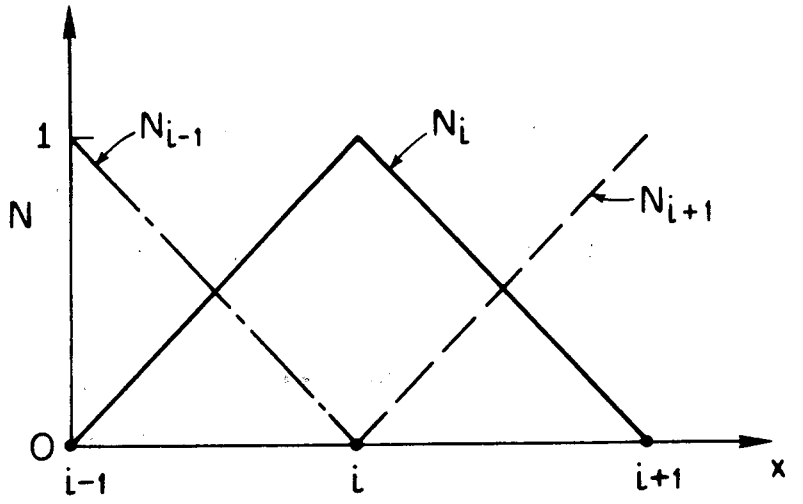

Figure 7: Linear 'chapeau' basis functions.

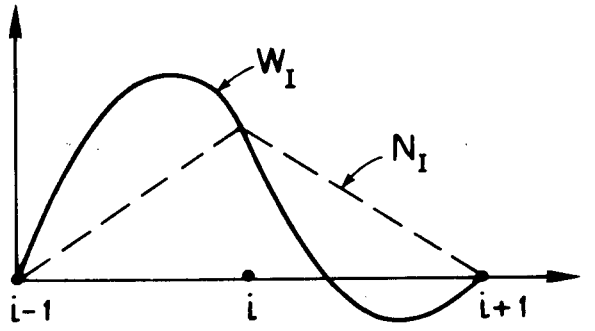

XBL 795-9553

Figure 8: Asymmetric weighting function w_i.

(5.83f) $$\beta(x,t) \approx \hat{\beta}(x,t) = N_J(x)\beta_J(t)$$

(5.83g) $$H(x,t) \approx \hat{H}(x,t) = N_J(x)H_J(t)$$

where summation notation is assumed, i.e., $N_J p_J \equiv \sum_{J=1}^{N} N_J p_J$. The functional form of $N_J(x)$ has not been specified but a number of possibilities exist: the simplest choice is the piecewise linear chapeau function illustrated in figure 7.

The method of weighted residuals assumes a residual exists when (5.83) is substituted into (5.81) and (5.82) i.e.,

(5.84) $$L_f(\hat{p}) = R_f$$

One then minimizes this residual in an average sense using weighting functions, $w_I(x)$.

(5.85) $$\int_x R_f w_I dx = \int_x L_f(\hat{p}) w_I dx = 0 \qquad I = 1,2,\ldots N$$

When $w_I(x) \equiv N_I(x)$, the method of weighted residuals becomes the Galerkin method. Substitution of (5.81), (5.82) and (5.83) into (5.85) yields:

(5.86) $$\int_x \left(\frac{\partial F}{\partial t} N_I - \frac{\partial}{\partial x} \left[\tau \frac{dN_J}{dx} p_J \right] w_I \right) dx = 0$$

$$(5.87)\qquad \int_x \left(\frac{\partial H}{\partial t} N_I - \left[\frac{\partial}{\partial x} \left(\lambda \frac{dN_J}{dx} p_J \right) + \frac{\partial}{\partial x} \left(\beta \frac{dN_J}{dx} h_J \right) \right] w_I \right) dx = 0$$

Note that in (5.86) and (5.87) we have used $w_I \equiv N_I$ for the time derivative. The remaining w_I functions are asymmetric basis functions designed to accommodate upstream weighting (see figure 8).

One normally modifies (5.86) and (5.87) using Green's theorem to transform the second derivative terms:

$$(5.88)\qquad \int_x \left(\frac{\partial F}{\partial t} N_I + \tau \frac{dw_I}{dx} \frac{dN_J}{dx} p_J \right) dx - \tau \frac{\partial \hat{p}}{\partial x} w_I \Big|_{x_o}^{x_\ell} = 0$$

$$I = 1,2,\ldots N$$

$$(5.89)\qquad \int_x \left(\frac{\partial H}{\partial t} N_I + \frac{dw_I}{dx} \frac{dN_J}{dx} (\lambda p_J + \beta h_J) \right) dx$$

$$- \left(\lambda \frac{\partial \hat{p}}{\partial x} + \beta \frac{\partial \hat{h}}{\partial x} \right) w_I \Big|_{x_o}^{x_\ell} = 0 \qquad I = 1,2,\ldots N$$

Thus, we have 2N equations in the 2N unknowns p_J and h_J, provided, of course, one performs the appropriate integration. The remaining task is to investigate the boundary terms, i.e., those terms located at x_ℓ and x_o. Let us rewrite the last term on (5.89) as

$$(5.90)\qquad \left(\lambda \frac{\partial \hat{p}}{\partial x} + \beta \frac{\partial \hat{h}}{\partial x} \right) w_I \Big|_{x_o}^{x_\ell} = w_I \kappa \frac{\partial \hat{T}}{\partial x} \Big|_{x_o}^{x_\ell} + w_I \Theta \frac{\partial \hat{p}}{\partial x} \Big|_{x_o}^{x_\ell}$$

where $\Theta = \lambda - \kappa \left. \frac{\partial T}{\partial p} \right|_h$.

The first term on the right hand side of (5.90) is the conductive heat flux and is generally known (assuming $\hat{T}$ itself is not available). The second term is generally unknown and thus must be carried as part of the coefficient matrix. We will return to this problem shortly.

5.6.4 Solution of Approximating Equations:

The non-linear equations (5.88) and (5.89) are solved using a Newton-Raphson procedure. The resulting linear algebraic equations are solved directly: a trivial task since the problem is one-dimensional. Inasmuch as we have not described the Newton-Raphson procedure to this point, we will now do so using the relatively simple system of (5.88) and (5.89).

5.6.4.1 Newton-Raphson Approximation:

The Newton-Raphson procedure is modified slightly to account for discontinuities in the derivatives of the non-linear coefficients when phase conversion occurs. Let us first define the equations (5.88) and (5.89) using operator notation

$$(5.91) \qquad R_I \equiv \int_x \left(N_I \frac{F^{n+1} - F^n}{\Delta t} + \tau \frac{dw_I}{dx} \frac{dN_J}{dx} p_J^{n+1} \right) dx$$

$$(5.92) \qquad G_I \equiv \int_x \left(N_I \frac{H^{n+1} - H^n}{\Delta t} + \frac{dw_I}{dx} \frac{dN_J}{dx} (\lambda p_J^{n+1} + \beta h_J^{n+1}) \right) dx$$

where we have temporarily dropped the boundary terms. In a completely implicit formulation, we also assume the non-linear coefficients λ and τ are to be evaluated at the n+1 level. When a solution for (5.88) and (5.89) is achieved $R_I = G_I = 0$. We now generate a Taylor series expansion

around the desired zero residual, i.e.,

$$(5.93)\qquad R_I\Big|_{k+1} = 0 = R_I\Big|_k + \frac{\partial R_I}{\partial p_J}\Big|_k (p_J^{k+1} - p_J^k) + \frac{\partial R_I}{\partial h_J}\Big|_k (h_J^{k+1} - h_J^k)$$

where the superscript of p_J and h_J has been suppressed.

$$(5.94)\qquad G_I\Big|_{k+1} = 0 = G_I\Big|_k + \frac{\partial G_I}{\partial p_J}\Big|_k (p_J^{k+1} - p_J^k) + \frac{\partial G_I}{\partial h_J}\Big|_k (h_J^{k+1} - h_J^k)$$

Let us now examine the form of the derivatives $\frac{\partial G_I}{\partial p_J}$ etc.

$$(5.95)\qquad \frac{\partial R_I}{\partial p_J} = \int_x \left(\frac{N_I}{\Delta t} \frac{\partial F^{n+1}}{\partial p_J} + \frac{dw_I}{dx} \left\{ \tau \frac{dN_J}{dx} + \frac{dN_J}{dx} p_J \frac{\partial \tau}{\partial p_J} \right\} \right) dx$$

$$(5.96)\qquad \frac{\partial R_I}{\partial h_J} = \int_x \left(\frac{N_I}{\Delta t} \frac{\partial F^{n+1}}{\partial h_J} + \frac{\partial \tau}{\partial h_J} \frac{dw_I}{dx} \frac{dN_J}{dx} p_J \right) dx$$

$$(5.97)\qquad \frac{\partial G_I}{\partial p_J} = \int_x \left(\frac{N_I}{\Delta t} \frac{\partial H^{n+1}}{\partial p_J} + \frac{dw_I}{dx} \frac{dN_J}{dx} \left[\lambda + p_J \frac{\partial \lambda}{\partial p_J} + h_J \frac{\partial \beta}{\partial p_J} \right] \right) dx$$

$$(5.98)\qquad \frac{\partial G_I}{\partial h_J} = \int_x \left(\frac{N_I}{\Delta t} \frac{\partial H^{n+1}}{\partial h_J} + \frac{dw_I}{dx} \frac{dN_J}{dx} \left[p_J \frac{\partial \lambda}{\partial h_J} + \beta + h_J^{n+1} \frac{\partial \beta}{\partial p_J} \right] \right) dx$$

We can now combine (5.91 - 5.98) to yield

$$(5.99)\qquad \int_x \left(\frac{N_I}{\Delta t} \frac{\partial F^{n+1}}{\partial p_J} + \frac{dw_I}{dx} \left\{ \tau \frac{dN_J}{dx} + \frac{dN_J}{dx} p_J \frac{\partial \tau}{\partial p_J} \right\} \right) dx \Bigg|_k \Delta p_J^{n+1}$$

$$+ \int_x \left(\frac{N_I}{\Delta t} \frac{\partial F^{n+1}}{\partial h_J} + \frac{\partial \tau}{\partial h_J} \frac{dw_I}{dx} \frac{dN_J}{dx} p_J \right) dx \Bigg|_k \Delta h_J^{n+1}$$

$$+ \int_x \left(N_I \frac{F^{n+1} - F^n}{\Delta t} + \tau \frac{dw_I}{dx} \frac{dN_J}{dx} p_J^{n+1} \right) dx \Bigg|_k = 0$$

$$(5.100)\qquad \int_x \left(\frac{N_I}{\Delta t} \frac{\partial H^{n+1}}{\partial p_J} + \frac{dw_I}{dx} \frac{dN_J}{dx} \left[\lambda + p_J \frac{\partial \lambda}{\partial p_J} + h_J \frac{\partial \beta}{\partial p_J} \right] \right) dx \Bigg|_k \Delta p_J$$

$$+ \int_x \left(\frac{N_I}{\Delta t} \frac{\partial H^{n+1}}{\partial h_J} + \frac{dw_I}{dx} \frac{dN_J}{dx} \left[p_J \frac{\partial \lambda}{\partial h_J} + \beta + h_J^{n+1} \frac{\partial \beta}{\partial p_J} \right] \right) dx \Bigg|_k \Delta h_J$$

$$+ \int_x \left(N_I \frac{H^{n+1} - H^n}{\Delta t} + \frac{dw_I}{dx} \frac{dN_J}{dx} \left[\lambda p_J^{n+1} + \beta h_J^{n+1} \right] \right) \Bigg|_k = 0$$

(5.101a) where $\Delta p_J = p_J^{k+1} - p_J^k$

(5.101b) $\Delta h_J = h_J^{k+1} - h_J^k$

Equations (5.99 - 5.101) can be written in matrix form

$$(5.102) \qquad [A] \begin{Bmatrix} \Delta p \\ \Delta h \end{Bmatrix} = \begin{Bmatrix} f \\ g \end{Bmatrix}$$

$$(5.103a) \quad \text{where } f_I = - \int_x \left(\frac{dw_I}{dx} \tau \frac{dN_J}{dx} p_J^k + \frac{N_I}{\Delta t} [F^{n+1,k} - F^n] \right) dx$$

$$(5.103b) \quad g_I = - \int_x \left(\frac{dw_I}{dx} \frac{dN_J}{dx} [\lambda p_J^k + \beta h_J^k] + \frac{N_I}{\Delta t} [H^{n+1,k} - H^n] \right) dx$$

$$(5.103c) \qquad [A_{ij}] = \begin{bmatrix} a_{IJ} & b_{IJ} \\ c_{IJ} & d_{IJ} \end{bmatrix}$$

$$(5.103d) \qquad a_{IJ} = \int_x \left(\frac{N_I}{\Delta t} \frac{\partial F^{n+1}}{\partial p_J} + \frac{dw_I}{dx} \left\{ \tau \frac{dN_J}{dx} + \frac{dN_J}{dx} p_J \frac{\partial \tau}{\partial p_J} \right\} \right) dx \Bigg|_k$$

$$(5.103e) \qquad b_{IJ} = \int_x \left(\frac{N_I}{\Delta t} \frac{\partial F^{n+1}}{\partial h_J} + \frac{\partial \tau}{\partial h_J} \frac{dw_I}{dx} \frac{dN_J}{dx} p_J \right) dx \Bigg|_k$$

$$(5.103f) \qquad c_{IJ} = \int_x \left(\frac{N_I}{\Delta t} \frac{\partial H^{n+1}}{\partial p_J} + \frac{dw_I}{dx} \frac{dN_J}{dx} \left[\lambda + p_J \frac{\partial \lambda}{\partial p_J} + h_J \frac{\partial \beta}{\partial p_J} \right] \right) dx \Bigg|_k$$

$$(5.103g) \qquad d_{IJ} = \int_x \left(\frac{N_I}{\Delta t} \frac{\partial H^{n+1}}{\partial h_J} + \frac{dw_I}{dx} \frac{dN_J}{dx} \left[p_J \frac{\partial \lambda}{\partial h_J} + \beta + h_J^{n+1} \frac{\partial \beta}{\partial p_J} \right] \right) dx \Bigg|_k$$

The procedure from this point forward can be summarized as:

1) Solve (5.102) for the incremental pressures (Δp_J) and enthalpies (Δh_J)

2) The increments are used to update p_J and h_J

3) The new values, p_J and h_J are used to update the coefficients in [A] and the right-hand-side vectors.

4) Steps 1) - 3) are repeated until the increments Δp_J and Δh_J are within a prescribed tolerance

The derivatives of the non-linear coefficient τ, F etc. are approximated by a chord slope determined using nodal values p_J^k and h_J^k and taking small increments from them. These increments are taken such that one avoids the possibility of crossing the phase boundary, i.e., either a positive or negative increment may be used, depending upon the location of the point (p_J^k, h_J^k). We have not presented the formulation for the boundary terms but they are approximated using a procedure analogous to that outlined above.

5.6.5 Example Problems:

Two one-dimensional problems were simulated. The first was the Arihara experiment mentioned in earlier examples. A solution which suitably matched the experimental data was obtained. The second problem was a modification of the first. Using the same experimental set up, the sandstone core was initially filled with hot water and then subjected to a rapid pressure drop. This is a severe test of the ability of the model to accommodate highly non-linear flow. Mass lumping, which is the diagonalization of the matrix associated with the time derivative, produced good results in both of the above problems. Using a convergence criteria of 0.05 percent satisfactory mass and energy balance checks were achieved.

5.6.6 Model Evaluation:

The Huyakorn and Pinder model is important only in the sense that it demonstrates that finite element schemes, suitably modified, can be used to simulate geothermal reservoir behavior. The model in its present form cannot be considered an important reservoir engineering tool. The iterative scheme is interesting and effective. The treatment of the downstream boundary of the Arihara experiment appears to work well (this is discussed at length in the paper (Huyakorn and Pinder, 1977)).

5.7 Model of Thomas and Pierson

The three dimensional finite difference model of Thomas and Pierson is described in Thomas and Pierson (1976). It is capable of handling multiphase flow using an implicit pressure, explicit saturation formulation.

5.7.1 Governing Equations:

The governing equations are not formally developed. The combined water and steam mass and energy balances are presented

$$(5.111)\qquad \frac{\partial}{\partial t}(\varepsilon\rho_s S_s + \varepsilon\rho_w S_w) - \underset{\sim}{\nabla}\cdot\left[\frac{\underset{\approx}{k}k_{wr}\rho_w}{\mu_w}\cdot(\underset{\sim}{\nabla}p_w - \rho_w\underset{\sim}{g}) + \frac{\underset{\approx}{k}k_{sr}\rho_s}{\mu_s}\cdot(\underset{\sim}{\nabla}p_s - \rho_s\underset{\sim}{g})\right] - R_w - R_s = 0 \qquad \text{(mass)}$$

(5.112) $$\frac{\partial}{\partial t}\left[\epsilon(\rho_w S_w U_w + \rho_s S_s U_s) + (1-\epsilon)\rho_f c_p T\right]$$

$$\underset{\sim}{\nabla}\cdot\left[\left(\frac{\underset{\approx}{k}k_{wr}\rho_w h_w}{\mu_w} + \frac{\underset{\approx}{k}k_{sr}\rho_s h_s}{\mu_s}\right)\underset{\sim}{\nabla}p_f - \underset{\sim}{\nabla}\cdot\kappa\underset{\sim}{\nabla}T - R_w h'_w - R_s h'_s - Q\right.$$

$$= 0$$

In addition, Thomas and Pierson provide the following relationships to further determine the physical state of the water

(5.113a) $S_s^{n+1} - S_s^n = - S_s^n$ (water phase only)

(5.113b) $p_f = p_{sat}(T)$ (saturated steam)

(5.113c) $S_w^{n+1} - S_w^n = - S_w^n$ (superheated steam)

5.7.2 Assumptions:

The standard assumptions have been made in this model. It would appear that additional assumptions regarding the gravity force term are employed in (5.112) although this may be a misprint or my misinterpretation.

5.7.3 Numerical Approximation and Solution of Approximating Equations:

The governing equations are approximated using standard finite-difference procedures. Because the scheme employed in the solution of these equations is rather unusual and not considered heretofore in this report, we now consider it in some detail. Let us first expand the time

derivative of (5.111)

$$(5.114a)\quad \frac{\partial}{\partial t}(\varepsilon\rho_s S_s + \varepsilon\rho_w S_w) = \varepsilon\rho_s \frac{\partial S_s}{\partial t} + \varepsilon\rho_w \frac{\partial S_w}{\partial t} + \varepsilon S_s \left(\frac{\partial \rho_s}{\partial T}\right)_{p_f} \frac{\partial T}{\partial t}$$

$$+ \varepsilon S_w \left(\frac{\partial \rho_w}{\partial T}\right)_{p_f} \frac{\partial T}{\partial t} + \varepsilon S_s \left(\frac{\partial \rho_s}{\partial p}\right)_T \frac{\partial p_f}{\partial t} + \varepsilon S_w \left(\frac{\partial \rho_w}{\partial p}\right)_T \frac{\partial p_f}{\partial t}$$

In finite difference form, this becomes:

$$(5.114b)\quad \frac{\partial}{\partial t}(\varepsilon\rho_s S_s + \varepsilon\rho_w S_w) \simeq \frac{1}{\Delta t}\Big\{\left[\varepsilon^{n+1}\rho_s^{n+1} - \varepsilon^{n+1}\rho_w^{n+1}\right]\delta S_w$$

$$+ \left[\varepsilon^{n+1} S_w^n \left(\frac{\partial \rho_w}{\partial T}\right)_{p_f} + \varepsilon^{n+1} S_s^n \left(\frac{\partial \rho_s}{\partial T}\right)_{p_f}\right]\delta T$$

$$+ \Big[S_w^n\, \varepsilon^{n+1}\rho_w^{n+1} c_w + S_w^n \varepsilon_i \rho_w^n c_f + S_s^n\, \varepsilon^{n+1}\left(\frac{\partial \rho_s}{\partial p_f}\right)_T$$

$$+ S_s^n \rho_s^n \varepsilon_i c_f\Big]\delta p_f$$

(5.115) where $\delta S_w = S_w^{n+1} - S_w^n$ or, in general, $\delta(\cdot) = (\cdot)^{n+1} - (\cdot)^n$

c_w is the compressibility of water

c_f is the formation compressibility

ε_i is the initial porosity

Note that (5.115) can be written

$$(\cdot)^{n+1} = \delta(\cdot) + (\cdot)^n$$

such that the second term in (5.111) can be written

(5.116) $$\underset{\sim}{\nabla}\cdot[M_w\rho_w(\underset{\sim}{\nabla}p_w - \rho_w\underset{\sim}{g}) + M_s\rho_s(\underset{\sim}{\nabla}p_s - \rho_s\underset{\sim}{g})] \simeq$$

$$\frac{\underset{\sim}{\Delta}}{V_b}[M_w\rho_w\underset{\sim}{\Delta}\delta p_f + M_s\rho_s\underset{\sim}{\Delta}\delta p_f] + \frac{\underset{\sim}{\Delta}}{V_b}[M_w\rho_w(\underset{\sim}{\Delta}p_w^n - \rho_w\underset{\sim}{g}) + M_s\rho_s(\underset{\sim}{\Delta}p_s^n$$

$$- \rho_s\underset{\sim}{g})]$$

where $\underset{\sim}{\Delta}$ is the standard finite difference spatial operator.
Combination of (5.116), (5.114), and (5.113) yields

(5.117) $$\underset{\sim}{\Delta}\cdot[(M_w\rho_w + M_s\rho_s)\underset{\sim}{\Delta}\delta p_f] = c_{11}\delta S_w + c_{12}\delta T + c_{13}\delta p + R_1 \qquad \text{(mass)}$$

where the c_{1i} are

$$c_{11} = \frac{V_b}{\Delta t}[\epsilon^{n+1}\rho_w^{n+1} - \epsilon^{n+1}\rho_s^{n+1}]$$

$$c_{12} = \frac{V_b}{\Delta t}\left[\epsilon^{n+1}\left(S_w^n\left(\frac{\partial\rho_w}{\partial T}\right)_{p_f} + S_s^n\left(\frac{\partial\rho_s}{\partial T}\right)_{p_f}\right)\right]$$

$$c_{13} = \frac{V_b}{\Delta t}\left[S_w^n(\epsilon^{n+1}\rho_w^{n+1}c_w + \rho_w^n\epsilon_i c_f) + S_s^n\,\epsilon^{n+1}\left(\frac{\partial\rho}{\partial p_f}\right)_T + S_s^n\rho_s^n\,\epsilon_i c_f\right]$$

where c_w is water compressibility and c_f is formation compressibility.

R_1 is given by the second term on the right-hand-side of (5.116) plus the source terms. One can follow a similar development and arrive at the following expression for energy

$$(5.118) \qquad \underset{\sim}{\Delta}[(h_w M_w \rho_w + h_s M_s \rho_s)]\underset{\sim}{\Delta}\delta p_f = c_{21}\delta S_w + c_{22}\delta T + c_{23}\delta p + R_2$$

(energy)

where c_{2i} are non-linear coefficients and R_2 is once again the known information at the n^{th} level. Now, following the same logic as Coats (1977) we recognize that the constraints of (5.113) arise from the fact that only two of δp_f, δT, δS_w are independent in any given phase. Thus, (5.117) and (5.118) must be modified to account for this. Thomas and Pierson accomplish this through an additional constraint equation

$$(5.119) \qquad c_{31}\delta S_w + c_{32}\delta T + c_{33}\delta p + R_3 = 0$$

To illustrate the use of (5.119) let us consider the case when steam and liquid water coexist at n+1. From (5.113b)

$$\delta_p = p_{sat}(T^n) + \left(\frac{\partial p}{\partial T}\right)_{p_f} \delta T - p^n$$

where

$$\left(\frac{\partial p}{\partial T}\right)_{p_f} = \frac{p_{sat}(T^{n+1}) - p_{sat}(T^n)}{T^{n+1} - T^n}$$

Thus, the coefficients of (5.119) become

$$c_{31} = 0; \quad c_{32} = \left(\frac{\partial p}{\partial T}\right)_{p_f} \quad ; \quad c_{33} = 1; \; R_3 = p^n - p_s^n$$

One can now visualize (5.117), (5.118) and (5.119) as a system of three equations in three unknowns. The solution procedure involves the following steps (Thomas and Pierson, 1976).

1) eliminate δS_w and δT from (5.117 - 5.119) by multiplying (5.118) and (5.119) by appropriate coefficients and adding (5.117 - 5.119)

2) solve the resulting equation in one unknown using the reduced band width direct solution method (Price and Coats, 1974).

3) eliminating δS_w from equations (5.117) and (5.118) we have the following explicit relationship for δT.

(5.120)
$$\delta T = \frac{c_{31}}{c_{12} - c_{11}c_{32}} \left\{ \underset{\sim}{\Delta} \cdot [(M_w\rho_w + M_s\rho_s)\underset{\sim}{\Delta}\delta p_f] - R_1 \right.$$

$$\left. \frac{-(c_{13}c_{31} - c_{11}c_{33})}{c_{31}} \delta p + \frac{c_{11}}{c_{31}} R_3 \right\}$$

4) calculate the change in water saturation from (5.117)

(5.121)
$$\delta S_w = \frac{1}{c_{11}} \{ \underset{\sim}{\Delta} \cdot [(M_w\rho_w + M_s\rho_s)\underset{\sim}{\Delta}\delta p_f] - R_1 - c_{12}\delta T - c_{13}\delta p \}$$

5) steps 1-4 are repeated using updated coefficients until a prescribed convergence criteria is achieved. Thomas and Pierson (1977) report two to three iterations per time step.

This scheme is known as the implicit pressure explicit saturation method (IMPES) and was discussed in Coats (1977) for geothermal simulation.

5.7.3.1 Implicit Production Rate:

The production rate can be considered implicitly (e.g. Faust and Mercer, 1978b; Coats, 1977). In the Thomas and Pierson model, this is achieved using the following approach. Let the production rate be written

$$(5.122) \qquad R = R^n + \left(\frac{\partial R}{\partial p_f}\right)_{S_w,\rho_{wf}} \delta p_f + \left(\frac{\partial R}{\partial S_w}\right)_{p_f,\rho_{wf}} \delta S_w + \left(\frac{\partial R}{\partial p_{wf}}\right)_{s_w,p_f} \delta p_{wf}$$

where p_{wf} is flowing bottom-hole pressure

- R^n is the explicit production rate defined by

$$(5.123) \qquad -R^n = \frac{2\pi T^* k_r (\rho/\mu)(p_f - p_{wf})}{\left(\ell n \left(\frac{r_e}{r_w}\right) + s - 1/2\right)}$$

where T^* is the vertically integrated permeability [L^3]

r_e is external radius,

r_w is well-bore radius,

s is skin effect [L°], and

V_g is grid block bulk volume

The derivative $\frac{\partial R^n}{\partial p_f}$ is obtained from R^n

$$(5.124) \qquad -\frac{\partial R^n}{\partial p_f} = \frac{2\pi T k_r \rho/\mu}{\left(\ell n \left(\frac{r_e}{r_w}\right) + s - 1/2\right)}$$

This term is kept in the implicit pressure calculation. This type of development can be extended to multiwell simulations. The final step is the determination of the fractional flow of water, f_w. The procedure described by Thomas and Pierson (1976) is

> "After pressure and temperature convergence is reached and δS_w is calculated explicitly, an implicit δS_w calculation is made using implicit production rates with respect to water saturation. The difference between implicit and explicit production is given by

$$(5.125) \qquad -Rf_w^{n+1} + R_w^n = \frac{V_p^{n+1}}{\Delta t}(\delta S_w - \delta S_w^*)$$

> where δS_w^* is saturation change calculated using explicit production rates and δS_w is the implicit saturation change. The term f_w is the fractional flow of water and R is the total production rate.

$$R = R_w + R_s$$

Fractional water flow is written at time n+1 as

$$f_w^{n+1} = \frac{\lambda_w^n + \left(\frac{\partial \lambda_w}{\partial S_w}\right)_{p_f} \delta S_w}{\lambda_w^n + \left(\frac{\partial \lambda_w}{\partial S_w}\right)_{p_f} \delta S_w + \lambda_s^n + \left(\frac{\partial \lambda_s}{\partial S_w}\right)_{p_f} \delta S_w}.$$

where $\lambda_w^n = \frac{k_{rw}^n}{\mu_w^n}$

$$\lambda_s^n = \frac{k_{rs}^n}{\mu_s^n}$$

Substituting the above expressions into (5.125) yields a quadratic equation which can be solved directly for δS_w."

Note that equation (5.125) appears to contain a typographical error since the dimensions on each side of the equation do not match.

5.7.4 Example Problems:

One-dimensional, two-dimensional cylindrical and areal, and three-dimensional problems were simulated.

1) one dimensional problems: The problem considered is the laboratory experiment of Arihara wherein a core, initially saturated with hot water, is subjected to decreasing pressure until flashing occurs. It is worth noting that in this example the initial conditions dictated saturated water so the transition period was simulated. Pinder and Huyakorn also simulated the problem through the difficult transition period. Automatic time step selection yielded steps of one to ten seconds. Satisfactory results were achieved. There appear to have been 14 nodes used in the problem with $\Delta x/2$ spacing used for the first and last block.

2) areal two dimensions: This problem is the same as that treated by Toronyi, 1974 and discussed in section 5.4.5. The results were essentially identical to those obtained by Toronyi. A 36 node block centered grid was used.

3) radial two dimensions: This problem involved the simulation of the behavior of a reservoir initially containing subcooled water and subjected to production at a constant rate. The reservoir was initially at a temperature of 500°F and a pressure of 1000 psia. Seventy nodes were used in this example problem.

4) three-dimensional: A three-dimensional reservoir with a 10° dip is simulated. The model contained a well in the top five blocks and, due to symmetry, only half the region was modelled. The grid was 12x3x10 = 360 nodes. The model used implicit rates with respect to pressure and saturation and with implicit transmissivities. (this option is not discussed herein but can be found in Thomas and Pierson, 1976) Mass and energy balances of 1.0020 and 0.9998 respectively were achieved. Explicit transmissivities yielded mass and energy balances of 0.9998 and 1.0003. The implicit formulation required approximately 10% fewer time steps. Minor oscillations were observed at the bottom perforations of the well using the explicit scheme.

5.7.5 Model Evaluation:

The Thomas and Pierson model is similar to the Coats model in theoretical foundation and flexibility in application. Both models have some semblance of a well bore model, can be applied to a range of dimensions and geometries and appear to be both accurate and efficient. The principal differences involve solution technique (direct versus IMPES) and fracture representation (only attempted in Coats). The Thomas and Pierson model appears to have been more thoroughly tested, i.e., its solutions were compared with experiment and other numerical simulators, and mass and energy balances were reported. The Coats model would appear to be more computationally efficient although no direct comparisons were attempted. The methodology for crossing the water-two phase boundary is particularly interesting.

The model appears to satisfy most of the requirements of a geothermal reservoir simulator. It does not have some of the practical features of the Coats model such as an effective methodology for simulating flow from adjacent formations. It has the inherent limitations in discretization normally associated with standard finite difference schemes.

5.8 Model of Voss and Pinder

The Voss and Pinder model was designed to demonstrate that the finite-element method could be employed in a large scale simulator. There are several new concepts in this model including the governing equations and method of solution. The model has been used primarily as a research tool and consequently lacks the practical features which would qualify it as an effective reservoir engineering tool. This model is described in Voss (1978).

5.8.1 Governing Equations:

The governing equations were formulated from the primitive point balance equations using the volume averaging approach (see section 3.0). In contrast to other workers, this formulation carries the kinetic and internal energy components through the entire development and then imposes simplifications based on the magnitude of the kinetic energy component. The mass balance expression written in terms of pressure and enthalpy is

$$(5.126)\qquad \varepsilon\left(\frac{\partial \rho_f}{\partial p_f}\right)_{h_f}\frac{\partial p_f}{\partial t} + \varepsilon\left(\frac{\partial \rho_f}{\partial h_f}\right)\frac{\partial h_f}{\partial t} - \underset{\sim}{\nabla}\cdot\left[\left(\frac{\underset{\approx}{kk}_{rs}\rho_s}{\mu_s} + \frac{\underset{\approx}{kk}_{rw}\rho_w}{\mu_w}\right)\cdot\underset{\sim}{\nabla} p_f\right] - \underset{\sim}{\nabla}\cdot\left[\left(\frac{\underset{\approx}{kk}_{rs}\rho_s^2}{\mu_s} + \frac{\underset{\approx}{kk}_{rw}\rho_w^2}{\mu_w}\right)\cdot\underset{\sim}{g}\right] = 0 \qquad \text{(mass)}$$

The energy equation without assumptions regarding the importance of kinetic or potential energy yields

$$(3.47)\qquad (1-\varepsilon)\rho_R \frac{\partial h_R}{\partial t} + \varepsilon\rho_f \frac{\partial r_f}{\partial t} + \varepsilon\rho_f \underset{\sim}{v}_f \cdot \underset{\sim}{\nabla} r_f + \underset{\sim}{\nabla}\cdot\left[\left(\frac{\varepsilon}{\rho_f}\right) S_s S_w \rho_s \rho_w (r_s - r_w)(\underset{\sim}{v}_s - \underset{\sim}{v}_w)\right]$$

$$- \underset{\sim}{\nabla}\cdot(\kappa \underset{\sim}{\nabla} T) - \varepsilon \frac{\partial p_w}{\partial t} - \varepsilon\rho_f (\underset{\sim}{v}_f \cdot \underset{\sim}{g}) = 0$$

where $r_f \equiv h_f + \frac{1}{2} v_f^2$.

If we assume $\frac{1}{2} \underset{\sim}{v}^2 << h_f$, then $r_f \tilde{} h_f$. Further, if we assume the derivatives in r and h_f are essentially the same, we obtain

$$(3.49)\qquad (1-\varepsilon)\rho_R \frac{\partial h_R}{\partial t} + \varepsilon\rho_f \frac{\partial h_f}{\partial t} + \varepsilon\rho_f \underset{\sim}{v}_f \cdot \underset{\sim}{\nabla} h_f$$

$$+ \underset{\sim}{\nabla}\cdot\left[\left(\frac{\varepsilon}{\rho_f}\right) S_s S_w \rho_s \rho_w (h_s - h_w)(\underset{\sim}{v}_s - \underset{\sim}{v}_w)\right] - \underset{\sim}{\nabla}\cdot(\kappa \underset{\sim}{\nabla} T) - \varepsilon \frac{\partial p_w}{\partial t} - \varepsilon\rho_f (\underset{\sim}{v}_f \cdot \underset{\sim}{g})$$

$$= 0$$

Let us now rewrite (3.49), using thermodynamic relationships, to obtain an expression in terms of enthalpy and pressure

$$(5.127)\quad \left[(1-\varepsilon)\rho_m\left(\frac{\partial h_m}{\partial p_f}\right)_{h_f} - \varepsilon\right]\frac{\partial p_f}{\partial t} + \left[(1-\varepsilon)\rho_m\left(\frac{\partial h_m}{\partial h_f}\right)_{p_f} + \varepsilon\rho_f\right]\frac{\partial h_f}{\partial t}$$

$$- \left[\left(\frac{\underset{\approx}{k}k_{rs}\rho_s}{\mu_s} + \frac{\underset{\approx}{k}k_{rw}\rho_w}{\mu_w}\right)\cdot\underset{\sim}{\nabla}p_f - \left(\frac{\underset{\approx}{k}k_{rs}\rho_s^2}{\mu_s} + \frac{\underset{\approx}{k}k_{rw}\rho_w^2}{\mu_w}\right)\cdot\underset{\sim}{g}\right]\cdot\underset{\sim}{\nabla}h_f$$

$$+ \underset{\sim}{\nabla}\cdot\left\{\left[\left(\frac{1}{\rho_f}\right)S_sS_w\rho_s\rho_w(h_s-h_w)\left(\frac{\underset{\approx}{k}k_{rw}}{S_w\mu_w} - \frac{\underset{\approx}{k}k_{rs}}{S_s\mu_s}\right) - \kappa\left(\frac{\partial T}{\partial p_f}\right)_{h_f}\underset{\approx}{I}\right]\cdot\underset{\sim}{\nabla}p_f\right\}$$

$$- \underset{\sim}{\nabla}\cdot\left(\kappa\frac{\partial T}{\partial h_f}\underset{\sim}{\nabla}h_f\right) - \underset{\sim}{\nabla}\cdot\left\{\left(\frac{1}{\rho}\right)S_sS_w\rho_s\rho_w(h_s-h_w)\left[\left(\frac{\underset{\approx}{k}k_{rw}\rho_w}{S_w\mu_w} - \frac{\underset{\approx}{k}k_{rs}\rho_s}{S_s\mu_s}\right)\cdot\underset{\sim}{g}\right]\right\}$$

$$- \varepsilon\rho_f(\underset{\sim}{v}_f\cdot\underset{\sim}{g}) = 0$$

5.8.2 Assumptions:

In the most general form, three of the generally accepted assumptions have been relaxed:

1) pressure work is not considered negligible
2) kinetic energy is not assumed negligible
3) no assumptions have been made regarding potential energy

5.8.3 Numerical Approximations

The governing equations (3.4a) and (5.127) are approximated using a Galerkin finite element method. The only modification to the basic theory is the use of asymmetric weighting functions for the convective term. Symmetric weighting is used for the dispersive term. The mass matrix was not lumped.

Isoparametric quadrilateral and brick finite elements defined in two and three space dimensions respectively were used. The isoparametric finite element has the advantage that the subspaces can be quite general in shape: those employing higher degree polynomials can actually have curved sides. In this model only straight-sided isoparametrics were employed. Thus, this model and that of Lasseter, Witherspoon and Lippmann both have greater flexibility in application than standard finite-difference schemes. Because it is impossible to summarize isoparametric finite element theory in a few paragraphs we refer the reader to Voss, 1978 and standard texts such as Pinder and Gray (1977).

5.8.4 Solution of the Approximating Equations:

The approximating equations are linearized using the total increment method of Settari and Aziz (1975). The scheme is similar to the Newton-Raphson method, yet quite different in some ways. Let us consider a nonlinear coefficient $S(\psi)\psi(t)$. From our earlier development

$$S^{n+1} = S^n + \delta S \tag{5.128}$$

$$\psi^{n+1} = \psi^n + \delta\psi \tag{5.129}$$

Thus, the non-linear product can be written

$$(S\psi)^{n+1} = (S^n+\delta S)(\psi^n+\delta\psi) = S^n\psi^n+\psi^n\delta S + S^n\delta\psi + \delta S\delta\psi \tag{5.130}$$

The change in the non-linear coefficient S can be written (considering only one node) as

(5.131) $$\delta S = \frac{\partial S}{\partial \psi} \delta\psi$$

Substitution of (5.131) into (5.130) yields

(5.132) $$(S\psi)^{n+1} = S^n \psi^n + \psi^n \frac{\partial S}{\partial \psi} \delta\psi + S^n \delta\psi + \frac{\partial S}{\partial \psi} \delta\psi\delta\psi$$

To handle the non-linearities, we introduce the iteration level k and define

(5.133a) $$\frac{\partial S^k}{\partial \psi} = \frac{S(\psi^{n+1,k}) - S(\psi^n)}{\psi^{n+1,k} - \psi^n}$$

(5.133b) $$\delta\psi^k = \psi^{n+1,k} - \psi^n$$

(5.133c) $$\delta\psi^{k+1} = \psi^{n+1,k+1} - \psi^n$$

(5.133d) $$\delta S = \frac{\partial S^k}{\partial \psi} \delta\psi^{k+1}$$

At convergence $\delta\psi^k = \delta\psi^{k+1} = \delta\psi$.

Substitution of (5.133) into (5.132) yields

(5.134) $$(S\psi)^{n+1} = S^n \psi^n + \psi^n \frac{\partial S^k}{\partial \psi} \delta\psi^{k+1} + S^n \delta\psi^{k+1} + \frac{\partial S^k}{\partial \psi} \delta\psi^{k+1} \delta\psi^{k+1}$$

We now apply the Newton-Raphson method to the last term in (5.134) and obtain (see Nolen and Berry, 1972).

$$(5.135) \qquad \frac{\partial S^k}{\partial \psi}\left(\delta\psi^{k+1}\delta\psi^{k+1}\right) \simeq \frac{\partial S^k}{\partial \psi}\left(\delta\psi^{k+1}\delta\psi^{k} + \delta\psi^{k}\delta\psi^{k+1} - \delta\psi^{k}\delta\psi^{k}\right)$$

The final relationship for $(S\psi)^{n+1}$ is obtained through combination of (5.135) and (5.134)

$$(S\psi)^{n+1} = S^n\psi^n + \left(\psi^n \frac{\partial S^k}{\partial \psi} + S^n + \frac{\partial S^k}{\partial \psi}\delta\psi^k + \delta\psi^k\right)\delta\psi^{k+1} - \frac{\partial S^k}{\partial \psi}\delta\psi^k\delta\psi^k$$

Notice that in this formulation, the derivative $\frac{\partial S^k}{\partial \psi}$ is not the tangent at the point $\psi^{n+1,k}$ but rather the chord slope between $\psi^{n+1,k}$ and ψ^n as determined by (5.133a). In practice, the derivatives would be taken with respect to each nodel value of ψ, i.e., ψ_k, k = 1,2,...N.

It is recognized that the situation may arise where the numerical solution will occur exactly on the two phase boundary. While this may seem unlikely, numerical experiments indicate certain problems are solvable only when this possibility is accounted for. An algorithm for achieving this goal is presented in Voss (1978).

The linear algebraic equations are solved using a block iterative scheme which circumvents the need to integrate the coefficients of the matrix equation after each iteration. This technique is rather involved and is described in Voss and Pinder (1978). The time integration parameters (i.e., 0.5 is Crank-Nicolson) were selected to minimize mass and energy balance errors.

5.8.5 Example Problem:

Several problems were considered in order to demonstrate the accuracy and applicability of the model. The following one-dimensional simulations were conducted:

1) single-phase flow with diffusion dominated energy transport

2) single phase flow with convection dominated energy transport

3) linearized two phase flow: a check on the pressure solution

4) two phase flow with phase change (several problems including the Arihara depletion experiment). Both Carey and Arihara permeabilities were employed. Twenty finite elements (21 nodes) were used with a varying time step size. Satisfactory solutions were obtained.

The two and three dimensional problems involved simulation of the production-reinjection problem. The two dimensional areal problem required 29 nodes (see figure 9). The three dimensional simulation required 73 nodes and 29 elements. No difficulties were encountered in the simulation of either of the above problems.

5.8.6 Model Evaluation

The Voss and Pinder model was developed as a prototype to evaluate new ideas in large scale geothermal reservoir simulation. Several concepts were introduced all the way from the formulation of the equations through to their numerical solution. By and large, the new aspects of this simulator have proven satisfactory and improved modelling efficiency. The model has been tested carefully and probably is the most accurate currently available.

The model does not incorporate certain features which are important in practical reservoir engineering. In particular, it does not include a well bore model or enhanced input-output devices. The program is highly complex because it attempts to utilize the ideosyncrasies of the IBM installation to achieve increased efficiency. It would probably be

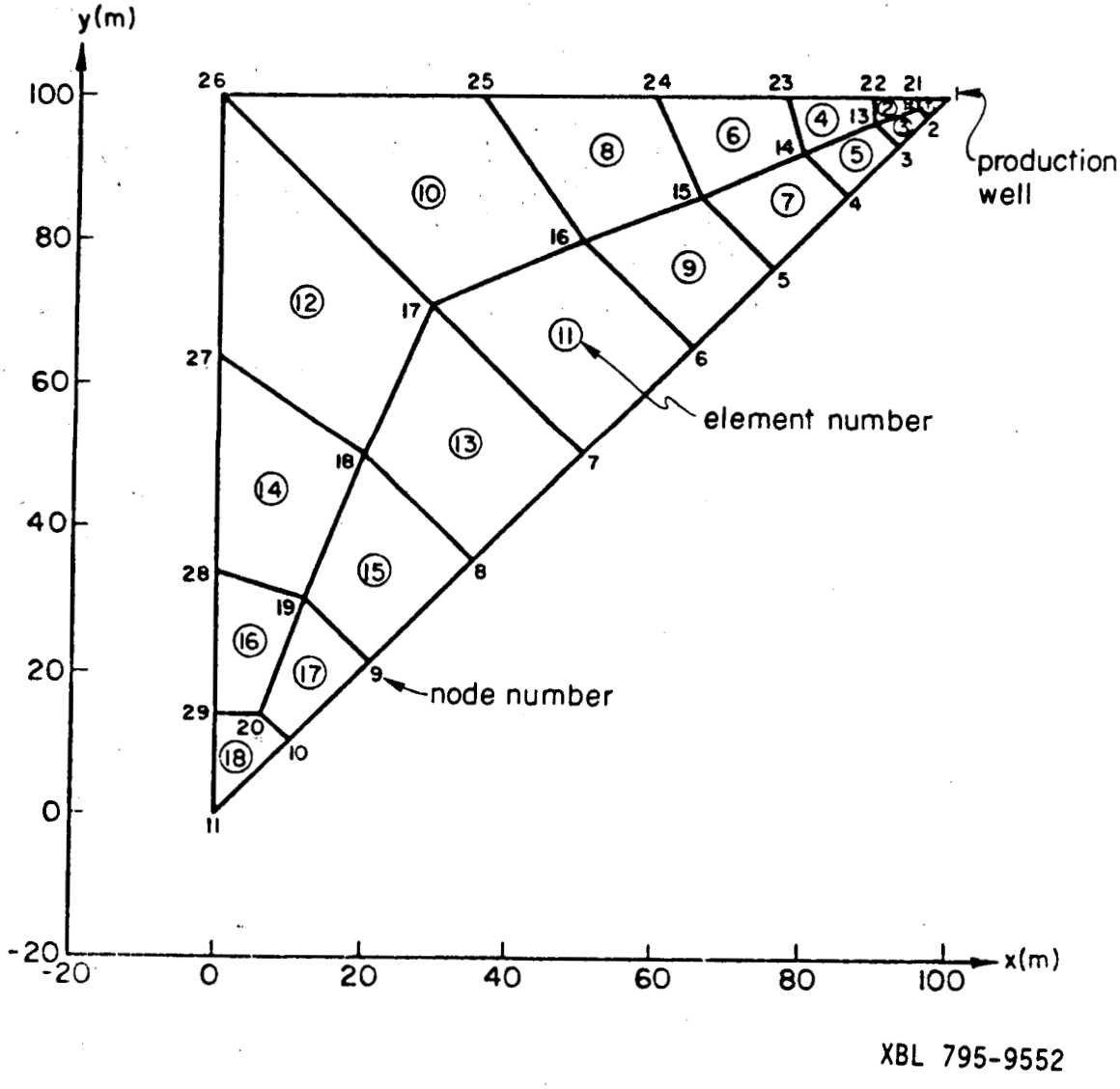

Figure 9: Two-dimensional finite element mesh for production-reinjection problem (after Voss, 1978).

difficult to convert the computer code to computers outside the IBM series.

The Voss and Pinder model should probably be viewed primarily as a research tool although problems of practical interest have been investigated during the course of its development. Many of the ideas introduced in this code should prove valuable in the formulation of the next generation of geothermal reservoir models.

6.0 SUMMARY AND CONCLUSIONS

6.1 Conceptual Model

Geothermal reservoirs are difficult to catalogue physically. They are relatively scarce and tend to be rather unique in their respective settings. Moreover, they are difficult to instrument because of the adverse nature of the geothermal environment. Fortunately, a few fields, particularly those at Wairakei in New Zealand, The Geysers in California, Larderello in Italy, and more recently Cerro Prieto in Mexico are monitored. With the exception of The Geysers, these installations are publicly administered and thus the field data is generally available.

While there is still a great deal to learn about geothermal reservoirs, a knowledge of the physics of the system is gradually emerging. Interaction between mathematical modellers and reservoir engineers has shed light on many aspects of the problem. By and large, this information tends to corroborate concepts formulated by earlier scientists and engineers working in the field. Nevertheless, fundamental questions remain. At the megascopic level, there is still speculation on the role of recharge in the overall system and the source of energy at depth is poorly understood. At the macroscopic scale, the role of fractures in mass and energy transport is not well understood and the interaction between fractures and porous blocks

is virtually unknown.

The conceptual model of the reservoir is particularly important in fabricating the initial and boundary conditions on the system and the source terms. In the short term, the flux terms are probably of the greatest concern. As the pressure decline approaches the boundaries of the reservoir, boundary conditions obviously begin to play an important role. Fortunately, or perhaps unfortunately in the case of newly developed fields, long term records in conjunction with geohydrologic information can provide important insight into boundary type and locations. To achieve reliable forecasts of productivity in an undeveloped geothermal reservoir new or improved geophysical techniques for the definition of reservoir geometry and properties will be required.

6.2 Reservoir Physics

By reservoir physics we refer to those physical phenomena that involve the transport of energy mass and momentum within a geothermal reservoir. The mathematical realization of these phenomena give rise to the governing equations of the reservoir simulator. Until very recently the procedure for establishing these equations was based on analogy with point equations derived using the concepts of continuum mechanics. This approach was extended, in the case of porous media, using mixture theory. Another methodology which appears to be gaining favour is based on the concepts of mass and volume averaging (see sections 3.0). This approach appears to provide enhanced physical insight into the interaction between the various phases encountered in the reservoir. I believe we are now at the stage where a rigorous development of the equations governing multiphase mass and energy transport in a porous medium reservoir is possible. The next challenge will be to establish techniques for measuring the parameters arising in these new and more comprehensive equations. While these develop-

ments will provide a better understanding of the physical processes encountered in the reservoir, they will probably not materially influence the accuracy of long-term reservoir performance.

The role of fractures in geothermal reservoir performance, however, is quite a different matter. Wairakei and The Geysers depend upon fracture permeability to achieve satisfactory mass flows. To date we know very little about modelling fractured reservoir systems and even less about how to determine accurately important properties such as fracture permeability, porosity, orientation and extent. Two schools of thought exist on how fractured reservoirs should be modelled. The first we denote as the discrete fracture approach: this conceptual model requires information on discrete fractures. These are subsequently modelled in combination with their neighboring porous medium blocks. Unless there are major advances in field measurement methodology, it is unlikely such data will even occasionally be available. The second approach is based on the concept of overlapping continua: one for the fractures and the other for the porous blocks. In this approach, several new sets of field parameters would be necessary: these would be volume averaged parameters similar to permeability. Although this may provide a viable tool for modelling fractured reservoirs, it is a rather recent concept and probably belongs within the realm of research at this time.

Unlike porous-flow physics, advances in fracture flow physics could result in important changes in our ideas about geothermal reservoir simulation.

6.3 Constitutive Equations

We have rather arbitrarily extracted this discussion of constitutive theory from the preceeding section on reservoir physics. It is a very important area which is receiving only token attention. The Stanford Geothermal program is responsible for the majority of research relevant to this topic. While it is possible to determine a great deal about the functional form of constitutive equations arising in reservoir physics, experiments are essential to verify hypotheses and measure parameters. Fundamental relationships such as relative permeability curves are not available; the existence or nonexistence of important capillary effects has yet to be established; the thermodynamic relationships for curved steam-water interfaces are not available; elasticity-plasticity models require additional investigation. Needless to say, the introduction of fracture flow, chemical precipitation and dissolution further aggravates the problem of an inadequate experimental program in this area.

Of more pressing importance to the reservoir engineer is the measurement of constitutive parameters at the field level. Given various rather reasonable assumptions, some of the constitutitve knowledge gaps outlined above can be set aside, at least momentarily. One cannot, however, disregard problems in the measurement of important parameters such as permeability, porosity and thermal conductivity. Accurate forecasts reflect accurate parameter estimates and these are exceedingly difficult to come by in the geothermal environment. The impact of this parameter uncertainty we will examine separately in a later section.

6.4 Numerical Approximations

The numerical schemes employed in existing geothermal models have been described in the body of this report (section 5.x). The salient features of each are also summarized in table 2. The important elements of the discussion can be briefly stated as follows:

DEPENDENT VARIABLES: variables solved for explicitly in the governing equations
- Variables are defined in list of variables

WELL APPROXIMATION: the utilization of a model of the well bore

EQUATION APPROXIMATION: the mathematical formalism employed in obtaining the governing porous medium equations
- MACRO designates a macroscopic balance
- MIX designates mixture theory methodology of continuum mechanics
- VINT denotes volume integration from the microscopic level to the macroscopic level.

DIMENSIONS: number of space dimensions employed in example problems

PHASES: The number of phases that can coexist at any given point in space and time.

SPACIAL APPROXIMATION: The numerical scheme used to approximate space derivatives
- IFD denotes integrated finite difference
- FD denotes finite difference
- FE denotes finite element

TEMPORAL APPROXIMATION: The numerical scheme used to approximate the time derivative
- FD denotes finite difference

VERTICAL INTEGRATION: The formal procedure of integrating the three dimensional equations vertically when generating a two-dimensional areal model

CONVECTIVE TERM: form in which the convective term appears in the model

CONVECTIVE TERM APPROX.: numerical scheme employed in approximating the convective term
- UFD denotes upstream weighted finite difference
- UFE denotes upstream weighted finite element

TIME INTEGRATION OF UNKNOWNS: type of time derivative approximation employed

- θ denotes a general formulation $0.5 \leq \theta \leq 1$
- CENT denotes a Crank-Nicolson scheme (i.e., $\theta = 0.5$)
- IMP denotes a backward difference approximation

TIME INTEGRATION COEFFICIENTS: The location in the time domain where the non-linear coefficients are evaluated. Nomenclature the same as previous case.

NON-LINEAR APPROX.: method used to linearize non-linear equations

- NRA denotes Newton-Raphson iteration
- IMPES denotes implicit pressure, explicit saturation
- TIM denotes the total increment method

PHASE CHANGE METHOD: technique used to more numerically across the phase change boundary

- LEX denotes limited excursion technique
- Δt ADJ denotes a modification of Δt as the phase boundary is approached
- TAN denotes a modification of Newton-Raphson to allow the tangent to be taken in a direction away from the phase boundary
- IMP denotes a formulation accounting for the phase change with the equations
- SLA denotes saturation line adjustment

SOLUTION SCHEME: The method used to solve the two coupled governing equations

- SEQ denotes the sequential solution of each, i.e., N equations are solved twice per iteration
- SIM denotes the simultaneous solution of 2N equations at each iteration

MATRIX SOLUTION: Technique used to solve linear algebraic equations

- ITR denotes an iterative method
- ADI denotes alternating direction implicit procedure
- D denotes a direct solution scheme
- SSOR denotes slice successive over relaxation
- IMPES denotes implicit pressure explicit saturation method
- BIFEPS denotes block iterative finite element preprocessed scheme

AVAILABILITY: designation of availability of model to the public

- PUB designates models funded through public monies and therefore available to the public
- PRIV designates models developed with private funds and thus probably proprietary.

Table 2b: Nomenclature for table 2a.

1) The sets of dependent variables employed in solving the flow and energy transport equations are (ρ_f, U_f), (p_f, h_f), (p_f, S_w), $(p_w, T; \rho_s, S_s)$ and $(\rho_w, T; S_w, T; \rho_s, T)$. The choice between (ρ_f, U_f) and (p_f, h_f) seems rather arbitrary since one is readily derived from the other for presentation.

2) The majority of models will accommodate one, two, and three space dimensions: the notable exceptions are Toronyi and Farouq-Ali and Huyakorn and Pinder.

3) With the exception of the Toronyi and Farouq-Ali model, all simulators can handle either one or two phase flow.

4) Finite difference, finite element, and integrated finite difference methods have been used in spacial approximations: the majority of models employ finite difference methods

5) All models approximate the time dimension using finite difference methods

6) Explicit, implicit, and mixed explicit-implicit schemes are employed in the representation of the non-linear coefficients: the majority of algorithms employ an implicit formulation

7) Where an implicit formulation is used, either Newton-Raphson or the total increment method is employed to linearize the approximating equations.

8) The only vertically integrated areal model is the one developed by Faust and Mercer.

9) All methods employ some form of upstream weighting for the convective term.

10) The transition across the phase boundary is accomplished in a number of ways. Most schemes involve some method of numerical damping which stops the oscillation across this boundary. Only the model of Voss and Pinder completely resolves the phase change problem. The approach of Thomas and Pierson deserves additional study: it was difficult to evaluate based on the available literature.

MODELS	DEPENDENT VARIABLES	WELL APPROXIMATION	EQUATION APPROX.	DIMENSIONS	PHASES	SPATIAL APPROX.	TEMPORAL APPROX.	VERTICAL APPROX.	CONVECTIVE TERM	CONVECTIVE TERM APPROX.	TIME INTEGRATION UNKNOWNS	TIME INTEGRATION COEFFICIENTS	NON-LINEAR APPROX.	PHASE CHANGE METHOD	SOLUTION SCHEME	MATRIX SOLUTION	AVAILABILITY
Toronyi and Farouq Ali	p_f S_w	YES	MACRO	2	2	FD	FD	NO	$\nabla \cdot v_f h_f$	UFD	IMP	IMP	NRA	-	SIM	D	PRIV
Lasseter, Witherspoon and Lippmann	p_f U_f	NO	MACRO	1 2 3	1 2	IFD	FD	NO	$\nabla \cdot v_f U_f$	UFD	θ	EXP	NONE	NONE	SEQ	ITR	PUB
Brownell Garg and Pritchett	p_f U_f	YES	MIX	1 2 3	1 2	FD	FD	NO	$\nabla \cdot v_f U_f$	UFD	CENT	IMP	NRA	LEX	SIM	ADI	PRIV
Faust and Mercer	p_f h_f	NO	VINT	1 2 3	1 2	FD (FE)	FD	YES	$\nabla \cdot v_f h_f$	UFD	θ	IMP EXP	NRA	TAN 2D/3D	SEQ/SIM	D/SSOR	PUB
Coats	p_w,T p_s,s_s	YES	MACRO	2 3	1 2	FD	FD	NO	$\nabla \cdot v_\alpha h_\alpha$	UFD	IMP	IMP	NRA	?	SIM	D	PRIV
Huyakorn and Pinder	p_f h_f	NO	MACRO	1	1 2	FE	FD	NO	$\nabla \cdot v_f h_f$	UFE	IMP	IMP	NRA	TAN	SIM	D	PUB
Thomas and Pierson	p_w,T s_w,T p_s,T	YES	MACRO	1 2 3	1 2	FD	FD	NO	$\nabla \cdot v_f h_f$	?	IMP	IMP EXP	IMPES	IMP	SIM	IMPES	PRIV
Voss and Pinder	p_f h_f	NO	VINT	2 3	1 2	FE	FD	NO	$v \cdot \nabla h_f$	UFE	θ	θ	TIM	SLA	SIM	BIFEPS	PUB

Table 2a: Comparison of Multiphase Distributed Parameter Geothermal Reservoir Models (*ratings are subjective)

11) A well bore model is included in the models of Toronyi and Farouq-Ali, Coats, Thomas and Pierson and Brownell, Garg and Pritchett.

The formulation of the approximating equations is relatively straightforward. The linearization of the resulting non-linear equations is rather challenging. The Achilles' heel of the methodology is the treatment of the phase change. For some problems, probably the majority of those encountered in the field, the problem can be treated rather crudely. For others, which are dominated by the phase change phenomenon, an accurate formulation is essential. Because there is no test which is sufficient to demonstrate the accuracy of geothermal reservoir simulators, we can only speculate on the adequacy of this element of the development.

6.5 Solution Scheme

The flow and energy equations can be solved either sequentially or simultaneously. The sequential solution employs estimates of the energy variable when solving the flow equation and estimates of the flow variable when solving the energy equation. This uncoupling is desirable because it is more efficient to solve N equations twice than 2N equations once. The disadvantage is that it is generally necessary to iterate between the equations and convergence is not, in general, guaranteed. The majority of existing models solve the two equations simultaneously and employ Newton-Raphson type schemes to accommodate the non-linearity which arises. The two dimensional model of Faust and Mercer and the formulation of Lasseter, Witherspoon and Lippmann are exceptions to this general rule.

The matrix equations which arise in either approach may be solved either directly or iteratively. Direct methods are based on Gaussian elimination and are reliable when applied to a well behaved system of equations. Iterative methods tend to be more efficient for large problems (e.g., more than 500 equations) but generally require a higher level of numerical ingenuity to program and apply effectively. The majority of iterative schemes are block iterative and thus incorporate a direct solution module in the iterative algorithm. This is true for the models considered with the exception of Lasseter, Witherspoon and Lippmann.

The primary factors to consider in the selection of a solution scheme are accuracy and efficiency. Ease of programming will probably play a secondary role because of the considerable computer costs involved in geothermal reservoir simulation. Because a comparison of the accuracy and efficiency of the models outlined in table 2 has never been undertaken, one cannot select an optimal approach directly.

The complexity of geothermal reservoir physics essentially precludes the verificiation of existing codes using analytical solutions. One can, however, compare solutions generated by a model against other numerical solutions or experimental data. This has been done to varying degrees by the majority of modellers.

6.6 The Question of Uncertainty

In this section, we attempt to address the question of simulation uncertainty. In fact, each of the preceeding sections 6.x have addressed this problem indirectly. Because the history of geothermal reservoir simulation is very short, we have little experience on which to estimate the accuracy of our forecasts. Thus, this discussion must draw on personal experience and studies in related areas. In figure 10, we present a completely subjective estimate of the distribution of uncertainty in the reservoir simulation process. We wish to emphasize that uncertainty does not reside within the technology of equation solving but rather in the formulation of the equations and the measurements of field parameters.

The classical approach to estimating the impact of parameter uncertainty on calculated solutions is through sensitivity analysis. The method involves simulation using maximum and minimum parameter estimates from a reasonable ensemble of values. Thus, the range of solution uncertainty is, in some sense, bracketed. We will not pursue this approach further because this data is not currently available for the geothermal case.

Let us consider a more generic approach wherein we investigate the impact of parameter uncertainty for an operator of the form encountered in geothermal reservoir simulation. The objective is to estimate imput uncertainty and compute the resultant output uncertainty. The approach and results are taken from Tang and Pinder (1977;1978).

The coupled non-linear set of equations has not been considered in the literature. A set of equations similar to a linearized version of the geothermal reservoir equations has been examined. These equations are

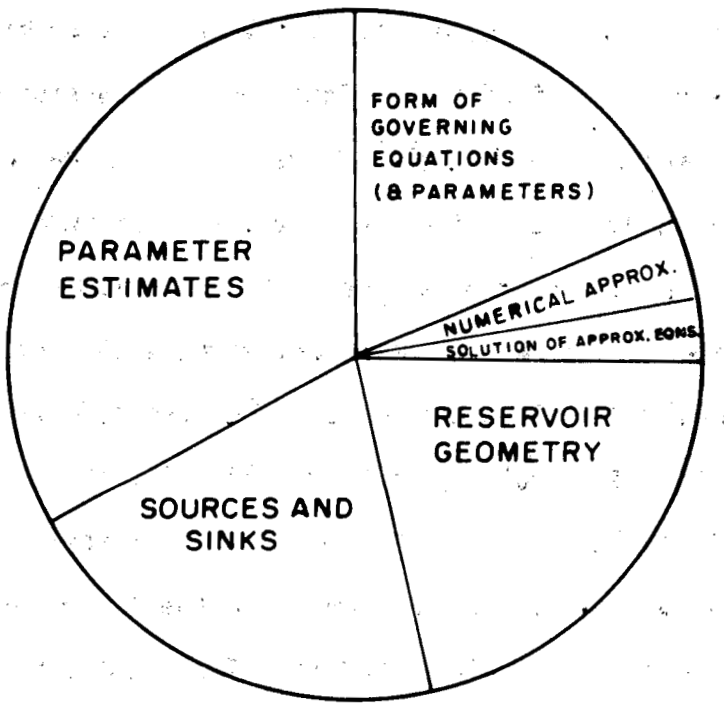

Figure 10: Estimate of the uncertainty distribution among elements of geothermal reservoir simulation.

$$(6.1) \qquad T\frac{\partial^2 u}{\partial x^2} + T\frac{\partial^2 u}{\partial y^2} - \beta\frac{\partial u}{\partial t} - R_w\delta(x-x_o, y-y_o) = 0 \qquad \text{(mass)}$$

where

T is transmissivity,

u is fluid potential,

β is the storage coefficient

δ is the Dirac delta function, and

$$(6.2) \qquad \frac{\partial u}{\partial t} + v\frac{\partial u}{\partial x} - \frac{\partial}{\partial x}\left(D\frac{\partial u}{\partial x}\right) = 0 \qquad \text{(energy)}$$

where

u would be temperature,

v the x velocity component,

D the dispersion coefficient,

$D = D(\alpha, v)$ and

α is the medium dispersivity

Equations (6.1) and (6.2) were solved using uncertain values for T, v, and α. While a rather extensive analysis was performed, we will consider here only an overview of the results.

Let us define a measure of coefficient uncertainty using the coefficient of variation i.e. $CV = \frac{\sigma_\alpha}{\langle\alpha\rangle} \times 100$ where σ_α is the variance and $\langle\alpha\rangle$ the mean of the parameter α. In equation (6.1) we employed input parameters of $\sigma_T = 6.6 \times 10^{-7}$ cm^2/sec. and $\langle T\rangle = 6.6 \times 10^{-6}$ cm^2/sec. The

coefficient of variation is

$$C.V. = \frac{6.6 \times 10^{-7}}{6.6 \times 10^{-6}} \times 100 = 10\%$$

For the case of a radial flow problem defined on a rectangular net, we obtain as a solution $\sigma^2_{u,max} = 6.0 \times 10^2$ and $\langle u \rangle = 0.5 \times 10^2$.

$$C.V. = \frac{24.49}{1.2 \times 10^2} \times 100 = 20.40\%$$

Thus, the uncertainty in the input generated uncertainty in output of about the same magnitude.

The transport equation exhibits a simular tendency. The input parameters in this case were $\sigma^2_D = 87.10^{-12}(cm^2/sec)^2$ and $\langle D \rangle = 6.6 \times 10^{-5}$ cm^2/sec which yields a coefficient of variation of

$$C.V. = \frac{2.94 \times 10^{-6}}{6.6 \times 10^{-5}} \times 100 = 4.45\%$$

The solution to a one dimensional transport problem yields $\sigma^2_u = 2.4 \times 10^{-4}$ and $\langle u \rangle = 0.82$ with a coefficient of variation of

$$C.V. = \frac{0.015}{0.82} = 1.8\%$$

The results of the above analyses suggest that the flow equation tends to amplify uncertainty while the transport equation tends to dampen uncertainty. An examination of the results in their entirety would reveal that, as time elapses, the variance in the solution tends to decrease. Thus, the impact of initial uncertainty in parameter values is less as

boundary values begin to influence the solution.

With respect to geothermal reservoir simulation we are led to conclude that uncertain input data generates solution uncertainty of about the same magnitude (using the coefficient of variation as the uncertainty measurement). The greatest uncertainty in the solution occurs during the period of maximum change in the system. As the system approaches steady state the solution uncertainty decreases. The problem that remains to be considered is the estimation of the input uncertainty.

7.0 NOMENCLATURE

7.1 Upper Case Roman Letters

A	grid cross-sectional area perpendicular to flow direction
D_{nm}	distance between node n and m
E	total energy $(U + \frac{v^2}{2} + \Phi)$
F	$\varepsilon\rho$
G	net production
H	$\varepsilon\rho_f h_f + (1-\varepsilon)\rho_R h_R$
$\underset{\sim}{K}_m$	medium thermal conductivity and dispersion
M	$\varepsilon\rho_f$
M_α	$\frac{kk_{r\alpha}}{\mu_\alpha}$; mobility of the α phase

$(M\rho)^*_{nm}$	$\dfrac{D_{nm}(M\rho)^*_n(M\rho)^*_m}{d_{nm}(M\rho)^*_m + d_{mn}(M\rho)^*_n}$
$(M\rho^2)^*_{nm}$	$\dfrac{(M\rho^2)^*_n(M\rho)^*_{nm}d_{nm} + (M\rho^2)^*_m(M\rho)^*_n d_{mn}}{d_{nm}(M\rho)^*_m + d_{mn}(M\rho)^*_n}$
N	basis function
Q	internal energy injection rate per volume
$\bar{Q}$	$\rho_s/(\rho_w + \rho_s)$
R	mass injection rate per volume
R_f	residual
S	volume saturation
S_{sc}	critical steam saturation
S_{wc}	irreducible water saturation
S^*_w	$(S_w - S_{wc})/(1-S_{wc} - S_{sc})$
$\mathcal{S}$	entropy per unit mass
T	temperature
T^*_w	$\dfrac{kA\rho_w k_{rw}}{\ell\mu_w}$
T^*_s	$\dfrac{kA\rho_s k_{rs}}{\ell\mu_s}$
T^*_h	$T^*_w h_w + T^*_s h_s + \dfrac{K_m A}{\ell} \left(\dfrac{\partial T}{\partial p_f}\right)_{h_f}$

T_c^* $\frac{K_m A}{\ell} \left(\frac{\partial T}{\partial h_f}\right)_{p_f}$

U internal energy per unit mass

w weighting functions

X_m $\left(\frac{\partial (M\rho)^*}{\partial \rho_f}\right)_{nm} \left(\frac{p_m - p_n}{D_{nm}}\right) - \left(\frac{\partial (M\rho^2)^*}{\partial \rho_f}\right)_{nm} \gamma_{nm} g$

7.2 Lower Case Roman Letters

b reservoir thickness

c_w compressibility of water

c_f formation compressibility

c_v heat capacity

c_r rock compressibility

d_{nm} distance between nodal point n and interface between nodes n and m

$\underset{\sim}{\dot{e}}$ deviatoric part of the strain rate tensor

$\underset{\sim}{g}$ gravitational force vector

h enthalpy per unit mass

$\underset{\sim}{k}$ intrinsic permeability tensor

k_r relative permeability

ℓ length increment in the flow direction

m_p	total mass per cell containing the well
$\underset{\sim}{n}$	unit outward normal vector
p	pressure
p_c	capillary pressure
p_T	$(1-\varepsilon)p_R + \varepsilon p_f$
p_{sat}	pressure of saturated steam
p_{wf}	bottom well-bore pressure
q	heat flux vector
$\underset{\sim}{w}$	velocity of the interface
Δt	time step

7.3 Upper Case Greek Letters

$\underset{\approx}{\kappa}$	thermal conductivity tensor
Δ	finite difference operator
χ	$\varepsilon\rho_f h_f + (1-\varepsilon)\rho_R h_R$
Θ	$\lambda - \kappa \left(\frac{\partial T}{\partial p_f}\right)_{h_f}$
Λ	$\frac{\mu_s \rho_w}{\mu_w \rho_s}$

7.4 Lower Case Greek Letters

α	$\left[\frac{1}{\kappa_R} - (1-\varepsilon_o)/\kappa\right]/\varepsilon_o$
β	$\kappa \left(\frac{\partial T}{\partial h_f}\right)_{p_f}$
β_w	$\frac{1-\bar{Q}}{S_w}\left(1-\bar{Q}\ \frac{U_{vap}}{U_f \rho_f}\right)$
β_s	$\frac{\bar{Q}}{S_s}\left[1 + (1-\bar{Q})\ \frac{U_{vap}}{U_f \rho_f}\right]$
γ_{mn}	directional cosine between normal from node m to n and $\underset{\sim}{g}$
θ	weighting factor in numerical scheme
$\bar{\varepsilon}$	bulk volumetric strain
ε	porosity
ε_α	V_α / V
ε^e	rock grain volumetric strain
$\underset{\sim}{\xi}$	microscopic position vector
$\delta(\cdot)$	$(\cdot)^{n+1} - (\cdot)^n$
μ	dynamic viscosity

μ_p skew modulus of the porous rock

λ $\kappa \left(\frac{\partial T}{\partial p_f}\right)_{h_f} + h_s\tau_s + h_w\tau_w \qquad h_w \leq h \leq h_s$

$\kappa \left(\frac{\partial T}{\partial p_f}\right)_{h_f} + \tau_\alpha h_\alpha$

ρ density

τ $\frac{k_{r_\alpha}\rho_\alpha}{\mu_\alpha}$

$\underset{\sim}{\tau}$ stress tensor

Φ potential energy per unit mass

ψ example variable

7.5 Subscripts

f fluid

i,j,k position index in finite difference scheme

m mixture

n node index

R rock

s steam

w water (liquid)

nm	between nodes n and m
α,β	phases

7.6 Operators

$$\frac{D(\cdot)}{Dt} = \frac{\partial}{\partial t}(\cdot) + \underset{\sim}{v}\cdot\underset{\sim}{\nabla}(\cdot)$$

$$\langle\psi\rangle_\alpha = \frac{1}{d\forall}\int_{d\forall}\psi\gamma_\alpha dv_\xi$$

$$\bar{\psi}^\alpha = \frac{1}{\langle\rho\rangle_\alpha d\forall}\int_{d\forall}\rho E\gamma_\alpha dv_\xi$$

$$\tilde{\psi}^\alpha = \psi - \bar{\psi}^\alpha$$

$$\langle\psi\rangle^\alpha = \frac{\langle\psi\rangle_\alpha}{\varepsilon_\alpha}$$

$$\hat{I}^\alpha = \frac{1}{\langle\rho\rangle_\alpha d\forall}\sum_{\beta\neq\alpha}\int \underset{\sim}{n}^{\alpha\beta}\cdot\underset{\sim}{i}da$$

$$\tau^\alpha = \frac{1}{dA}\int_{dA}[\underset{\sim}{i} - \rho\tilde{\psi}^\alpha\tilde{\underset{\sim}{v}}^\alpha]\cdot\underset{\sim}{n}\gamma^\alpha da$$

$$\rho^\alpha = \frac{1}{\langle\rho\rangle_\alpha d\forall}\sum_{\beta\neq\alpha}\int_{dA}\rho\psi(\underset{\sim}{w}-\underset{\sim}{v})\cdot\underset{\sim}{n}^{\alpha\beta}da$$

Figure Captions

Figure 1: Representative elementary volume (REV) containing steam (s), water (w) and rock (R) ($V_w + V_s + V_R = V$)

Figure 2: Discrete fracture system modelled used finite differences (after Coats, 1977). The number of vertical blocks employed in the original experiment by Coats was 31.

Figure 3: Conceptual model for overlapping continua, curve (a) is the plot of a property ψ measured for different volume (REV) L^s of porous media; curve (b) is the plot of a property ψ measured for different volumes (REV) L^3 of fractured porous media. The region (c) is the common region where both the porous medium and fracture medium physics can be represented as though each were a continuum.

Figure 4: Discretization by the integrated finite difference method (after Lasseter, Witherspoon and Lippmann, 1975).

Figure 5: Pressure-enthalpy diagram for water and steam with thermodynamic regions 1) compressed water 2) two-phase steam and water and 3) superheated steam (after Faust and Mercer, 1977a)

Figure 6: Definition sketch for the vertical integration of the parameter $\psi(z) = \langle\psi\rangle + \hat{\psi}(z)$ (after Faust and Mercer, 1978a)

Figure 7: Linear 'chapeau' basis functions

Figure 8: Asymmetric weighting function w_i

Figure 9: Two-dimensional finite element mesh for production-reinjection problem (after Voss, 1978).

Figure 10: Estimate of the uncertainty distribution among elements of geothermal reservoir simulation.

References

Arihara, N., "A study of non-isothermal single and two-phase flow through consolicated sandstones", Stanford Geothermal Program Report SGP-TR-2, 1974.

Assens, G. E., "Derivation, by averaging, of the equations of heat, mass and momentum transfer in a geothermal reservoir", Summaries Second Workshop Geothermal Reservoir Engineering, Stanford University, Stanford, California, paper No. 5-7, December, 1976.

Bear, J., "Dynamics of fluids in porous media", Elsevier, New York, 1972.

Bear, J. and G. F. Pinder, "Porous medium deformation in multiphase flow", Jour. of the Engineering Mechanics Division, Amer. Soc. of Civil Engineers, EM4, p. 881, 1978.

Biot, M. A., "General theory of three dimensional consolidation", Jour. of Applied Physics, Vol. 12, p. 155, 1941.

Bird, R. B., W. E. Stewart and E. N. Lightfoot, "Transport and Phenomena" John Wiley and Sons, New York, 1960.

Brigham, W. E. and W. B. Morrow, "P/Z behavior for geothermal steam reservoirs", SPE 4899, presented at 44th annual California Regional Meeting of SPE, San Francisco, California, April, 1974.

Brownell, D. H., Jr., S. K. Garg, and J. W. Pritchett, "Computer simulation of geothermal reservoirs", SPE 5381, presented at the 45th Annual California Regional Meeting of the Society of Petrol. Engineers of AIME, Ventura, California, 1975.

Brownell, D. H., Jr., S. K. Garg, and J. W. Pritchett, "Governing equations for geothermal reservoirs", Water Resour. Res. 13(6), p. 929, 1977.

Budiansky, B., "Thermal and thermoelastic properties of isotropic composites: Jour. Composite Materials", V.4, p. 286, 1970.

Coats, K.H., "Simulation of steamflooding with distillation and solution gas", SPE 5015, presented at the 19th Annual Fall Meeting of Soc. Petrol. Engineers, Houston, Texas, Oct. 1974.

Coats, K. H., W. D. George, Chieh Chu, and B. E. Marcum, "Three-dimensional simulation of steamflooding", Soc. Petrol. Engineers Jour., 257, p.573, 1974.

Coats, K. H., "Geothermal reservoir modelling", SPE 6892, presented at 52nd Annual Fall Technical Conference and Exhibition of the Soc. of Petrol. Engineers, Denver, Colorado, October 1977.

Corey, A. T., C. H. Rathjens, J. H. Henderson and K. J. Wylie, "Three-phase relative permeability", Trans. AIME, V. 207, p 49, 1955.

Edwards, A. L., "TRUMP: A computer program for transient and steady state temperature distribution in multi-dimensional systems", Livermore, California, Lawrence Livermore Lab. Report UCRL-14754, Rev. 3, 1972.

Eringen, A. C., E. S. Suhubi, "Non-linear theory of simple micro-elastic solids - I", Int. Jour. of Engineering Sciences, V2, p. 189, 1964.

Evans, G. W., R. J. Brousseau and R. Keirstead, "Instability considerations for various difference equations derived from the diffusion equation", Livermore, Calif., Lawrence Livermore Lab Rept. UCRL-4476, 1954.

Farouq Ali, S. M., "Oil recovery by steam injection", Producers Publishing Company, Bradford, Pa., 1970.

Faust, C. R. and J. W. Mercer, "Mathematical modelling of geothermal systems", Proc. Second U. N. Symposium on the Development and Use of Geothermal Resources, Vol. 3, p. 1633, 1975.

Faust, C. W., "Numerical simulation of fluid flow and energy transport in liquid-and vapour-dominated hydrothermal systems", Ph.D. dissertation, Pennsylvania State University, University Park, Pa., 1976.

Faust, C. R. and J. W. Mercer, "Theoretical analysis of fluid flow and energy transport in hydrothermal systems", U. S. Geological Survey open file report 77-60.

Faust, C. R. and J. W. Mercer, "Finite-difference model of two-dimensional single- and two-phase heat transport in a porous medium - Version I", U. S. Geological Survey Open File Report 77-234, 1977a.

Faust, C. R. and J. W. Mercer, "Theoretical analysis of fluid flow and energy transport in hydrothermal systems", U. S. Geological Survey Open File Report 77-60, 1977b.

Faust, C. R., personal communication (1978).

Faust, C. R. and J. W. Mercer, "Geothermal reservoir simulation I: mathematical models for liquid- and vapour-dominated hydrothermal systems", Water Resources Res. (in press).

Faust, C. R. and J. W. Mercer, "Geothermal reservoir simulation II: numerical solution techniques for liquid- and vapour-dominated hydrothermal systems", Water Resources Res., (in press).

Garg, S. K., "Land surface subsidence associated with geothermal energy production", Workshop on Geothermal Reservoir Engineering, P. Kruger and H. J. Ramey, Jr. (ed), Stanford University Geothermal Report SGP-TW-12, p. 65, 1975.

Garg, S. K., J. W. Pritchett, and D. H. Brownell, Jr., "Transport of mass and energy in porous media", Proc. 2nd U. N. Symposium on Development and Use of Geothermal Resources, Vol. 3, p. 1651, 1975

Garg, S. K., personal communication reported by Lasseter, Witherspoon and Lippmann (1975).

Garg, S. K., J. W. Pritchett, M. H. Rice, and T. D. Riney, "U. S. Gulf coast geopressured geothermal reservoir simulation", Systems, Science and Software Report SSS-R-77-3147, La Jolla, California, 1977.

Garg, S. K. and J. W. Pritchett "On pressure-work, viscous dissipation and the energy balance relation for geothermal reservoirs", Advan. Water Resources, 1(1), p. 41, 1977.

Garg, S. K., J. W. Pritchett, D. H. Brownell, Jr., and T. D. Riney, "Geopressured geothermal reservoir and wellbore simulation", Systems, Science and Software Report SSS-R-78-3639, La Jolla, California, 1978.

Gray, W. G. and P. C. Y. Lee, "On the theorems for local volume averaging of multiphase systems", Int. Jour. of Multiphase Flow, p. 333, 1977.

Hassanizadeh, M. and W. G. Gray, "General balance equations for multiphase systems", Princeton Water Resources Report 79-WR-2, (1979)

Huyakorn, P. S. and G. F. Pinder, "A pressure-enthalpy finite element model for simulating hydrothermal reservoirs" in Advances in Computer Methods for Partial Differential Equations II, R. Vichnevetsky (ed.), IMACS, p. 284, 1977.

Kassoy, D. R., "Heat and mass transfer in models of underdeveloped geothermal fields", Proc. 2nd U. N. Symposium on Development and Use of Geothermal Resources, Vol. 3, p. 1707, 1976.

Kruger, P. and H. Ramey, Jr., "Stimulation and reservoir engineering of geothermal resources", Stanford Geothermal Program Report SGP-TR-1, 1974.

Lasseter, T. J., "SHAFT: A computer program for the numerical simulation of heat and mass transfer in multidimensional two-phase geothermal reservoirs", Prelim. Report by Geonuclear Nobel Paso, Geneva, Switzerland, to the Lawrence Berkeley Lab., Berkeley, California, 1975.

Lasseter, T. J., P. A. Witherspoon, and M. J. Lippmann, "The numerical simulation of heat and mass transfer in multidimensional two-phase geothermal reservoirs", Proc. 2nd U. N. Symposiun on Development and Use of Geothermal Resources, Vol. 3, p. 1715, 1975.

Lippmann, M. J., C. F. Tsang and P. A. Witherspoon, "Analysis of the response of geothermal reservoirs under injection and production procedures", SPE 6537, presented at the 47th Annual California Regional Meeting of Soc. of Petrol. Engineers of AIME, Bakersfield, California 1977.

Mercer, J. W. and G. F. Pinder, "A finite element model of two-dimensional, single phase heat transport in a porous medium", U. S. Geol. Survey Open File Report, 75-574, 1974.

Mercer, J. W. and C. R. Faust, "Simulation of water-and vapour-dominated hydrothermal reservoirs", SPE 5520 presented at the 50th Annual Fall Meeting of the Soc. Pet. Eng. AIME, Dallas, Texas, 1975.

Nolen, J. S. and D. W. Berry, "Tests of the stability and time-step sensitivity of semi-implicit reservoir simulation techniques", Soc. Petrol. Engrs. Jour., p. 253, 1972.

O'Neill, K., "The transient three-dimensional transport of liquid and heat in fractured porous media", Ph.D. dissertation, Dept. of Civil Engineering, Princeton University, 1977.

Pinder, G. F. and W. G. Gray, "Finite element simulation in surface and subsurface hydrology", Academic Press, 295pp, 1977.

Price, H. S. and K. H. Coats, "Direct methods in reservoir simulation", Soc. Pet. Eng. Jour. 14(3), p. 295, 1974.

Pritchett, J. W., S. K. Garg, D. H. Brownell, and H. B. Levine, "Geohydrological environmental effects of geothermal power production phase I", Systems, Science and Software Report SSS-R-2733, La Jolla, California, 1975.

Pritchett, J. W. , "Numerical calculation of multiphase fluid and heat flow in hydrothermal reservoirs", Workshop on Geothermal Reservoir Engineering, P. Kruger and H. J. Ramey, Jr., (eds), Stanford University Geothermal Report SGP-TR-12, p. 201, 1975.

Pritchett, J. W., S. K. Garg, D. H. Brownell, Jr., L. F. Rice, M. H. Rice, T. D. Riney, R. R. Hendrickson, "Geohydrological environmental effects of geothermal power production phase IIA", Systems, Science and Software Report SSS-R-77-2998, La Jolla, California, 1976.

Pritchett, J. W., personal communication, 1978.

Pritchett, J. W., "Geohydrological environmental effects of geothermal power production - phase IIB", Systems, Science and Software Report SSR-R-78-3631, La Jolla, Californai, 1978.

Riney, T. D., J. W. Pritchett and S. K. Garg, "Salton Sea geothermal reservoir simulations", 2nd Workshop on Geothermal Reservoir Engineering, P. Kruger and H. J. Ramey, Jr. (ed), Stanford University Geothermal Report SGP-TR-25, p. 178, 1977.

Safai, N., "Simulation of saturated and unsaturated deformable porous media", Ph.D. dissertation, Dept. of Civil Engineering, Princeton University, 1977.

Settari, A. and K. Aziz, "Treatment of non-linear terms in the numerical solution of partial differential equations for multiphase flow in porous media, Int. J. Multiphase Flow, 1, p. 817, 1975.

Sorey, M. L., "Numerical modelling of liquid geothermal systems", Ph.D. dissertation, Univ. of California, Berkeley, 1975.

Tang, D. H. and G. F. Pinder, "Simulation of groundwater flow and mass transport under uncertainty", Advances in Water Resources, 1(1), 1977.

Tang, D. H. and G. F. Pinder "Analysis of mass transport with uncertain physical parameters", Water Resources Research (in press).

Thomas, L. K. and R. Pierson, "Three dimensional geothermal reservoir simulation", SPE 6104, presented at the 51st Annual Fall Technical Conference and Exhibition of the Society of Petroleum Engineers of AIME, New Orleans, 1976.

Toronyi, R. M., "Two-phase, two dimensional simulation of a geothermal reservoir and the wellbore system", Ph.D. dissertation, Pennsylvania State University, 1974.

Toronyi, R. M. and S. M. Farouq Ali, "Two-phase, two-dimensional simulation of a geothermal reservoir and the wellbore system", SPE 5521, presented at the 50th Annual Fall Meeting of the Soc. Pet. Eng. AIME, Dallas, Texas, Sept. 1975.

Toronyi, R. M. and S. M. Farouq Ali, "Two-phase, two-dimensional simulation of a geothermal reservoir", Soc. Petrol. Engineers Jour., p. 171, June 1977.

Verruijt, A., "Elastic Storage in Aquifers", Flow through Porous Media, R.J.M. deWiest, ed., Academic Press, New York, N. Y., p. 331, 1969.

Voss, C. I., "Finite element simulation of multiphase geothermal reservoirs", Ph.D. dissertation, Dept. of Civil Engineering, Princeton University, 1978.

Voss, C. I. and G. F. Pinder, "Block iterative finite element preprocessed scheme for simulation of large non-linear problems, Int. J. Num. Methods Engrg. (in press), 1978.

Wartenburger, R. A. and D. H. Thurnaw, "Application of SSOR to three-dimensional reservoir problems, SPE 5728, presented at the Fourth Symposium of Numerical Simulation of Reservoir Performance", Soc. Pet. Eng. AIME, Los Angeles, Calif., 1976.

Weinstein, H. G., J. A. Wheeler, and E. G. Woods, "Numerical model for steam simulation", SPE 4759, presented at the Improved Oil Recovery Symposium of Soc. Petrol. Engineers, Tulsa, Oklahoma, April 1974.

Whiting, R. L. and H. J. Ramey, Jr., "Application of material and energy balances to geothermal steam production", Jour. Petrol. Tech., p. 893, July 1969.

U.S.GPO:1980-693-924/83